MECHANICAL ENGINEERING DEPARTMENT

AUTO-IGNITION MODELING IN A SPARK IGNITION INTERNAL COMBUSTION ENGINE FUELED WITH GASEOUS FUELS WITH VARIABLE METHANE NUMBER

by

GERMAN JAVIER AMADOR DIAZ

A dissertation submitted in partial fulfillment of the requirements

for the Degree of Doctor in Mechanical Engineering

Department of Mechanical Engineering

Universidad del Norte

Barranquilla, Colombia

2017

AUTO-IGNITION MODELING IN A SPARK IGNITION INTERNAL COMBUSTION ENGINE FUELED WITH GASEOUS FUELS WITH VARIABLE METHANE NUMBER

Submitted by: German Javier Amador Diaz

Advisor: Ph.D. Lesme Antonio Corredor Martinez

Universidad del Norte

Co-advisor: Ph.D. Daniel B. Olsen

Colorado State University

Examinig Committee

Ph.D. Helmer Acevedo Gamboa

Ph.D. Mauricio Carmona Garcia

Ph.D. Octavio Armas Vergel

Ph.D. Jhon Agudelo Santamaría

Barranquilla, Abril 23, 2017

ACKNOWLEDGEMENTS

I would like to thank my advisors, professor Lesme Corredor Martinez of the Universidad del Norte and Daniel B. Olsen of the Colorado State University, for their support, advice and encouragement during the development of this thesis.

Thank to staff of Engines and Energy Conversion Laboratory, for their support during the development of experiments.

Thank to Dr. Antonio Bula by his advice and invaluable help.

Thank to COLCIENCIAS for their financial support.

Finally, my thanks go to my wife, Yeimy and my aunts Palmira, Julia e Isabel Amador to whom this work is dedicated.

ABSTRACT

A semi-empirical model for determining Knock Occurrence Crank Angle (KOCA) in a Cooperative Fuel Research (CFR) engine was developed. The model is based on the Integral Model approach and experimental data collected in a factorial 2^3 with axial and central runs experiment. Mixtures of CH_4/H_2 were employed as fuel. The model was accurate enough to predict KOCA with a maximum and minimum error of just 3.6 and 0.9 degrees in crank angle respectively.

To study the auto-ignition chemistry and its relationship with the knock resistance of gaseous fuels, the Methane Number of $CO/CO_2/H_2$ mixtures were measured through a method analogous to the standard method for Octane Number measurement**.** A correlation for estimating Methane Number as a function of fuel compositions was proposed. The proposed correlation is a good tool for estimating the Methane Number of fuels with high concentration of carbon dioxide, carbon monoxide and hydrogen. Relationship between Methane Number, KOCA, Laminar Flame Speed (S_L) and combustion parameters were examined.

A comprehensive evaluation of the accuracy of a detailed chemical kinetics mechanism for predicting KOCA in a CFR engine was carried out. The spark ignition engine model of Chemkin Pro® software coupled with Gri-Mech. 3.0 chemical kinetics mechanism was used to model auto-ignition A set of equations for calculating residual gas fraction (x_r), inlet valve close gas temperature (T_{IVC}) and residual gas temperature(T_r) were proposed. Moreover, a technique for estimating combustion parameters from the indicator diagram was developed. Polytropic coefficients, Combustion Duration (CD), Ignition Delay (ID) and Start of Combustion (SOC) are estimated by using this methodology. Results reveal that accuracy of the mechanism used for estimating KOCA decreases as compression ratio decreases. This result is consistent with the lack of accuracy of the mechanism for predicting ignition delay time of gaseous fuel at low temperature.

CONTENT

LIST OF FIGURES

LIST OF TABLES

NOMENCLATURE

A/F	Air fuel ratio
aBDC	After bottom dead center (deg.)
bTDC	Before top dead center (deg.)
CCR	Critical Compression Ratio
CD	Combustion duration (deg.)
CNG	Compressed Natural Gas
EOC	End of Combustion (deg.)
EVC	Exhaust Valve Close
EVO	Exhaust Valve Open
FFT	Fast Fourier Transform
ICE	Internal Combustion Engine
ID	Ignition delay (deg.)
IT	Ignition Timing (deg.)
IVC	Inlet Valve Close
IVO	Inlet Valve Open
Ki	Knock intensity
KI	Knock Integral
KOCA	Knock Occurrence Crank Angle (deg.)
LPG	Liquefied Petroleum Gas
m	Mass (kg)
MBT	Maximum Break Torque (kN-m)
MFB	Mass Fraction Burned
MHRR	Maximum Heat Release Rate (kJ/deg)

MN	Methane Number
ON	Octane Number
P	Pressure (kPa)
PRF	Primary Reference Fuel
p_e/p_i	Exhaust and inlet gas pressure ratio
Q_{LHV}	Low heating value (MJ/kg)
RON	Research Octane Number
ROP	Rate of Production (moles/m^3-s)
S_L	Unstretched laminar flame speed (cm/s)
SOC	Start of Combustion (deg.)
SI	Spark Ignition
t	Time (s)
T	Temperature (K)
TDC	Top Dead Center
V	Volume (m^3)
W	Engine power output (kW)

GREEK SYMBOLS

ω	Engine speed (rpm)
$\emptyset$	Equivalence ratio
β	Error parameter
σ	Standard deviation
ρ	Density [kg- m^{-3}]
λ	Excess of Air
τ	Ignition delay time (ms)
γ	Specific heat ratio

Chapter 1

Introduction

1.1 BACKGROUND

Auto-ignition modeling of fuels in Spark Ignited (SI) Internal Combustion Engine (ICE) can be categorized into two groups: zero-dimensional and multi-dimensional auto-ignition models as shown in Figure 1-1. Zero-dimensional models are further sub-divided into: integral model, single zone, two-zone and multi-zone auto-ignition models. These models are zero-dimensional because they do not involve any consideration of the flow field dimensions; therefore, time is the only independent variable. The Integral model was one of the most used approaches for auto-ignition modeling. It is based on Knock Occurrence Crank Angle (KOCA) and in-cylinder pressure measurements for determining ignition delay time functions. These functions can be determined for different fuels by using ICE as a reactor.

In the single zone, two-zone and multi-zone auto-ignition models, the working fluid in the engine is divided into different control volumes, which are assumed to be thermodynamic systems. These systems undergo energy and/or mass exchange with the surroundings. The energy released during combustion process is calculated by applying the first law of thermodynamic.

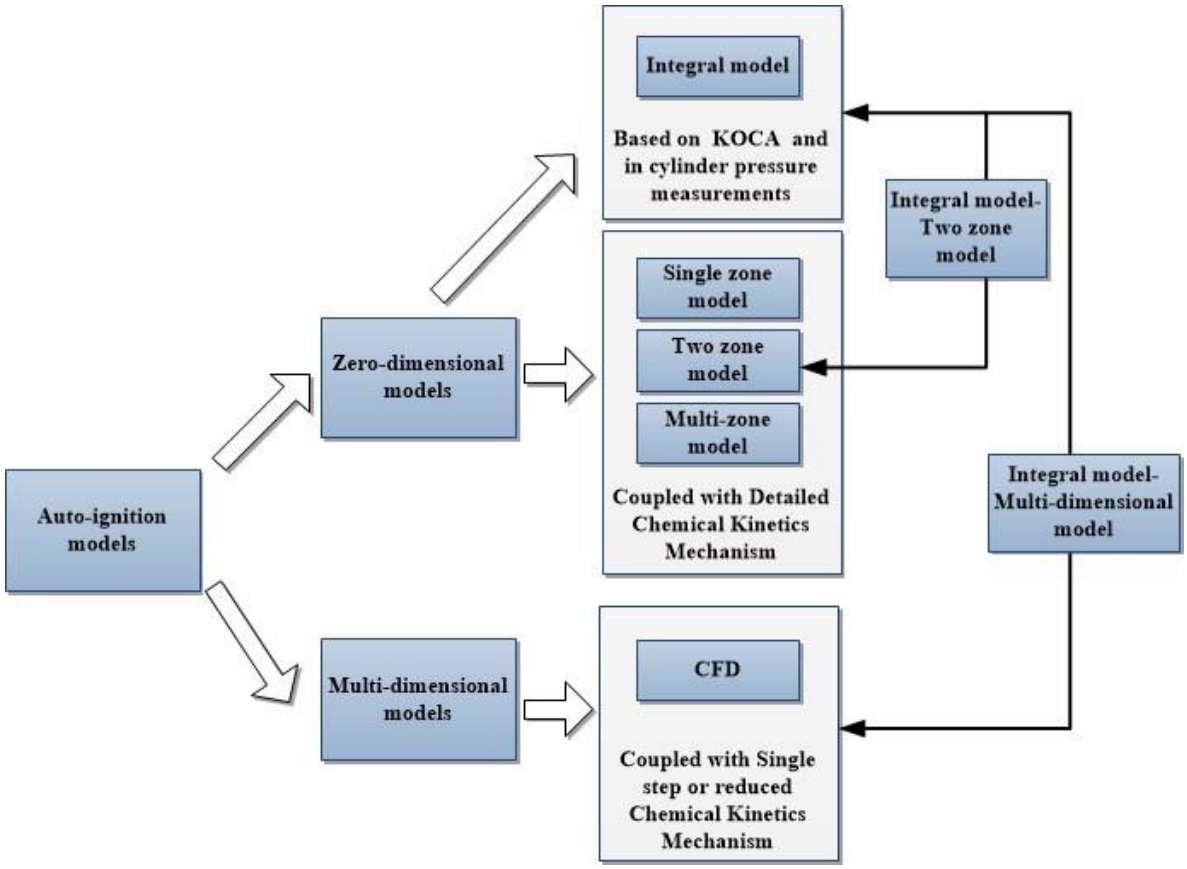

Figure 1-1 Classification of auto-ignition models found in the literature.

In two-zone models, the working fluid is divided into two thermodynamic systems: burned and unburned zones. The end gas properties are equal to the homogeneous unburned gas properties where low temperature unburned gas oxidation takes place. For low temperature gas oxidation and combustion analysis, detailed chemical kinetics mechanisms are used. According to the literature review, two-zone auto-ignition models are the most used zero-dimensional models. Its low computational cost and flexibility for studying engine emissions, chemical species interactions and thermal engine performance are the main reasons.

Multi-dimensional auto-ignition models involve spatial auto-ignition analysis, where flow turbulence, ignition development, flame-wall interactions, heat transfer and emissions modeling are considered. The implementation of these sub-models and the grid used in the CFD codes reduces its capacity for considering detailed chemical kinetics mechanism. To

overcome this issue, single step or reduced chemical kinetics mechanisms are considered both liquid and gaseous fuels combustion modeling. To improve auto-ignition models accuracy, the integral model approach has been coupled with two-zone and multi-dimensional engine codes. This strategy has been successfully implemented both hydrocarbons fuels and natural gas auto-ignition predictions.

In the next section, a detailed review of the most important auto-ignition models is described.

1.1.1 Zero-dimensional auto-ignition models. As mentioned above empirical integral approach and two- zone model are the most used zero-dimensional auto-ignition models. The first approach was proposed by Livengood and Wu (1955) who considered a hypothetic zero-dimensional reactor where a global reaction occurs. This approach establishes that auto-ignition takes place when intermediate species achieve a critical value in the combustion chamber. Equation 1-1 relates auto-ignition timing of fuels with an ignition delay time function (τ), which depends on the unburned gas pressure and temperature. The parametersθ_{ref}, $\theta_{koca}$and x_c are the reference timing, auto-ignition timing in crank angle degree and critical specie concentration respectively.

$$\frac{x_c}{x} = \int_{\theta_{ref}}^{\theta_{koca}} \frac{d\theta}{\tau} = 1 \qquad \text{Eq. 1-1}$$

The Four Octane Number Method was proposed by Douaud and Eyzat (1978) where SI engines are used as a reactor for determining ignition delay time functions. This method was employed for determining anti-knock properties of commercial fuels and Primary Reference Fuels (PRF) ranging from 80 to 100 Octane Number (ON). The method is based on in-cylinder pressure, KOCA, and unburned gas temperature deduced from thermodynamics relations or zero-dimensional engine models. Constants of ignition delay time function are generally used as tuning parameters for fitting numerical estimations with experimental data. Several ignition delay time functions have been determined by using this methodology for conventional fuels and different engine designs. Wayne, Clark and

Atkinson (1998) developed a correlation for 89 and 94 ON gasoline and Elmqvist et al.(2003) for 95 Research Octane Number (RON) fuel, including in its analysis engine speed and equivalence ratio effects. Recently Song and Song (2016) employed a modified integral model for knock predictions of iso-octane and n-heptane mixtures.

Few works on the development of auto-ignition integral model for gaseous fuels have been published. An auto-ignition integral model for natural gas/propane mixture was developed by Soylu and Van Gerpen (2003) in a six in line, 112 kW turbocharged engine . This work considers up to 15% of propane in mixtures with natural gas, and evaluates ignition timing and equivalence ratio effects. The method employed is based on the Douaud and Eyzat (1978) methodology. Mixtures of gasoline and propane were tested by Beccari, S. et al.(2016) in a Dresser Wuakesha CFR (Cooperative Fuel Research) engine for calibrating two knock onset models: the Knock Integral Model and the Ignition Delay Model. Their results showed that the calibrated models were accurate enough to predict knocking occurrence phenomena, with a maximum error of just 4 degrees in crank angle. Table 1.1 shows a summary of the most important correlations developed for gasoline, PRF and Natural Gas. For more correlations, refer to (Chen, Li, Yin, and Zheng, 2014).

The hypothesis of a global reaction for predicting auto-ignition phenomenon has been demonstrated to be a good approach. Integral model is attractive because it is simple and requires a low computational cost for implementation. However, kinetics of pre-reactions even for pure hydrocarbons such as ethane and methane are complex. In this sense, a global reaction is not suitable for explaining actual phenomena that involve thousands of elementary reactions and critical intermediate species. To solve this issue, zero-dimensional engine models coupled with detailed chemical kinetics mechanism have been proposed to predict auto-ignition of fuels. These approaches are classified as single zone, two- zone and multi- zone models. An important contribution was made by Karim and Gao (1992), who developed a knock model that combine chemical reactions of methane air gas mixture during compression and combustion phase with engine operating conditions. This model considers a comprehensive reaction scheme of 105 elementary reactions with 31 species, which was coupled with a two-zone engine model. Kinetics and thermodynamic properties

Table 1-1 Summary of the most important integral models reported in the literature

Model	*Fuel*	*Reference*
$\tau = 0{,}01869\left(\frac{ON}{100}\right)^{3.4017} p^{-1{,}7}\exp\left(\frac{3800}{T}\right)$	80<ON<100	(Douaud and Eyzat, 1978)
$\tau = 0{,}389\left(\frac{ON}{100}\right)^{7{,}202} p^{-1{,}15}\exp\left(\frac{5200}{T}\right)$	89 and 94 ON	(Wayne et al., 1998)
$\tau = 0{,}021 p^{-1{,}7}\exp\left(\frac{3800}{T}\right)$	95 RON	(Elmqvist et al., 2003a)
$\tau = 18{,}33\left(\frac{ON}{100}\right)^{3{,}402} p^{-1{,}7}\exp\left(\frac{3800}{T}\right)$	PRF 87	(Shao and Rutland, 2014)
$\tau = 305{,}731\omega * p^{-c_2}\exp\left(\frac{3188{,}7424}{T}\right)$ Where $C_2 = 1{,}7914(1{,}03 - 3\times 10^{-5}\omega)$	96 RON	(Ganestam, 2010)
$\tau = 0{,}985 p^{-0{,}8870}\exp\left(\frac{7000X_3}{T}\right)$ Where $X_3 = (-0{,}575 + 10{,}058PR - 54{,}053PR^2)\emptyset + 1{,}456 - 8{,}703PR + 43{,}615PR^2$	Natural gas/Propane	(Soylu and Van Gerpen, 2003)
$\tau = 17{,}68\left(\frac{ON}{100}\right)^{3{,}402} p^{-2{,}005}\exp\left(\frac{3450}{T}\right)$	Natural gas/Gasoline Engine: Turbocharged	(Rostampour and Toosi, 2015)
$\tau = p^{-4{,}85}\exp\left(\frac{5450}{T}\right)$	Gasoline	(Pipitone, Beccari, and Genchi, 2015)
$\tau = 0{,}0185 p^{-5{,}45}\exp\left(\frac{11000}{T}\right)$	Propane	(Pipitone et al., 2015)
$\tau = 13{,}29\left(\frac{ON}{100}\right)^{3{,}665} p^{-1{,}364}\exp\left(\frac{3093}{T}\right)$	Gasoline	(Chen, L., Li, T., Yin, T., & Zheng, B. 2014)
$\tau = 5{,}35\times 10^{-5}\left(\frac{p}{T}\right)^{-2{,}374}(1 - X_{EGR})^{-3{,}013}\lambda^{-1{,}927}\exp\left(\frac{3167}{T}\right)$	Gasoline with EGR ranging from 0 to 11%	(Chen et al., 2014)

Nomenclature. τ: ignition delay time (ms); $\emptyset$: equivalence ratio; PR: natural gas/propane ratio ; p: unburned gas pressure (kPa) ; T: unburned gas temperature (K) ;ω: engine speed (rpm) ; EGR: exhaust gas recirculation.

estimations by using chemical reactions are used for defining a knock criterion and therefore a limit knock region in the engine. Although KOCA was measured experimentally at different engine operating conditions, there was no evidence that KOCA

was determined with accuracy. Similar methodology was carried out by Trijselaar (2012) who estimated knock onset region in a 150 kW four stroke Natural Gas engine. In this work, kinetics of pre-reactions and combustion phase were modeled by considering Gri-Mech 3.0 as reference mechanism. The accuracy of mechanism on KOCA estimation was not evaluated.

Auto-ignition studies of hydrocarbons fuels have been carried out recently. An interesting study on low temperature oxidation of PRF by using chemical reactions was performed by Kitada et al.,(2015). This research employed a simplified gasoline PRF chemical reaction compound of 38 elementary reactions and 37 chemical species. Experimental data and simulations done in Chemkin Pro® software were employed to validate the estimations. Results showed a good agreement between the predictions and experimental data.

Accuracy of chemical reactions for estimating KOCA have been tested for gaseous and liquid hydrocarbons fuels. LPG auto-ignition timing (called KOCA in this chapter) has been measured experimentally and modeled by using a comprehensive chemical kinetic mechanism for C_1-C_4 hydrocarbons fuels and a two- zone engine model (Morganti et al., 2015). In this research, twelve C_3/C_4 mixtures were tested in a CFR engine. KOCA estimations improve when addition of Nitric Oxide (NO) was considered in the residual gas. For fuels composed primarily of paraffin the estimations of KOCA occur 1-3 crank angle degree more prematurely when NO concentration is considered. The accuracy in the results obtained was variable, depending on the composition of the tested fuel. The same methodology was employed by Chen et al.(2016) who considers as fuel Pentane isomers (n-neo-and iso- Pentane). The tests were carried out in a CFR engine and simulations used the C_5 mechanism from the National University of Ireland–Galway (NUI- Galway) and the gasoline mechanism from the Lawrence Livermore National Laboratory (LLNL). These mechanisms were coupled with a two-zone engine model, which was implemented in MATLAB ®. Chemical kinetics simulations were done by using CANTERA code. The results obtained showed low accuracy in the estimations being more evident in the auto-ignition estimations of iso-pentane. The importance of these researches is the study of the accuracy in the prediction of auto-ignition timing by using detailed chemical kinetics mechanism.

An important step to evaluate the actual effect of the accuracy of chemical kinetic mechanisms on the auto-ignition modeling was performed by Gersen et al. (2016). In this research, auto-ignition simulation for Liquefied Natural Gas, Natural Gas and H_2/CO mixtures was performed using the NUI 2010 mechanism. Through a two-zone engine model was found that an increment of the fresh unburned temperature was required for induce numerical auto-ignition. This methodology was required to fit numerical KOCA estimations with experimental values.

1.1.2. Multi-dimensional auto-ignition models. Multi-dimensional models have been proposed as auto-ignition occurrence is a spatial and time dependent combustion process. Multi-dimensional approaches can consider the fuel spray, turbulence, mixture formation, chemical kinetic and emissions formation, but they have the disadvantage of high computational cost. However, the work developed by Yavuz, Celik, and McMillian (2001) considers a detailed chemical kinetics mechanism for modeling multi-dimensional auto-ignition of natural gas. A detailed di-methyl ether chemistry with the methane sub-mechanism with 135 elementary reaction and 33 species was used. Two interesting points were examined in this research: the effect of initial unburned gas temperature on auto-ignition and the frequency of pressure fluctuations due to auto-ignition. Similar to the method used by Gersen et al. (2016) with a zero-dimensional model, the initial temperature was increased to promote fuel auto-ignition. The initial temperature was increased from 273 K to 350 K and 400 K, revealing the lack of accuracy of the mechanism used. The advantage of multi-dimensional auto-ignition simulation is the ability to replicate the characteristics auto-ignition frequency, which is close to 6 kHz. This research reported a characteristic frequency ranging from 5 to 14 kHz. It was observed that although knocking was detected, the accuracy with respect to the experimental auto-ignition timing was not evaluated.

The lack of accuracy of a single step reaction for auto-ignition timing estimation was evidenced in the work developed by Soylu and Van Gerpen (2003), who modeled Natural Gas auto-ignition by using KIVA 3V® code. The simplified combustion model used is a

single step oxidation model that converts fuel and oxygen to carbon dioxide and water. The pre-exponential factor of the reaction was used as tuning constant so that the deviation between the simulated and measured cylinder pressure trace is a minimum. Also the pre-exponential factor was arbitrarily multiplied by 100 after knock takes place so that the burning rate can be increased as the burning rate of auto-ignition. Deviation of the peak pressure of 20 % with respect to experimental pressure trace was observed by using natural gas as fuel and an equivalence ratio of 0.82. An interesting tool for improving the accuracy of zero-dimensional and multi-dimensional auto-ignition models was developed in this research. An integral model approach was obtained from experimental measurements and coupled to the zero and multi-dimensional engine models. Although KOCA predictions were accurate for the zero-dimensional model, the estimations with multi-dimensional model deviate with respect to experimental measurements.

Rostampour and Toosi (2015) implemented the methodology proposed by Soylu and Van Gerpen(2003) for improving the gasoline auto-ignition timing estimation in a multi-dimensional auto-ignition model. The integral model optimized for turbocharged conditions is calculated for all the cells of the grid. When the value of the integral model reaches 1, it is assumed that the cell ignites and the code starts to solve the main combustion reactions in that cell. The appearance of experimental pressure fluctuations and second flame front in the multi-dimensional auto-ignition model are used to identify the experimental and computational auto-ignition point respectively. Authors reported a deviation of 2 crank angle degrees between the experimental and estimated auto-ignition point. It was demonstrated that the modified KIVA-3V® code and the integral knock model can predict auto-ignition phenomenon accurately, although the knock fluctuations cannot be modeled with this approach.

Based on the ERC-PRF reduced mechanism compound of 132 elementary reactions and 47 species, Shao and Rutland (2014) used the integral model approach with a multi-dimensional auto-ignition model to predict gasoline auto-ignition timing. Multi-Dimensional-Integral model performance was compared with a new knock criterion based on chemical kinetics. The mole fraction of HO_2 was proposed as knock criterion for knock onset detection in the engine simulation. This research corroborates the assumption that

auto-ignition takes place when some auto-ignition initiator species achieve a critical concentration, previously established by Livengood and Wu in 1953. It is important to point out that the knock criterion was not validated with other chemical kinetics mechanism. Also, experimental auto-ignition timing were not reported and compared with the estimated auto-ignition timing.

A generalized research octane number (GRON) model was proposed by Wang et al. (2017) for predicting auto-ignition timing of gasoline with different octane numbers. The model consists of a reduced chemical mechanism that includes 21 elementary reactions and 22 species. The model was coupled with a multi-dimensional engine model to study the gasoline auto-ignition. The mechanism developed could predict normal combustion and knocking conditions similar than the experimental measurements for 100 and 90 PRF. These results show that auto-ignition hydrocarbon chemistry has been widely studied, which contrasts with the little knowledge on the auto-ignition chemistry of gaseous fuels such as Natural gas, Biogas, Syngas etc.

It was evidenced from literature, that auto-ignition simulation of gaseous fuels cannot be performed with accuracy by using single step, reduced or detailed chemical kinetic mechanisms. The auto-ignition studies of gaseous fuels have been focused in their knock resistance and MN measurements rather than auto-ignition timing prediction. Some examples of these researches are the work developed by Callahan et al. (1996) and Ryan, Callahan, and King, (1993) for natural gas. For hydrogen and gaseous Hydrocarbons fuels the work developed by Tanaka et al., (2016); for methane, hydrogen and carbon monoxide mixtures the work developed by Attar and Karim (2003) and Rodrigues and Shrestha (2006); for Producer gas the research developed by Arunachalam and Olsen (2012) and Wise (2007); for Propane Biogas mixtures the research developed by Montoya, Amell, and Olsen, (2016).

1.2. MOTIVATION

The production of alternative gaseous fuels from coal, biomass and different organic wastes has gained importance due to the increase of the natural gas price, to the desire of less dependency on fossil fuels, and to the priority of reducing greenhouse gasses emissions. Colombia has about 6700 million of tons of coal, the biggest reserve of South America. Also, it is estimated that in agri-chain around 40 % of biomass is left in the forest, and the remaining 40 % is leaved in the sawmill industry as chips, bark and sawdust. Residual biomass of sawdust, rice and coffee are abundant due to the extensive agricultural exploitation of rice and coffee (Vélez, et al., 2009). For these reasons, the alternative fuels production and its use as fuel in ICE for power generation has great relevance and national interest.

Table 1-1 shows three commercial gas engines and the service MN of some reference fuels. The engines considered are the Detroit Diesel S50GTK gas engine (SOUTHERN CALIFORNIA GAS COMPANY, 2009), the John Deere 6081HFN04 gas engine (McCaw, 2006) and the Cummins QSV91 gas engine. The service MN of the alternative fuels were measured experimentally and the service MN of the natural gas were estimated by means of AVL ® software. When these commercial gas engines are fueled with low MN gaseous fuels, the undesired auto-ignition of the fuel appears. For example, if the Cummins QSV91 gas engine is fueled with gas from coal gasification, the auto-ignition of the fuel will cause damages to the engine. If this fuel is used for John Deere and Detroit Diesel engines, auto-ignition will appear as well. To decrease the MN Required (MNR) of the engine, it is necessary to modify the nominal engine operating conditions. These modifications involve change in the engine efficiency and output power that must be studied.

For engine design and engine efficiency improvement, the use of accurate models for predicting fuel auto-ignition is important. ICE model has been calibrated for studying engine performance under normal combustion; however when abnormal combustion appears, engine model cannot predict this phenomenon.

Table 1-2. Comparative between service MN of gaseous fuels and MNR of commercial gas engines

References	*Fuel*	*MN*	*MNR=75*		*MNR=52*
			Detroit Diesel S50G TK engine. Output Power: 186-208 kW	***John Deere 6081HFN04 gas engine. Output power:186-208 kW***	***Cummins QSV91 gas engine. Output power: 1540 kW***
Malenshek and Olsen (2009)	Reformed NG	62.4	A	A	
	Coal Gas	30.0	A	A	A
	Wood Gas	61.5	A	A	
	Digester Gas	139.1			
	Land fill Gas	139.6			
UPME (2014)	NG Ariana *	97.2			
	NG Guepaje*	95.5			
	NG Ballena*	98.2			
	NG Creciente*	95.7			
	NG Cusiana*	67.5	A	A	

Nomenclature. A: fuel auto-ignite. NG : Natural Gas

*** The name that appears, correspond to the gas production fields's name.**

Because the auto-ignition is a thermochemical phenomenon, detailed chemical kinetics mechanisms must be used, which are the main source of the lack of accuracy of the zero and multi-dimensional models. The relationships between ignition delay time (τ), fuel auto-ignition, engine operating conditions and their kinetic implications are difficult to study experimentally. The use of computational tools and experimental measurements are required for improving the understanding of auto-ignition phenomenon of alternative gaseous fuels.

1.3. STATEMENT OF THE PROBLEM

The use of alternative gaseous fuels with different MN in ICE has two problems: a) the removal of solid impurities from the thermochemical process that produces the fuel (Vargas, 2012), and b) the high auto-ignition tendency of these fuels, which decreases the efficiency and causes severe damage to the engine. Auto-ignition is an abnormal combustion phenomenon caused by the increment in the concentration of intermediate

species such as HO_2, H_2O_2, H, OH, O during compression stage in the engine (Hernandez et al., 2006). The production of these species depends both on unburned gas pressure and temperature (therefore, of the engine operating conditions) and on the MN of the fuel. The lower MN is, the higher auto-ignition tendency is (Leiker et al., 1972). According to measurements done by Malenshek and Olsen (2009) the MN of alternative gaseous fuels (syngas, producer gas) can change from 25 to 60 depending on the fuel composition. Moliere (2002) mentions that in the coal gasification process, hydrogen percentage can vary between 5 and 50% in the syngas, which modifies the MN of the fuel produced (Cavaliere, 2010). The variability of the MN of these fuels and their high auto-ignition tendency require that the auto-ignition prediction must be considered in ICE models.

Because the auto-ignition is a thermochemical phenomenon, the detailed chemical kinetics mechanisms play an important role on the auto-ignition modeling process. However, the use of chemical kinetics mechanisms is limited by their lack of accuracy for modeling low temperature oxidation of gaseous fuels. These lack of accuracy were examined by Petersen (2007) who estimated the ignition delay time of $CO/CO_2/H_2$ mixtures by using five kinetics models. A similar trend was observed when three new kinetics models were evaluated in this thesis. The kinetics models were: the Marinov model (Marinov et al., 1998), the Gri-Mech 3.0 model (Smith et al.,1999), and the AramcoMech model (Metcalfe et al.,2013). Figure 1-2 shows the strong deviations between the ignition delay times estimated and the experimental ignition delay times for temperatures ranging from 600 K to 900 K. The lack of accuracy observed is similar to that observed by Petersen (2007) for the same reference mixtures. *Based on the analysis performed previously is concluded that chemical kinetics mechanisms developed so far cannot predict with accuracy ignition delay times of gaseous fuels at low temperature; therefore, the detailed kinetics models coupled with ICE models are not suitable for estimating auto-ignition points (KOCA) with accuracy.* This demonstrates that auto-ignition chemistry is more complex than flame chemistry (Williams and Li, 2000).

Some authors have established methods for improving auto-ignition point predictions. Increasing the Nitric Oxide (NO) concentration in the residual gases, increasing the unburned gas temperature at IVC timing and coupling integral models to zero and multi-

dimensional engine models are some techniques used for this purpose. However, an accurate auto-ignition model must be able to predict KOCA and knock intensity with accuracy without adjusting fuel-air mixture properties and residual gas composition (Gersen et al., 2016). These approaches do not represent actual measurements in the engine and are used to compensate the lack of accuracy of the kinetics models. The efforts must be focused on the study of ignition delay time and auto-ignition chemistry for developing accurate two- zone and multi-dimensional auto-ignition models. In this regard, Cavaliere et al.(2010) proposed an enhanced San Diego chemical kinetic model for ignition delay times estimations of $H_2/CO_2/CO/O_2/N_2$ mixtures. Through a sensitivity analysis was demonstrated that the chain branching reaction $2OH(+M)=H_2O_2(+M)$ and the chain propagating reaction $H+H_2O_2=HO_2+H_2$ are dominant in the prediction of ignition delay times.

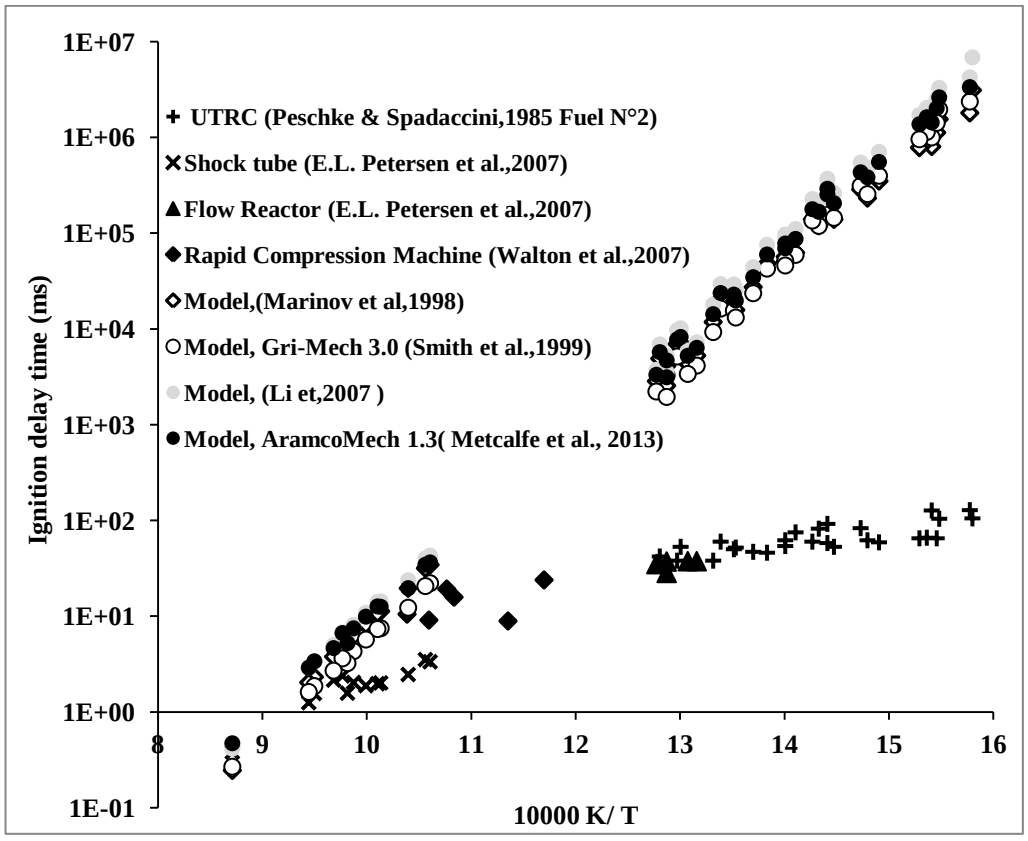

Figure 1-2 Ignition delay time obtained experimentally and predicted by different mechanism reported in the technical literature. UCI flow reactor data were normalized P^{-1} to compare with the new shock tube and UTRC data (Petersen et al., 2007). Fuel: mixtures of $CO/CO_2/H_2$. Fuel N°2: 38.6%H_2 /10.3%CO_2 /51.1% CO.

Improvement in the predictions was obtained by splitting these reactions in forward and backward reactions. The rate constants of these reactions were modified for improving the accuracy of the kinetic model. Although this thesis used a chemical kinetics model different from those used by Petersen et al. (2007), similar results were observed. Figure 1-3 shows the improvements achieved with this modification over a wide range of temperature. In this thesis, this modification is called Modification III; the other alternatives were tested and are examined in detail in Chapter 2.

According to the literature reviewed, the performance of the modified kinetic model for modeling auto-ignition of gaseous fuels in ICE has not been examined yet. *The strong relationship between ignition delay time and auto-ignition previously studied by Livengood and Wu in 1955 lead to the following research question: Can a detailed chemical kinetic model optimized for low temperature ignition delay time estimations improves the accuracy of a two-zone auto-ignition model for predicting auto-ignition points of gaseous fuels in an ICE?*

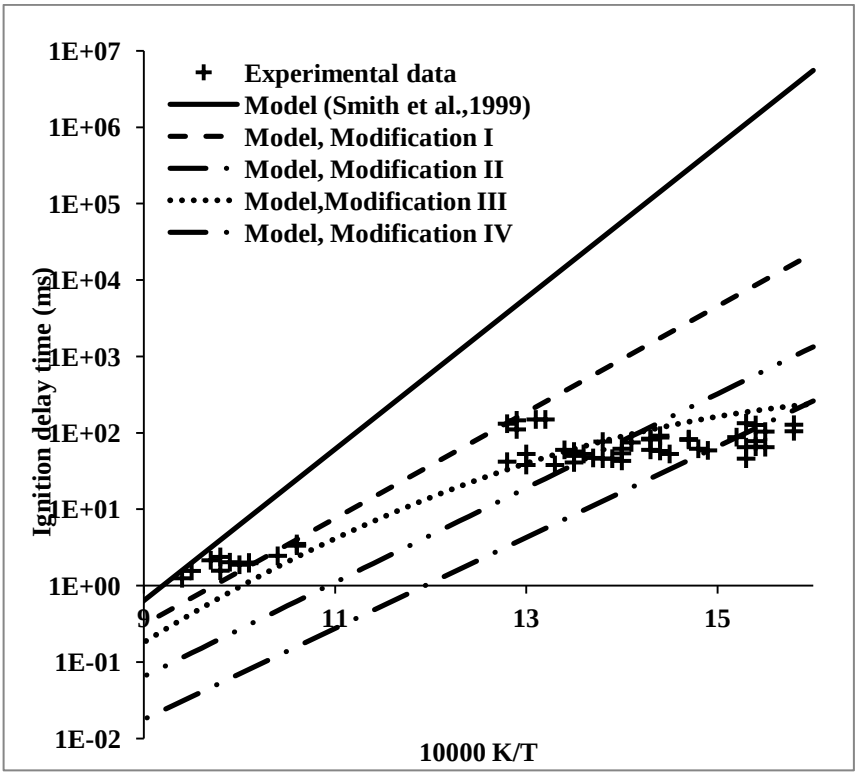

Figure 1-3 Comparative of the improvement of accuracy obtained with modifications I, II, III and IV. The estimations are based on GrimMech 3.0 kinetic model.

The modifications of the rate constants of the key elementary reactions influence the KOCA values; therefore the kinetic mechanism can be adjusted for fitting numerical with experimental KOCA. Accurate unburned gas temperature and residual gas fraction must be estimated to reduce the uncertainties in the KOCA predictions. This is accomplished by estimating actual IVC and residual gas temperature in the engine cylinder. *The previous approaches correspond to the research hypothesis of this thesis.*

1.4. OBJECTIVE AND SCOPE OF THE THESIS

The main objective of this thesis is to *develop a model to predict the auto-ignition in a spark ignition internal combustion engine fueled with gaseous fuels with variable MN.* The specific objectives that must be accomplished are:

- ✓ To determine computationally the impact of the main elementary reactions and intermediate chemical species of a detailed chemical kinetic mechanism on ignition delay time and auto-ignition in a spark ignition internal combustion engine.
- ✓ To measure the MN of the reference fuels and the cycle by cycle Knock Occurrence Crank Angle (KOCA) at different engine operating conditions.
- ✓ To validate experimentally the model developed under different engine operating conditions.

The scopes of this thesis are described as follow:

The conclusions derived from the experiments developed in this thesis apply for stationary gas engines due to output power was considered constant during the tests. Output power of the engine is a critical factor that influences significantly KOCA. Its interaction and effect were omitted because of the technical restrictions of the MN measurement methodology and CFR engine configuration.

Commercial engines have defined a spark timing, which gives maximum brake torque (MBT), brake power and minimum brake specific fuel consumption at a fixed speed, gas composition and flow rate (Heywood, 1988). The performance of new engine designs, alternative fuels and their emissions are evaluated by using MBT timing as reference engine operating conditions. However, for evaluating the relationship between engine operating conditions, combustion parameters and auto-ignition, the ignition timing must be changed depending on the design of experiment used. The levels of ignition timing are chosen in order to facilitate the reading of KOCA from the in-cylinder pressure trace. For these reasons MBT is not used as reference engine operating condition.

The fuels tested are mixtures of $CO/CO_2/H_2/CH_4$. These species were selected due to the following reasons: 1) some of them are the main components of alternative gaseous fuels such as syngas, biogas and producer gas, etc; 2) there are few experimental data of ignition delay time of gaseous fuels at low temperature reported in the literature. These data were reported for mixtures of $CO/CO_2/H_2$ by Peschke and Spadaccini in 1985 and for natural gas by de Vries in 2005. The KOCA values measured for these fuels are strongly related with these experimental data and thermodynamic conditions of the air fuel mixture in the engine.

Levels of emissions of NOx (nitric oxide, NO, and nitrogen dioxide, NO_2), carbon monoxide, unburned hydrocarbons (HC) and particulates were not measured because of the unavailability of the apparatus required.

Although auto-ignition is a multi-dimensional combustion phenomenon, this thesis considers a two-zone auto-ignition model. The use of multi-dimensional models requires high computational capacity to solve hundreds or thousands of differential equations that describe the low temperature oxidation process in the engine. These equations must be solved into each cell of the grid defined previously. Considering that this capacity is limited, single step or reduced chemical kinetics mechanisms must be used. Because the auto-ignition chemistry has been not fully understood, single step or reduced kinetic models are not able to explain auto-ignition phenomenon with accuracy. Two- zones auto-ignition model is a good alternative for studying auto-ignition by using detailed chemical kinetics mechanism coupled with a two-zone engine model. This approach is suitable due to auto-

ignition is assumed to be a time dependent phenomenon where the spatial components are not considered.

1.5. THESIS ORGANIZATION AND METHODOLOGY

In this section a description of the thesis organization and the methodology employed for accomplishing the objectives were carried out. Figure 1-4 shows in detail the relationship between the methodology and the six Chapters of the thesis. The background, the motivation, the statement of the problem and the objectives of this research were described in ***Chapter 1***. Also, this section described the scopes of the research and the thesis organization for a better understanding of the document.

An analysis of the performance of 4 detailed chemical kinetics mechanisms for estimating low temperature ignition delay times of mixtures of $CO/CO_2/H_2$ and CH_4/H_2 was described in ***Chapter 2***. Modifications reported in the literature for improving ignition delay times estimations were evaluated by considering its effects on the laminar flame speed and the Rate of Production (ROP) estimations of key radical species. The numerical estimations were carried out by using the AURORA and PREMIX codes of Chemkin Pro ® software.

A comprehensive analysis for improving the understanding of auto-ignition phenomenon of fuels with variable MN in spark ignited ICE was carried out in ***Chapter 3***. An Analysis of Variance (ANOVA) for evaluating the effect of the Individual Knock Intensity (Ki) on KOCA at different engine operating conditions was performed in this chapter. For MN measurements of $CO/CO_2/H_2$ mixtures a CFR engine was employed by using a method analogous to the standard method for octane number measurements. The KOCA at standard engine operating conditions was estimated by using the methodology developed by Checkel and Dale (1986). A correlation between MN, KOCA, engine operating conditions and combustion parameters was determined. For comparative purposes, both test fuel ($CO/CO_2/H_2$ mixtures) and reference fuels (CH_4/H_2 mixtures) were employed.

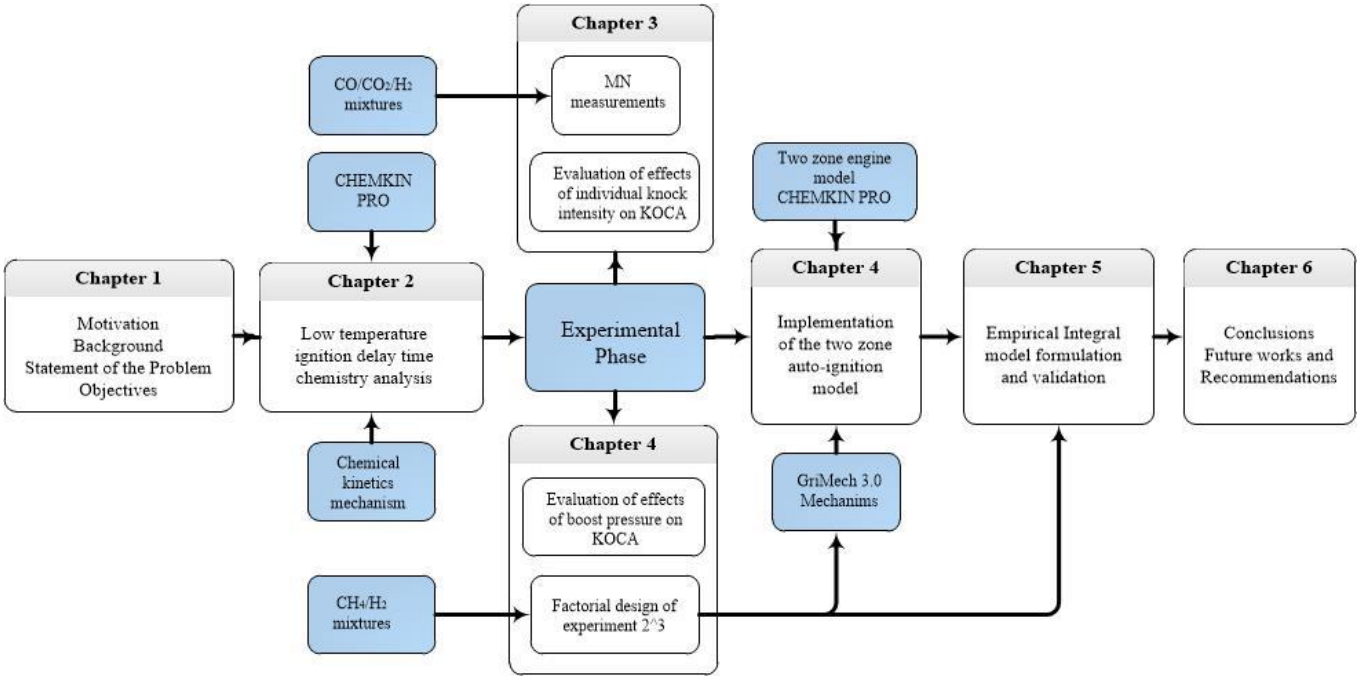

Figure 1-4 Thesis organization and methodology employed

Chapter 4 describes the two-zone auto-ignition model and the second stage of the experimental work carried out in this thesis. The observations done in Chapter 3 about the correlations of MN and engine operating conditions were evaluated by means of two designs of experiments. The former was a factorial design of experiment with axial and central runs performed in order to determine the effects of MN, Equivalence ratio (Ø) and Ignition timing (IT) on KOCA; the latter was an analysis of variance developed to examine the influence of boost pressure on KOCA.

In another hand, the two-zone engine model coupled with the Gri-Mech 3.0 mechanism was used for modeling auto-ignition of CH_4/H_2 mixtures at different engine operating conditions. The reference mechanism used was selected after an exhaustive performance analysis of several kinetics models carried out in Chapter 2. Numerical estimations were developed by using the adiabatic Closed Internal Combustion Engine Simulator of Chemkin Pro ® software.

A methodology for determining the start of combustion (SOC), the end of combustion (EOC) and the ignition delay period (ID) was described in this chapter. A set of equations

were developed for estimating IVC temperature, residual gas temperature and residual gas fraction. Moreover, an analysis was developed in order to estimate the polytropic coefficient of the compression and expansion process in the engine cycle. The combustion analysis ends with a heat release analysis carried out for evaluating the relationship between Maximum Heat Release Rate (MHRR) and KOCA for CH_4/H_2 mixtures. Analytic equations to estimate the unburned air fuel mixture temperature were proposed, based on the thermodynamic analysis.

Chapter 5 describes a method to find KOCA by using the integral model approach. A modified version of the integral model approach was used based on the Integral Mean Value Theorem. This version was developed by using a two stages optimization tecnique. The former was implemented to find the constants of the Arrhenious equation that belong to the integral model approach; the latter was used to find two thermodynamic parameters that describe the temperature and pressure path of the end gas prior to auto-ignition. These parameters were called in this thesis as the *characteristic temperature and pressure*. For the model formulation the cycle by cycle pressure trace and KOCA determined in Chapter 4 and the model to estimate the end gas temperature were required. The thermodynamic model for end gas temperature estimations is based on the ideal gas assumption and the compression polytropic coefficients determined in Chapter 4.

Finally, the conclusions, future works and recommendations are drawn in **Chapter 6**. Additional information can be found in the Appendices. Appendix A describes the standard operating procedure used for calibrating the flowmeters of the species used in the experiments. Appendix B examines the equations used to estimate the MN uncertainty based on the uncertainty of the flowmeters and the uncertainty caused by calibration of the flowmeters. Appendix C shows the computational tools developed for determining cycle by cycle KOCA, mass fraction burned (MFB) and the heat release curves. These codes implemented in Visual Basic for Applications of Excel® were developed to reduce the time for analyzing the data. The Matlab codes used in Chapter 5 are described in Appendix D and the methodology employed for estimating the standard uncertainty from experimental data is described in Appendix E.

Chapter 2

Low temperature ignition delay time and unstretched laminar flame speed of CH_4/H_2 and $CO/CO_2/H_2$ mixtures. Kinetic implications

2.1 INTRODUCTION

The combustion parameter linked with auto-ignition phenomenon in ICE is the ignition delay time τ, defined as the time that spends a fuel blend to self-ignite to a specified temperature and pressure (Livengood and Wu, 1955). According to the technical literature reviewed, this parameter has been measured by using different fuel compositions at medium and high temperatures (Lifshitz et al, 1971; Kalitan, 2007). However, the auto-ignition phenomenon within the combustion chamber takes place at low temperature (600-900K) where gaseous fuels oxidation has been little studied. For this reason detailed kinetic models cannot be used for modeling auto-ignition of gaseous fuels in ICE.

The objective of this Chapter is to evaluate numerically the performance of different modified chemical kinetic mechanisms for predicting the low temperature ignition delay time of $CO/CO_2/H_2$ and CH_4/H_2 mixtures. Also the effects of these modifications on the laminar flame speed and net production rate of critical intermediate species are examined.

2.2. NUMERICAL METHODOLOGY

2.2.1. Ignition delay time. In the literature the definition of computational or experimental ignition delay time varies depending on the author's criterion. In this Chapter the definition adopted by Hernandez et al. (2006) was used. This definition establishes that ignition delay time of any fuel is the time where temperature in the reactor reaches the initial temperature plus 400 ºC or K. The experimental data used as reference were measured by using different reactors such as: shock tube reactors (Petersen et al., 2007), flow reactor (Peschke and Spadaccini, 1985) and rapid compression machine (Walton,2007). According to some preliminary computational measurements, the ignition delay time of a gaseous fuel depends on the fuel composition and the initial temperature and pressure without regarding the reactor model used. Based on the foregoing, a Close Homogeneous Reactor model is considered. This model is assumed to be adiabatic, nearly spatially uniform due to high diffusion rates or forced turbulent mixing. It means that the rate of conversion of reactant to products is controlled by chemical reaction rates and not by mixing processes. In addition, is assumed that surface reactions do not take place (Reaction Design, 2013).

2.2.2. Laminar flame speed model. The flame speed model involves 1-D freely propagating unconstrained flame, wherein the point of reference where equations are solved is a fixed point on the flame. This configuration is used to determine the characteristic flame speed of a gas mixture at different pressures and inlet temperatures. The governing equations of energy, species, continuity, and state are solved by using PREMIX code of Chemkin Pro® software. According to the calculations of Kerommnes et

al., (2013) the thermal diffusions effects decrease by up to 8% for stoichiometric mixtures and 4% at ∅=2,5 the laminar flame speed of syngas and Hydrogen. Based on the foregoing, and the high concentration of hydrogen of the fuels studied, the thermal diffusion effects are considered. The transport properties are calculated by considering multicomponent option, and the initial temperature profile is estimated by using Equation 2-1 (Grupo de Ciencia y Tecnologia del Gas y Uso Racional de Energia [GASURE], 2011).

$$T = T_u + \frac{T_{ad} - T_u}{1 + exp\left[K\left(\frac{\delta}{2} - x\right)\right]} \qquad \text{Eq. 2-1}$$

The adiabatic flame temperature of each test fuel was previously determined by using EQUIL, a sub-routine of Chemkin Pro®. The constant K was fixed to 184.21 and the flame thickness was assumed to be 0.1 cm as initial approach. To guarantee convergence in the solution, the Chemkin Pro® convergence parameters were adjusted so that at least 1500 and 2000 grid points were used. To validate the results, the adiabatic flame temperature determined with EQUIL, was compared with the maximum products temperature in the simulations. If the temperature differences between these two values are less than 20 K, it was considered that an accurate result was obtained.

2.2.3. Chemical kinetic mechanisms. Since sixties, hundreds chemical kinetic mechanisms has been developed to model methane and hydrogen combustion in a wide range of temperatures (da Silva and Junior, 2011). Later, in the early years of the eighty it was proposed the first detailed mechanisms to model C_1 and C_2 hydrocarbons combustion (Westbrook and Pitz, 1990). A methodology to develop comprehensive kinetic mechanisms for modeling combustion of gaseous fuels was proposed by Frenklach et al.(1992). This methodology was used by Smith et al.(1999) and Hughes et al. (2001) to develop the well-known chemical kinetic mechanisms: Gri-Mech 3.0 and Leeds. From these kinetic models, hundred mechanisms have been developed for modeling natural gas and syngas combustion. These mechanisms have been optimized with experimental data at

temperature starting from 850 K as shown in Table 2-1. As previously mentioned, Petersen et al. (2007) examined the accuracy of the first five mechanisms reported in Table 2-1 for estimating low temperature ignition delay times of $CO/CO_2/H_2$ mixtures. However, to get more robust conclusions, three additional mechanisms were examined in this Chapter: Gri-Mech. 3.0 (Smith et al., 1999), the Marinov mechanism (Marinov et al., 1998) and Aramco Mech. 1.3 mechanism (Metcalfe, Burke, Ahmed, and Curran, 2013).

2.2. EXPERIMENTAL DATA FROM LITERATURE

The experimental ignition delay time data of $CO/CO_2/H_2$ mixtures plotted in Figure 2-1 were measured from different reactors, compositions, and initial temperature and pressure. Peschke and Spadaccini (1985) used a Flow Reactor for determining the ignition delay times of five fuels with different hydrogen, carbon monoxide and carbon dioxide concentrations. The data collected in this research have been used for studying the syngas oxidation at low temperature. The fuel Nº 2 from this research (38.6% H_2, 10.3%CO_2 and 51.1%CO) was selected as reference mixture. Later, ignition delay times of this mixture was measured by Petersen et al. (2007) by using a shock tube reactor at 20 atm and Ø=0.5. The results obtained were similar to those obtained by Peschke and Spadaccini in 1985. In the same research, ignition delay time of a fuel blend of 50% H_2 and 50% CO were measured with a flow reactor at 5 atm, and low temperature range. Finally, Walton et al.(2007) determined the ignition delay of a set of lean H_2/CO mixtures at 880-930 K by using a rapid compression machine at 10 atm. Actual initial pressure and equivalence ratio were considered in the simulations. Trend line was not considered to verify the variability and the actual trend of the estimations as shown in Figure 2-1.

Ignition delay time measurements of CH_4, C_2H_6, C_3H_8, C_4H_{10}, and C_5H_{12} mixtures were carried out in a high-pressure shock tube reactor by de Vries (2005).

Table 2-1 Summary of the most important chemical kinetic mechanisms developed to date for modeling etanol, natural gas and syngas combustion

Name	Nº elementary reactions	Nº species	T (K)	P	Observations	References
RAMEC Mechanism	190	38	1040-1500	40-260 atm	Based on the GRI-Mech. 1.2 mechanism, with additional important reactions in methane oxidation at lower temperature	(Petersen, Davidson, and Hanson, 1999)
Davis Mechanism	30	14	880-2625	1-64 atm	Allows to model combustion of fuel blends of Hydrogen, Carbon monoxide, Water, Nitrogen and Argon.	(Davis, Joshi, Wang, and Egolfopoulos, 2005)
San Diego Mechanism	235	46	Above 1000	Below 100 bar		(Saxena, 2007)
Sun Mechanism	33	16	Above 900	Below 40 atm	Allows to model laminar flame speed, counter-flow ignition temperatures and species reaction profiles	(Sun, Yang, Jomaas, and Law, 2007)
Li Mechanism	84	18	850-950	1.5-6 bares	It was optimized to model natural gas and syngas oxidations.	(Li et al., 2007)
Gri-Mech. 3.0 Mechanism	325	53	1000-2500	10 Torr-10 atm	It is an optimized mechanism used to model the combustion of natural gas (Methane), including the NO formation.	(Smith et al., 1999)
Marinov Mechanism	383	57	Above 1250	0.8- 2.2 atm	Developed to model ethanol oxidation	(Marinov,1999)
Aramco Mechanism	1543	253	1050-2500	1-260 atm	Developed to model oxidation of C_1-C_2 base hydrocarbons in a wide range of pressure and temperature	(Metalcafe, 2013)

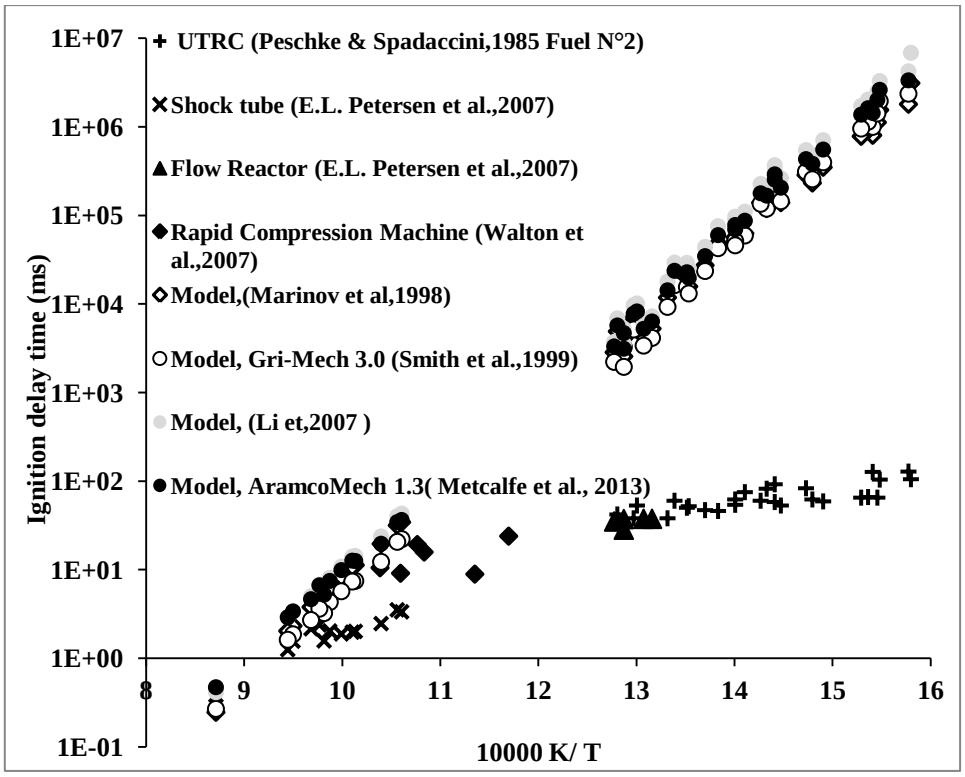

Figure 2-1 Ignition delay times obtained experimentally and predicted by using different mechanisms reported in the technical literature. UCI flow reactor data were normalized P^{-1} to compare with the new shock tube and UTRC data (Petersen et al., 2007).

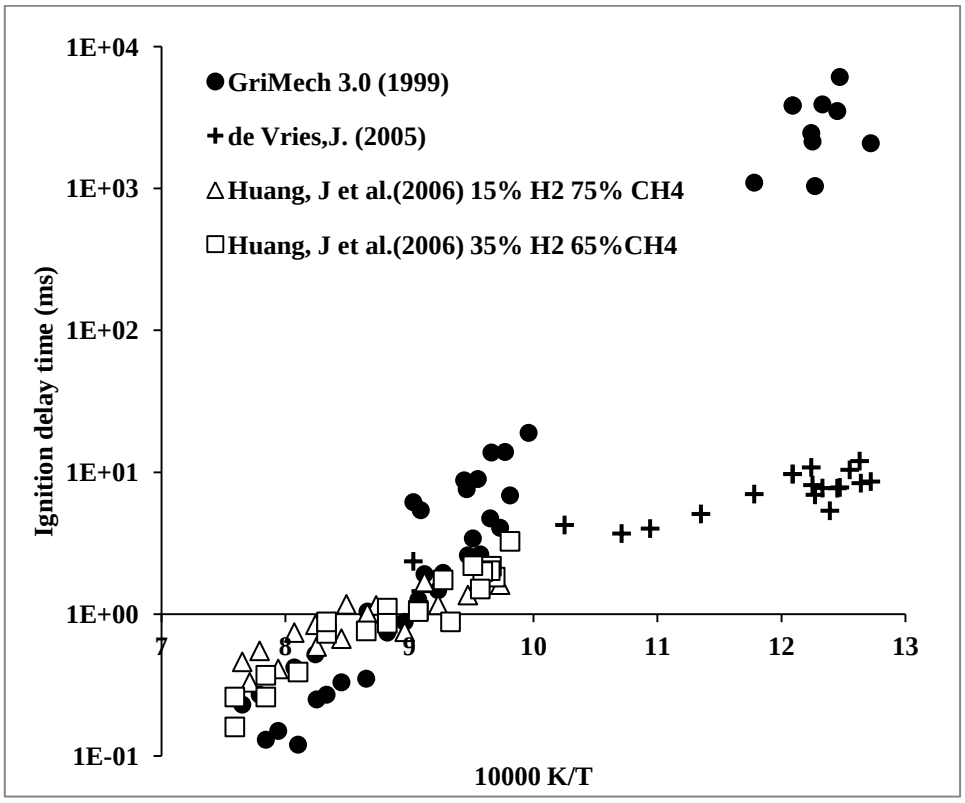

Figure 2-2 Ignition delay times of NG and CH_4/H_2 mixtures obtained experimentally and predicted by using Gri-Mech. 3.0 mechanism

These data were taken at intermediate temperature and pressure ranging from 8 to 20 atm. Additional data from the research developed by Huang et al. (2006) were considered who measured the ignition delay times of two stoichiometric methane/hydrogen/air mixtures in a shock tube facility at pressure ranging from 16 to 40 atm and temperature ranging from 1000 to 1300 K. The former composition used is 15% H_2 and 75% CH_4 and the latter is 35% H_2 with 65% CH_4. Figure 2-2 shows the experimental data reported and the estimations done by using a Close Homogeneous Reactor model coupled with Gri-Mech. 3.0 mechanism. It is observed that natural gas (NG) estimations deviate from the experimental data at low temperature even though an optimized mechanism for natural gas combustion modeling is used. This trend is similar to the trend observed in Figure 2-1 for $CO/CO_2/H_2$ mixtures. This interesting result reveals that auto-ignition chemistry at low temperature is complex and it is not dependent on the high molecular hydrogen concentration in the fuels.

2.3. SENSITIVITY ANALYSIS FOR CH_4/H_2 AND $CO/CO_2/H_2$ IGNITION DELAY TIME

A sensitivity analysis for highlighting the dominant elementary reactions that influence the ignition delay time chemistry of CH_4/H_2 and $CO/CO_2/H_2$ mixtures was carried out in this section. The analysis was performed by considering pressure ranging between 15 and 25 bar and temperature ranging between 750K and 770K. The normalized sensitivity coefficient was calculated with Equation 2-2 (Kéromnes et al., 2013):

$$\sigma = \frac{ln\left(\frac{\tau'}{\tau}\right)}{ln\left(\frac{2,0}{0,5}\right)} \qquad \text{Eq. 2-2}$$

where τ and τ' are the calculated ignition delay time with the elementary reaction acentric coefficient increased and decreased a factor of two respectively. This analysis was performed by assuming an adiabatic close homogeneous reactor model and Gri-Mech 3.0 as the reference mechanism. Figure 2-3 shows the sensitivity analysis developed for $CO/CO_2/H_2$, CH_4/H_2 and CH_4/air mixtures.

For evaluating the low temperature chemistry of $CO/CO_2/H_2$ ignition a fuel blend of 51.1%CO/ 10.3%CO_2/ 38.6% H_2 was considered at Ø=0.59, 769 K, and 14.5 atm. The initial conditions and the composition correspond to the actual conditions used by Peschke and Spadaccini in 1985. The chemistry is based on the generation of reactive radical species from hydroperoxyl radical (HO_2). From a pool of HO_2 radicals H_2O_2 species is produced through the chain propagating reaction $2HO_2 \Leftrightarrow O_2+H_2O$. Later, the chain branching reaction $2OH(+M) \Leftrightarrow H_2O_2(+M)$ consumes H_2O_2 and releases OH radicals. Because the high concentration of carbon monoxide in the test fuel, the chain propagating reaction $CO+HO_2 \Leftrightarrow CO_2+OH$ plays an important role in the ignition; however it has been demonstrated that this reaction is not sensitive to the temperature (Chaos and Dryer, 2007).

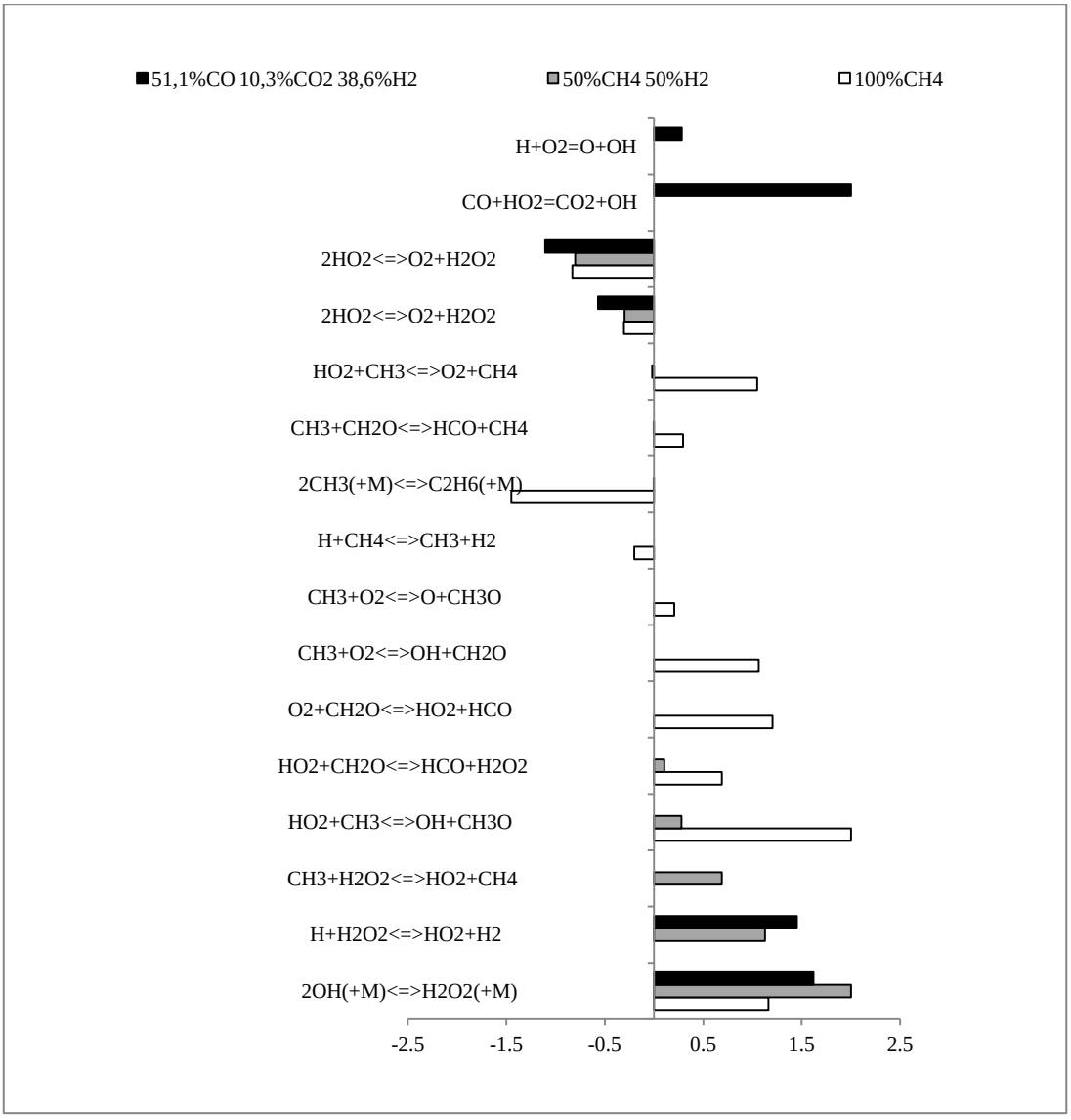

Figure 2-3 Sensitivity analysis for ignition delay times of CH_4 /air , CH_4/H_2 and / $H_2/CO/CO_2$ mixtures

The low temperature chemistry of CH_4/H_2 mixtures is governed by the hydrogen sub-mechanism. According to the sensitivity analysis, the production of the reactive radical OH follows the same path described for the $CO/CO_2/H_2$ ignition chemistry. However, additional H_2O_2 is produced through the reaction $2HO_2 \Leftrightarrow O_2+H_2O_2$, which is not sensitive for the $CO/CO_2/H_2$ ignition chemistry. Because the concentration of methane in the mixture, the chain propagating reaction $CH_3+H_2O_2 \Leftrightarrow HO_2+CH_4$ plays an important role for producing H_2O_2 later used by the reaction $2OH(+M) \Leftrightarrow H_2O_2(+M)$ to release OH. The sensitivity analysis was developed by considering a stoichiometric mixture of 50%H_2 50%CH_4 at 750 K and 25 bar.

In another hand, the radical OH and HO_2 are two of the most important active radicals for methane oxidation according to the sensitivity analysis developed. The radical OH is formed mainly through the chain branching reactions $HO_2+CH_3 \Leftrightarrow OH+CH_3O$, $2OH(+M) \Leftrightarrow H_2O_2(+M)$, and the chain propagating reaction $CH_3+O_2 \Leftrightarrow OH+CH_2O$. The radical HO_2 is formed through the reaction $O_2+CH_2O \Leftrightarrow HO_2+HCO$ and the chain initiation reaction $HO_2+CH_3 \Leftrightarrow O_2+CH_4$. Later, HO2 radical reacts with methyl (CH_3) to form methoxy (CH_3O) radical and hydroxyl (OH) through reaction $HO_2+CH_3 \Leftrightarrow OH+CH_3O$. The chain terminating reaction $2CH_3(+M) \Leftrightarrow C_2H_6(+M)$ is an important reaction; however is an ignition inhibiting reaction because consumes CH_3 radicals that could be used by reaction $HO_2+CH_3 \Leftrightarrow OH+CH_3O$ to release OH radicals . For this analysis, a stoichiometric CH_4/ air mixture was evaluated at 750 K and 25 bar.

The sensitivity analysis reveals that the elementary reactions that explain the ignition of the CH_4/air mixtures are not the same that explain the ignition of CH_4/H_2 and $CO/CO_2/H_2$ mixtures. When CH_4 is mixed with H_2 the reactions are almost the same that the reactions of $CO/CO_2/H_2$ mixtures. This means that the ignition chemistry of these mixtures is dominated by the H_2 sub-mechanism.

2.4. ATTEMPTS TO IMPROVE THE LOW TEMPERATURE IGNITION DELAY TIME ESTIMATIONS FOR $CO/CO_2/H_2$ AND H_2/CH_4 MIXTURES

It is relevant to present in this section a brief discussion about the different hypothesis that have been presented to explain the poor accuracy of the kinetic models developed

to date. From the literature reviewed, three approaches have been proposed and are evaluated in this chapter: gradient pressure effect, constant equilibrium modifications and catalytic effects.

2.4.1. Pressure history. The thermodynamic state of the air fuel mixture, located behind of the reflected wave in a shock tube reactor was taken into account by Lieuwen et al. (2009) and Pang et al. (2009). They considered the non-uniformity of pressure and temperature within the reactor. According to the observations carried out by Reehal et al. (2007), the pressure and temperature gradient varies with respect to the time. Some authors affirm that these non-idealities are caused by the incident shock attenuation, boundary layer growth and boundary layer interactions (Lieuwen et al. 2007). Taking into account the above, the assumption that the shock tube reactor can be modeled as a constant volume reactor with constant internal energy is not suitable. In this chapter, a simplified version of the recommendations done by Lieuwen et al., (2009) was considered. A pressure gradient was included as input data in the close homogeneous reactor model. The pressure profile in the reactor model has the form $P = \alpha * t$ where α is the gradient pressure and t is the time that spend the air fuel mixture to self-ignite. It was observed that ignition delay times by considering shock tube and constant volume reactor models have similar results. The gradient pressure considered are 0.55 atm/ms and 1 atm/ms. These values were chosen because the estimations agree with the experimental data available as shown in Figure 2-4. The improvement of the predicted ignition delay time by using the mechanism developed by Li et al. (2007) is evident. In the same way, it is possible to verify the discrepancy with respect to the experimental data when a constant volume reactor is considered.

To evaluate the kinetic implications a sensitivity analysis was performed for ignition delay time estimations of $CO/CO_2/H_2$ mixtures. The results are compared with the ignition delay time estimated by considering the assumption of ideal constant pressure as shown in Figure 2-5. The gradient pressure enhances the production and the subsequent consumption of the radical HO_2 as illustrated in Figure 2-6a.

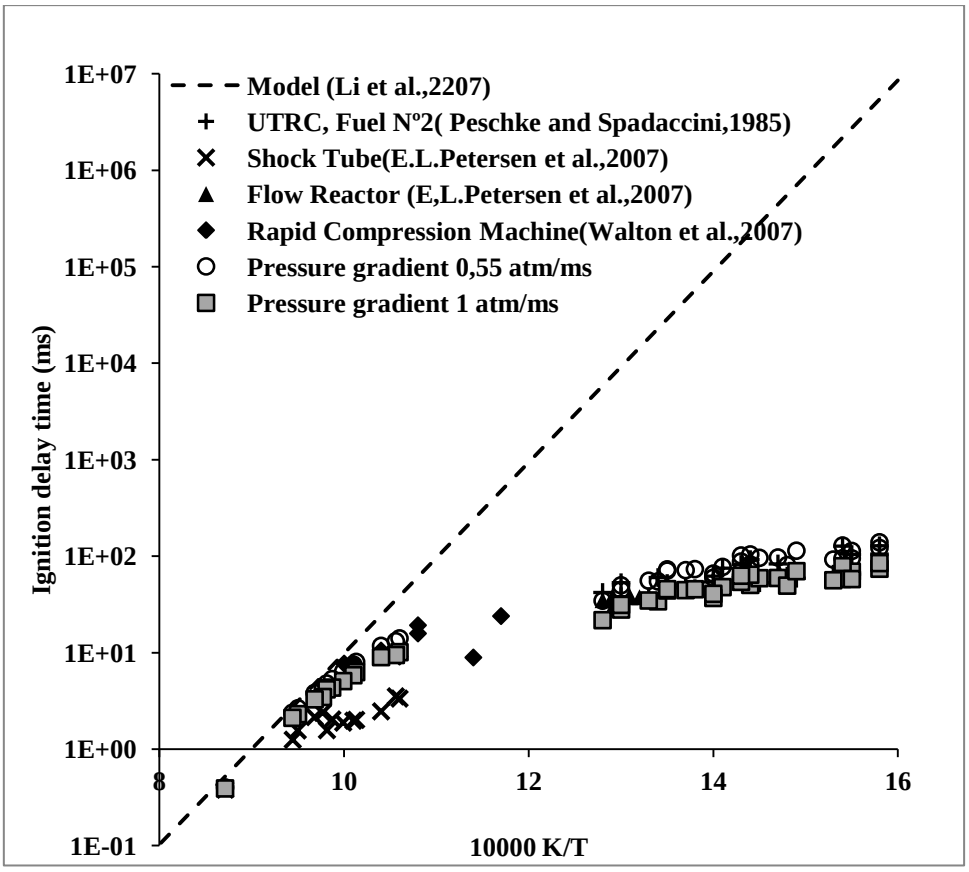

Figure 2-4 Comparative between the ignition delay times obtained experimentally and the estimated by using the kinetic model developed by Li et al. (2007). The pressure gradient considered are 0.55 atm/ms and 1 atm / ms. Solid line: model (Li et al.,2007)

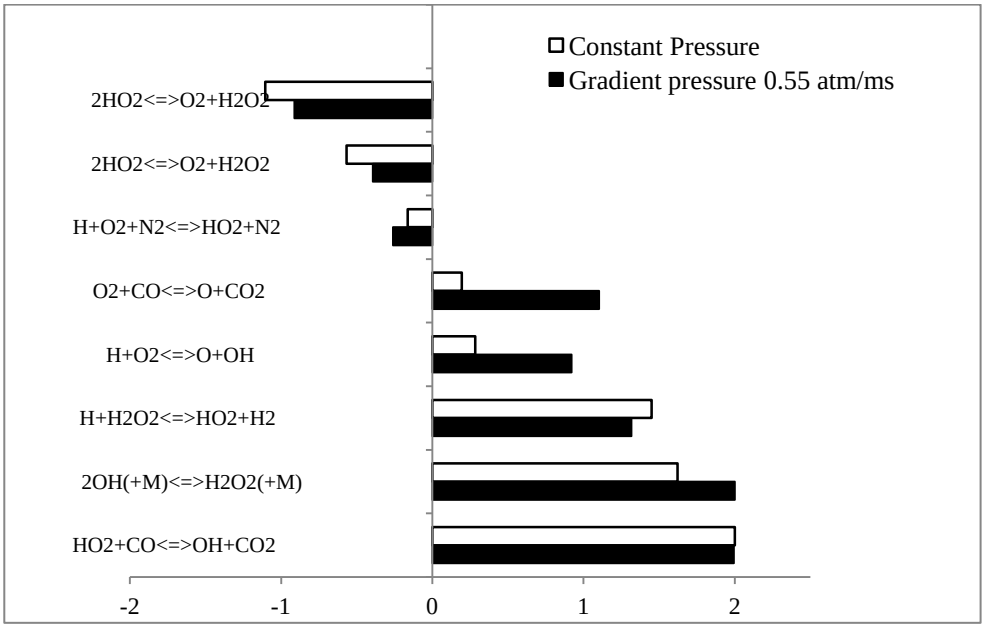

Figure 2-5 Sensitivity analysis at 769 K and 14.6 atm. Mixture : 51.1%CO/ 10.3%CO_2/ 38.6% H_2

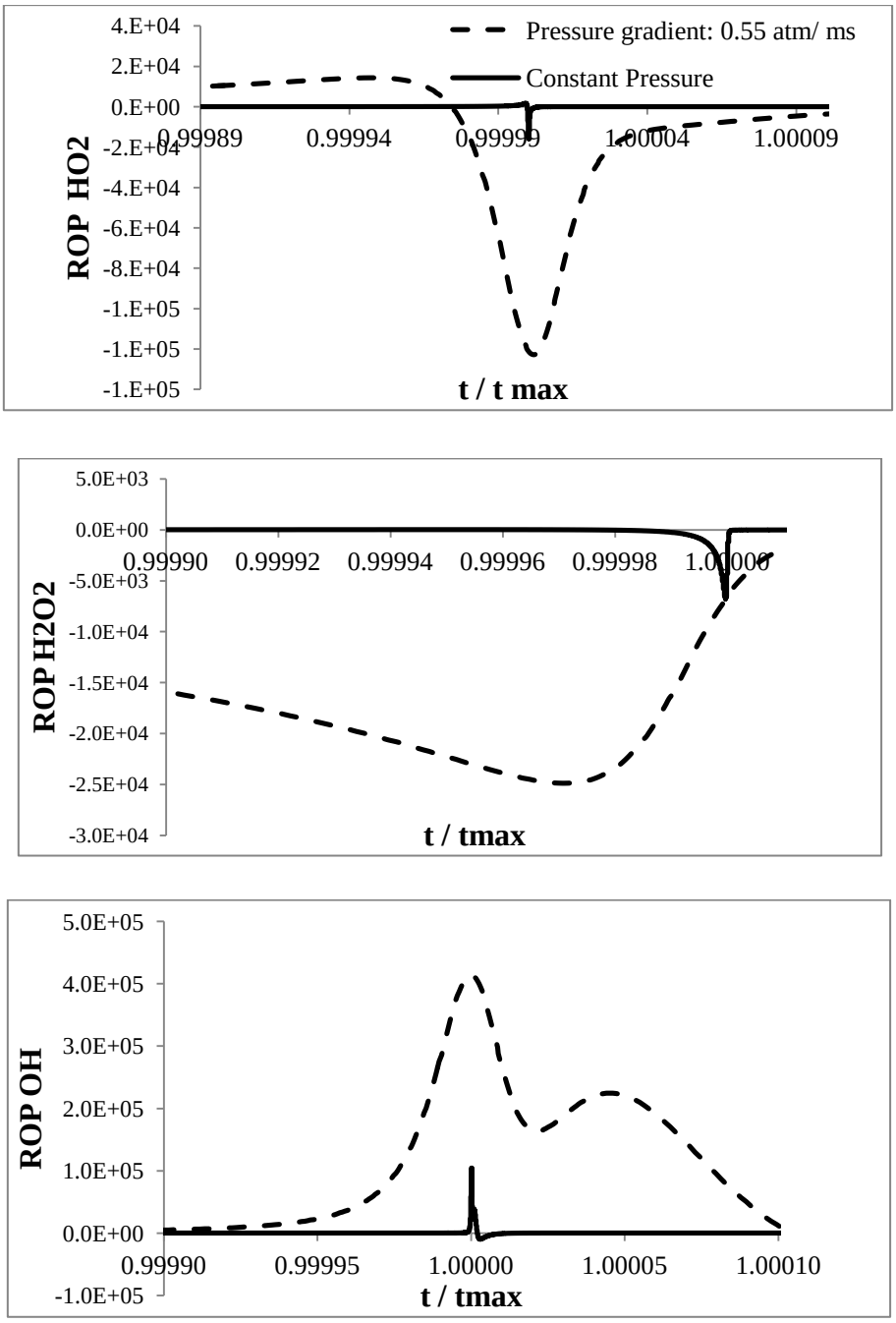

Figure 2-6 Rate of production of critical intermediate species such as: a) HO_2, b) H_2O_2 and c) OH. Ignition delay time estimations at 769 K and 14.6 atm. Mixture: 51.1%CO/ 10.3%CO_2/ 38.6% H_2

The high concentration of this radical promotes the formation of hydrogen peroxide (H_2O_2) through the chain propagating reaction $H+H_2O_2 \Leftrightarrow HO_2+H_2$. The gradient pressure contributes to the formation of OH radical species through the reaction $2OH (+M) \Leftrightarrow H_2O_2(+M)$ as this reaction is a pressure dependent reaction. The increasing production of HO_2 radical and the high concentration of carbon monoxide (CO) in the fuel promote the formation of OH radical through the reaction $HO_2+CO \Leftrightarrow OH+CO_2$.

The production of H radical from the chain propagating reaction $H+H_2O_2 \Leftrightarrow HO_2+H_2$ is then used by the reaction $H+O_2=O+OH$ for hydroxyl radical formation.

According to the sensitivity analysis, constant pressure and gradient pressure assumptions share the same key reactions. However, the sensitivity coefficient of the reactions H+O2=O+OH and $O_2+CO=O+CO_2$ increases significantly with respect to the coefficient estimated by considering constant pressure assumption. The rate of production (ROP) of H_2O_2 increases for promoting the formation of the reactive radical OH as shown in Figure 2-6b and 2-6c respectively. In these figures an adimensional factor was defined as t/t_{max} for decreasing the effect of the time-lag between the estimated ignition delay times. The parameter t_{max} corresponds the time where the maximum ROP is reached in each species.

2.4.2. Rate constant modifications. In this section a quantitative analysis for evaluating the performance of the different modifications suggested in the literature to improve the accuracy of detailed chemical kinetic mechanisms was carried out. Cavaliere et al.(2010) suggested to modify the rate constant of the most sensitive elementary reactions of the San Diego mechanism (Williams, 2005). In this thesis, each recommended modification was implemented in the Gri-Mech. 3.0 kinetic model, which is the reference mechanism. This mechanism was selected due to its good accuracy for estimating the ignition delay time and laminar flame speed of natural gas at intermediate and high temperature ranges. The ignition delay time estimated by using the reference mechanism without any modification is considered as baseline case. Moreover, the gradient pressure assumption was also examined for comparative purposes. Table 2-2 shows a detailed description of the modifications considered, the error obtained and the authors who suggested these modifications. These modifications were defined as *modification I, II, III* and *IV* in this thesis.

To evaluate the performance of these modifications, an error coefficient β was defined. This parameter quantifies the relative difference between the experimental and estimated ignition delay times. The coefficient was defined as:

Table 2-2. Description of the modifications proposed and the error with respect to experimental data

Item	Observations	β	Reference
Base line	Mechanism used as reference in the present research	1.13E+13	(Smith et al., 1999)
Pressure effect	Effect of non-uniformity of pressure within a shock tube reactor	6.44E+04	(Reehal et al.,2007)
Modification I	The elementary reaction $2OH(+M) \Leftrightarrow H_2O_2(+M)$ was splitted into two elementary reactions defined as $H_2O_2(+M) => 2OH(+M)$ and $2OH(+M) => H_2O_2(+M)$.	2.65E+08	(Cavaliere et al.,2010)
Modification II	The elementary reaction $2OH(+M) \Leftrightarrow H_2O_2(+M)$ was splitted into two elementary reactions defined as $H_2O_2(+M) => 2OH(+M)$ and $2OH(+M) => H_2O_2(+M)$. The ascentric factor of the reaction $H+H2O2 \Leftrightarrow HO_2+H_2$ was multiplied by 20	7.79E+05	(Cavaliere et al.,2010)
Modification III	The elementary reaction $2OH(+M) \Leftrightarrow H_2O_2(+M)$ was splitted into two elementary reactions defined as $H_2O_2(+M) => 2OH(+M)$ and $2OH(+M) => H_2O_2(+M)$. The elementary reaction $H+H_2O_2 \Leftrightarrow HO_2+H_2$ was also splitted into two elementary reactions defined as $H+H_2O_2 => HO_2+H_2$ and $HO2+H_2 => H+H_2O_2$	1.75E+05	(Cavaliere et al.,2010)
Modification IV	The elementary reaction $2OH(+M) \Leftrightarrow H_2O_2(+M)$ was splitted into two elementary reactions defined as $H_2O_2(+M) => 2OH(+M)$ and $2OH(+M) => H_2O_2(+M)$. The ascentric factor of the reaction $H+H_2O_2 \Leftrightarrow HO_2+H_2$ was multiplied by 100	9.72E+04	(Cavaliere et al.,2010)

$$\beta = \sum_{i=1}^{n} \left[\frac{\tau_{exp,i} - \tau_{model,i}}{\sigma_i} \right]^2 \qquad \text{Eq. 2-3}$$

where σ_i is the standard deviation of the experimental data considered. The standard error of regression is the better estimations of the experimental uncertainty of the data reported by Pscheke and Spadaccini (1985). This methodology was exposed by Currell (2009) and was employed previously by Sheen and Wang (2011) to estimate the standard uncertainty of a large data set of ignition delay data for ethylene. The standard uncertainty estimated for the data reported by Pscheke and Spadaccini (1985) was $\sigma_u = \mp 1{,}51\ ms$. For details of the regression model proposed as well as the statistical analysis developed see Appendix E. The results reveal that prediction of ignition delay time by considering pressure effect, modification III, and IV have the best estimations. Figure 2-7 shows a comparative of the results by considering the modifications defined. Although the modification III shows a good accuracy compared with modification IV, it is easy to realize that the latter has values close to the experimental data both high temperature and low temperature. The apparent deviation is caused by the logarithmic scale used.

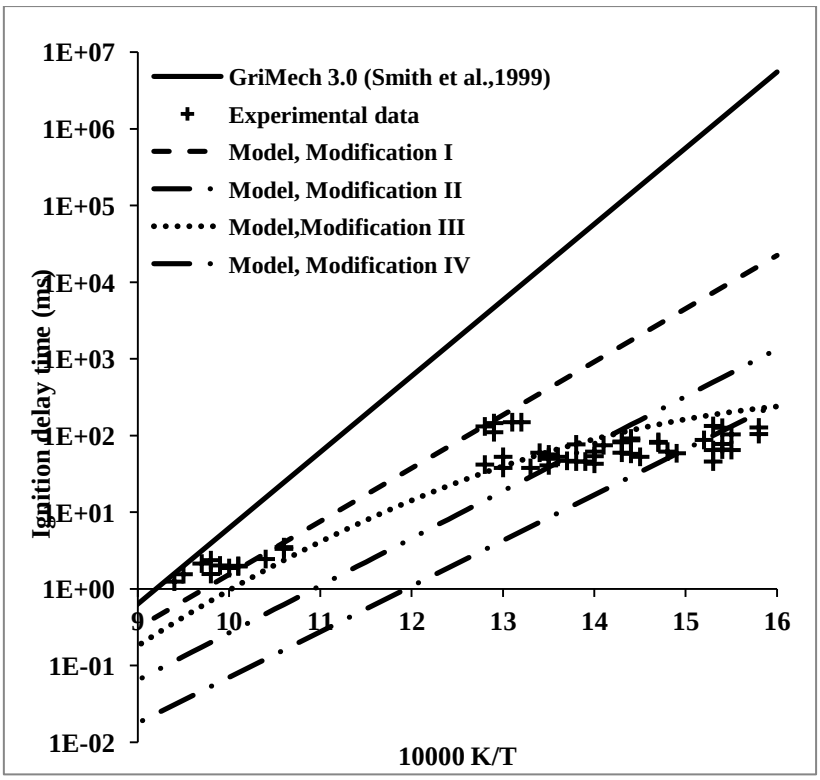

Figure 2-7 Comparative of the estimations of ignition delay time for $CO/CO_2/H_2$ mixtures by applying the modifications defined in Table 2-2. The reference mechanism used was Gri-Mech.3.0

The effect on ignition delay time of CH_4/H_2 mixtures at low temperature by considering the modification III was evaluated. The dispersion in the estimations observed in Figure 2-8 contrasts with the improvement in the estimations plotted in Figure 2-7 for $CO/CO_2/H_2$ mixtures. The increment of methane concentration in the mixture increases the ignition delay time of the fuels. This occur due to reduced production of reactive radicals through the chain branching reactions that react with the methane reactions for consuming radicals, especially OH that are needed in the ignition (Thiessen et al., 2010).

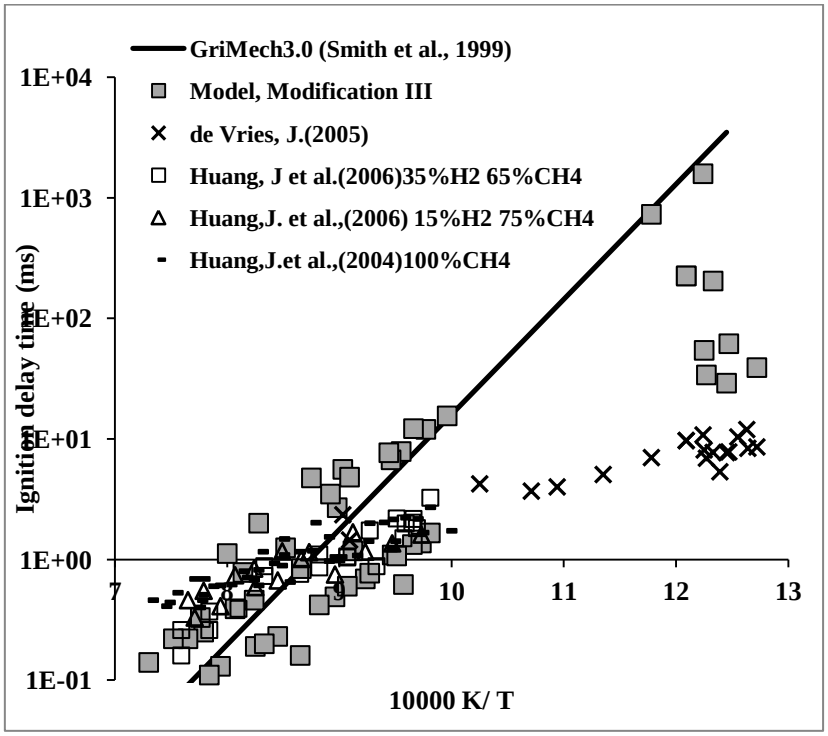

Figure 2-8 Comparative of the estimations of ignition delay time for CH_4/H_2 mixtures by applying the modifications defined in Table 2-2. The reference mechanism used was Gri-Mech.3.0

Figure 2-9 shows a sensitivity analysis developed for examining the kinetic implications of the modification III. This analysis includes the most sensitivity elementary reactions by considering the baseline case, gradient pressure assumption and the modification III. The analysis reveals that the modified reaction $HO_2 + H_2 \Rightarrow H + H_2O_2$ plays an important role in the production of H radicals. This is concluded due to the rate of formation of H_2O_2 is negligible compared with the production of HO_2 and OH as shown in Figure 2-10. The H radical is consumed by the chain propagating reactions $OH + H_2 = H + H_2O$ and $OH + CO = H + CO_2$ to release the reactive hydroxyl radical. The reaction

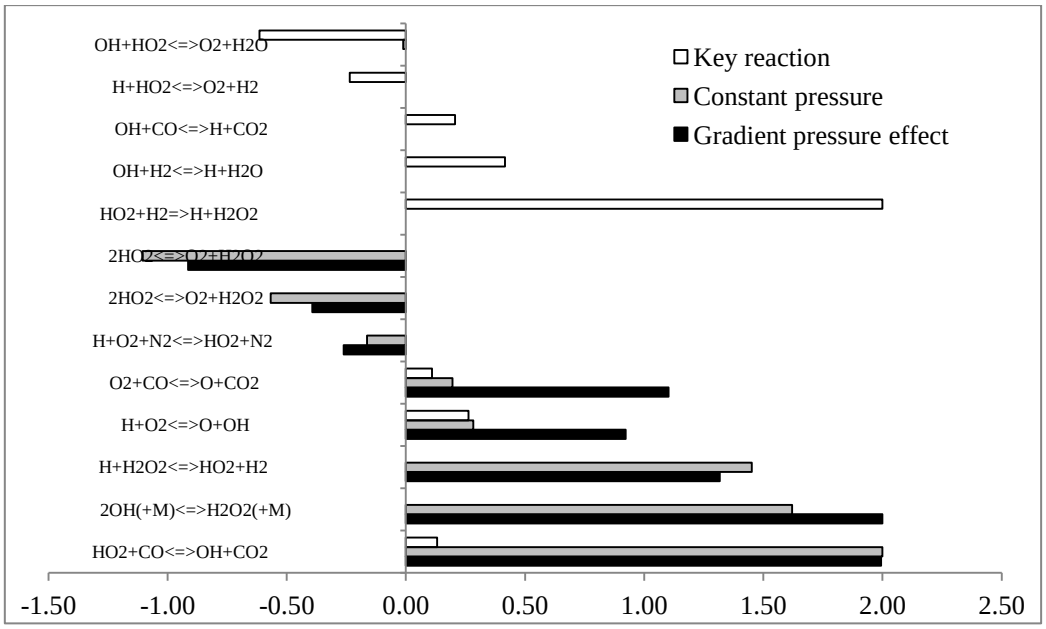

Figure 2-9 The most sensitive elementary reaction by considering base line case, gradient pressure assumption and the modification III

$H+H_2O_2=>HO_2+H_2$ is not sensitive because there is not formation of H_2O_2 and the produced radical H is consumed for the formation of OH.

The original reaction $H+H_2O_2=HO_2+H_2$ is strongly sensitive due to produce H_2O_2 from HO_2 radical due the high concentration of hydrogen in the fuel. The absence of H_2O_2 does not promote the formation of OH via $H_2O_2(+M)=>2OH(+M)$ and the consumption of OH radical for promoting the ignition makes not possible that the reaction $2OH(+M) => H_2O_2(+M)$ takes place .

The reaction $OH+HO_2 \Leftrightarrow O_2+H_2O$, which was not important in the baseline case became to be the second most important reaction by considering modification III. It is observed that the most important reactions with the modification III are not the same when baseline and gradient pressure approach was considered. In this case the most influential species, which play an important role in the fuel self-ignition are H, HO_2 and OH. The ROP of species under modification III are compared with ROP of the other approaches. As conclusion, two important considerations are highlighted in this section. The former is the close ROP of radicals OH and HO_2 to those obtained by considering the base line case without any abrupt increment at self-ignition point; the latter consideration is the negligible production of H_2O_2 although the ignition delay time predictions improved through the Modification III.

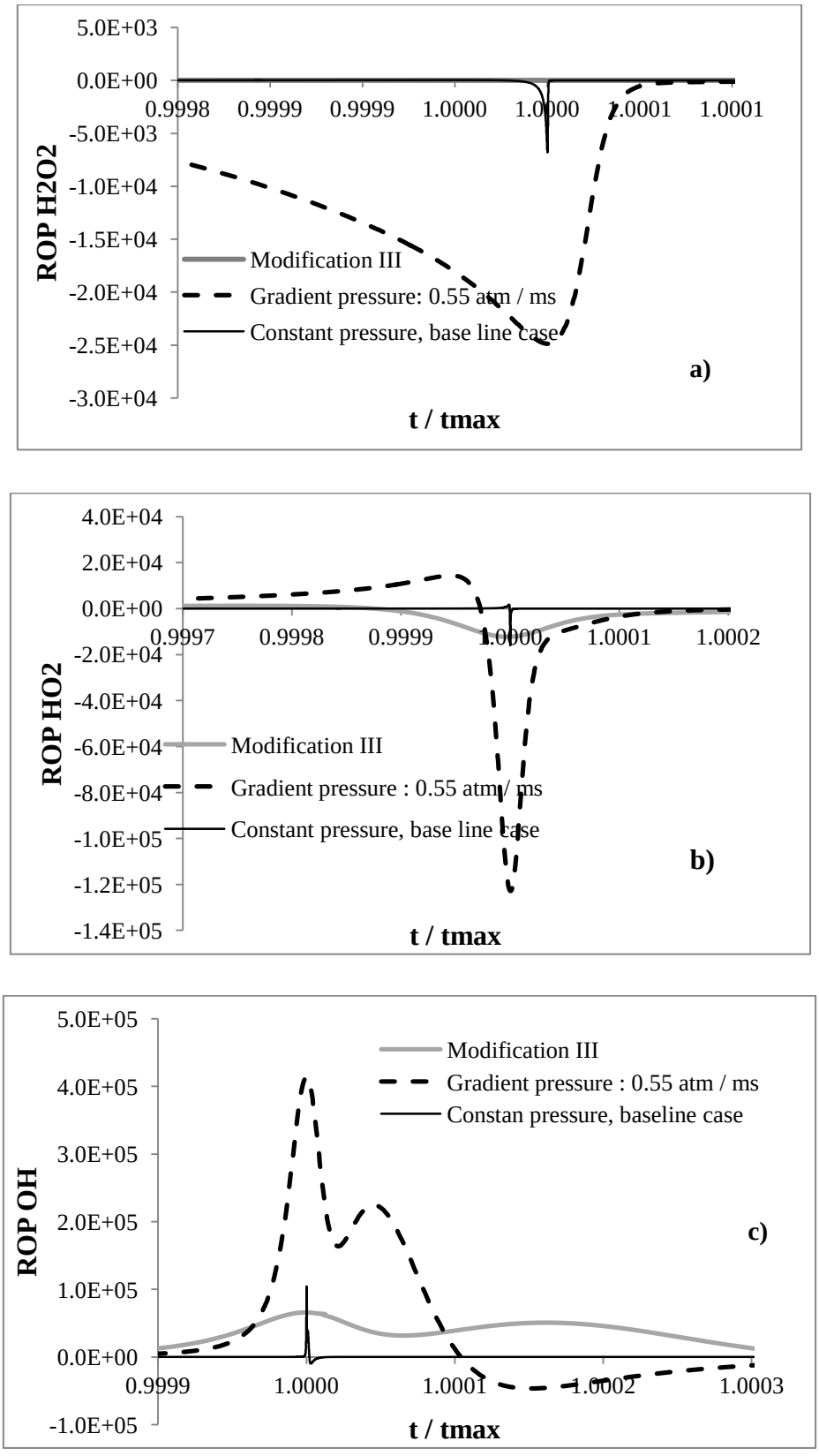

Figure 2-10 Rate of production of critical intermediate species such as: a) H_2O_2 b) HO_2 and c) OH by considering the different approaches. Ignition delay time measurements at 769 K and 14.6 atm. Mixture: 51.1%CO/ 10.3%CO_2/ 38.6% H_2

2.4.3. Catalytic effects. Chaos and Dryer (2008) revealed that the lack of accuracy of the mechanism for predicting auto-ignition point is not caused only by the absence of elementary reactions and intermediate species but also by other effects. The non-homogeneity of the auto- ignition in a shock tube reactor due to the slight auto-ignition occurred near to the reactor walls is an example of these effects. This is based on the data reported by Blumenthal et al.(1996) plotted in Figure 2-11. It is observed that the strong auto-ignition is well predicted by the chemical kinetic mechanism represented by black spots. However, the slight auto-ignition that occur at temperature below of 1100 K represented by white spots was not predicted by the Li et al. (2007) mechanism. In addition to the localized auto-ignition, Chaos and Dryer (2008) also consider the influence of impurities in the air fuel mixture that cause catalytic effects that accelerates the auto-ignition phenomenon. Their hypothesis is based on the additions of catalytic agents applied to the elementary reaction $H_2O_2+M \Leftrightarrow OH+OH$ and $H_2+HO_2 \Leftrightarrow H_2O_2+H$. This methodology was previously employed by Deutschmann et al. (1996) who developed a superficial chemical reaction mechanisms to measure the catalytic auto-ignition temperature of a mixture of $CH_4/CO/H_2$ over Paladium and Platinum atmosphere. Figure 2-11 shows the results obtained by using a small concentration of this impurity. The dotted curve shows the improvements in the estimations in a wide range of temperature. The grey area shows the ignition delay time range obtained when the magnitude of the impurity (catalyst) concentration is multiplied or divided by a factor of 10.

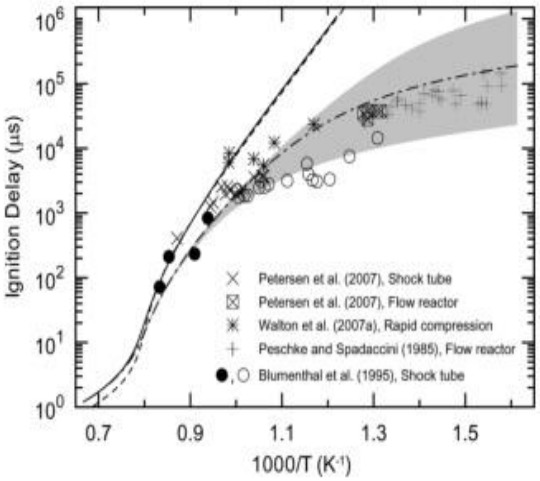

Figure 2-11 Ignition delay time obtained experimentally and estimated by using the kinetic model developed by Li et al.(2007) by considering catalytic effects. Adapted from (Chaos & Dryer, 2008)

2.5. EFFECT OF MODIFICATIONS ON LAMINAR FLAME SPEED OF $CO/CO_2/H_2$ AND CH_4/H_2MIXTURES

Although the modifications proposed by Cavaliere et al.,(2010) improve the accuracy of the kinetic models, it is necessary to study the actual effects of the modification III on the laminar flame speed and auto-ignition predictions. The laminar flame speed was computed at different fuel blends composition and equivalence ratio. These estimations were compared with the estimations done with the reference mechanism Gri-Mech.3.0.

2.5.1. Experimental data. In this section, a brief description of the measurement technique, fuel compositions and initial conditions of the reference experimental data was developed. Taylor (1991) measured the laminar flame speed of fuel blends of Methane, Hydrogen, Ethane, Propane, and Ethylene over a wide range of pressure and equivalence ratio. The measurements were done by using the expanding spherical flames technique. The same methodology was employed by Hassan et al.(1997) for H_2/CO mixtures. The laminar flame speed for this technique is defined as:

$$S_L = \frac{\rho_b}{\rho_u}\frac{dr_f}{dt} \qquad \text{Eq. 2-4}$$

where ρ_b/ρ_u corresponds to the burned and unburned gas density ratio in the bomb, and dr_f/dt correspond to the variation of flame radius with respect to the time. The average temperature and pressure in both cases in the estimations were 298K and 1 atm respectively. Bouvet (2009) used the outwardly propagating and the conical flame (Bunsen flame) technique to measure laminar flame speed of different CO/H_2 ratios over a wide range of equivalence ratios. The results obtained show similar results at the same fuel compositions and equivalence ratio by using the techniques referenced.

2.5.2. Laminar flame speed estimations. The objective of this section is to evaluate the influence of the Modification III on the laminar flame speed estimations for CH_4, CO/H_2, and CH_4/H_2 mixtures. The use of Gri-Mech3.0 mechanism is suitable for this analysis, due to the deviations with respect to the experimental data were small. These estimations were made by using PREMIX code from Chemkin Pro® software over a wide range of equivalence ratios.

To validate the kinetic model, laminar flame speed estimations were compared with the experimental laminar flame speed data of 50% H_2 / 50% CO and 5%H_2 / 95% CO mixtures. Agreement between experimental and numerical flame speeds were obtained both lean and reach mixture for the fuel blends examined. Figure 2-12 shows the performance of the kinetic model and the effect of the hydrogen concentration on the estimations.

It was observed that the model slightly overpredicts the laminar flame speed at rich mixture when high concentration of hydrogen is present in the fuel. However, for the mixture with low concentration of hydrogen (5% H_2 and 95% CO) numerical estimations agree with the experimental data. Figure 2-13 shows the estimated laminar flame speeds of the fuel Nº 2 of the research developed by Peschke and Spadaccini in 1985 for a wide range of equivalence ratios. For these estimations were considered the reference mechanism and the same mechanism with the modification III. From Figure 2-13 is concluded that effects of Modification III on the estimations are neglect. This important result means that improvement in the ignition delay time can be achieved without decrease the accuracy of the laminar flame speed predictions for $CO/CO_2/H_2$ mixtures.

In this section CH_4/ H_2 mixtures were considered due to its importance in the MN measurement and knock intensity definition. Figure 2-14 and Figure 2-15 show the experimental measurement of laminar flame of CH_4 and CH_4/H_2 mixtures respectively. In both cases, the overpredictions of laminar flame speed close to the stoichiometric point with the modification III are not significative. These differences do not change the conclusions that could be inferred from these estimations. The main reason of these results is the sensitive elementary reactions of the burning rate of this mixture, which are different from the sensitive reactions that influence the auto-ignition of the mixture.

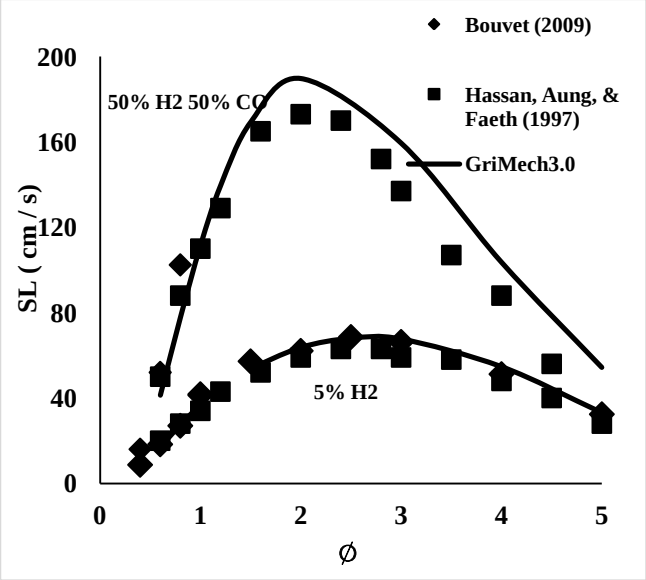

Figure 2-12 Estimations of laminar flame speed of H_2/CH_4 mixtures by using Gri-Mech3.0 chemical kinetics mechanism. Tu= 298 K, p = 1 atm

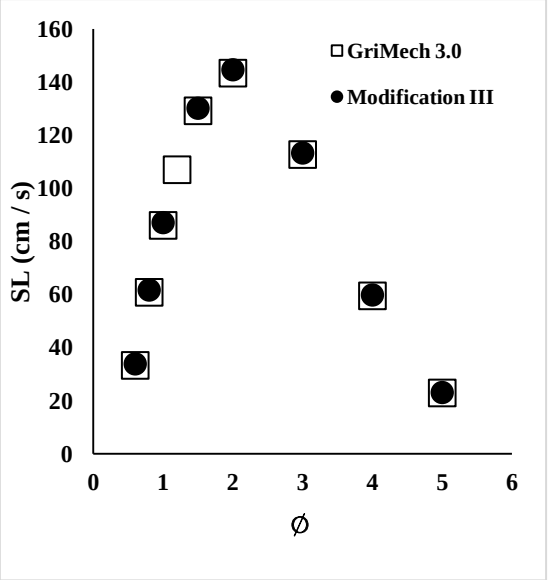

Figure 2-13 Estimations of laminar flame speed by using Gri-Mech3.0 and the same mechanism with Modification III. Mixture: CO=51.1% CO_2=10.3% H_2=38.6%. Tu=298 K, p = 1 atm.

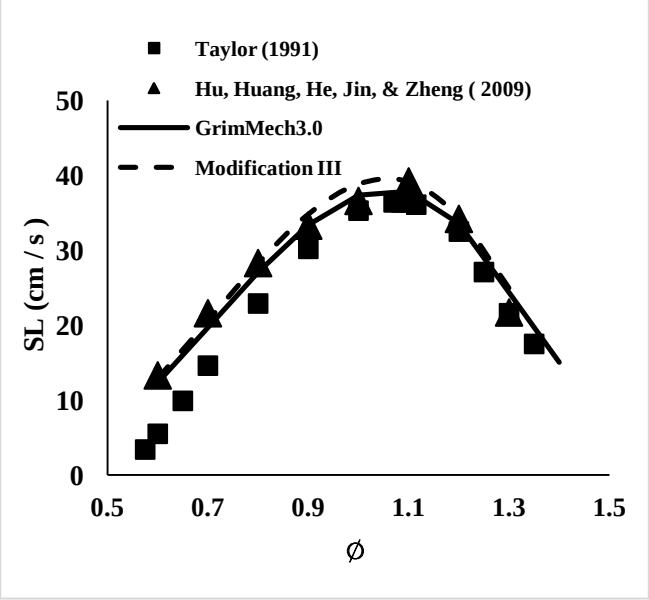

Figure 2-14 Estimations of laminar flame speed by using Gri-Mech3.0 and the same mechanism with Modification III. Fuel: CH_4=100 %. Tu=298 K, p = 1 atm.

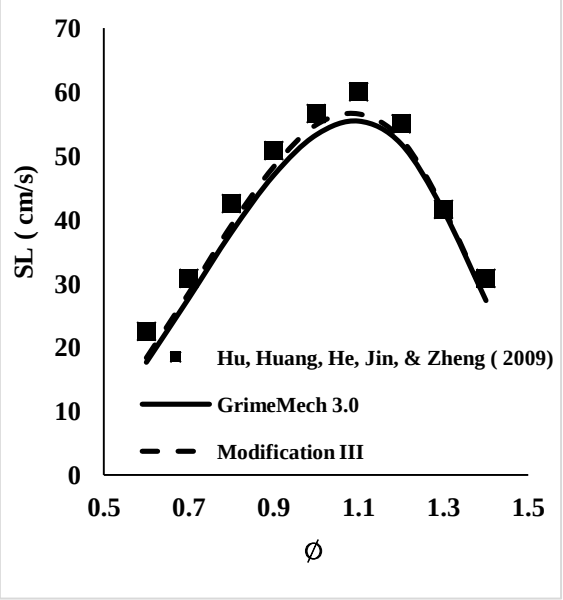

Figure 2-15 Estimations of laminar flame speed by using Gri-Mech3.0 and the same mechanism with Modification III. Mixture: CH_4=60% / H_2=40%. Tu=298 K, p = 1 atm.

According to the literature the chemistry of ignition delay and laminar flame speed does not share critical elementary reactions.

2.6. CONCLUSIONS

The most important conclusions derived from this chapter are described as follows:

- ✓ Strong deviation between numerical and experimental ignition delay time at low temperature range was obtained for CH_4 / H_2 mixtures. This trend agrees with the observations of Petersen et al. (2007) for $CO/CO_2/H_2$ mixtures.

- ✓ The gradient pressure improves the ignition delay time estimations at low temperature; however the methodology employed cannot be applied for ICE applications.

- ✓ The modifications proposed by Cavaliere et al., (2010) are suitable for improving ignition delay estimations without decreasing the accuracy for determining the laminar flame speed of $CO/CO_2/H_2$ and CH_4/H_2 mixtures.

- ✓ The most sensitive elementary reactions that govern the auto-ignition phenomena for $CO/CO_2/H_2$ mixtures are $2OH(+M) \Leftrightarrow H_2O_2(+M)$ and $H+H_2O_2 \Leftrightarrow HO_2+H_2$. Another elementary reaction that plays an important role in the ignition chemistry is $HO_2+CO \Leftrightarrow OH+CO_2$. However, the best estimations were obtained with the modifications done to the first two elementary reactions.

- ✓ When Modification III is implemented in the detailed chemical kinetic mechanism, the ROP of H_2O_2 specie is equal to zero. Although maximum and minimum ROP of the reactive radicals HO_2 and OH species are equal to the ROP of the base line case, there is not an abrupt increment of the their concentration near to auto-ignition point.

- ✓ The Gri-Mech 3.0 kinetic model is suitable for estimating laminar flame speeds of Syngas, NG and CH_4/H_2 mixtures. This mechanism is used as reference mechanism for the implementation of the two-zone auto-ignition model.

- ✓ The estimations of the laminar flame speed of $CO/H_2/CO_2$ and CH_4/H_2 mixtures are not affected by the Modification III implemented at different compositions and equivalence ratios.

Chapter 3

Methane Number and Knock Occurrence Crank Angle Measurements for $CO/CO_2/H_2$ Mixtures

3.1 INTRODUCTION

Environmental effects caused by the use of conventional fuels and the uncertainty of future of energy supply, have been a concern in the recent years. The use of alternative fuels from a variety of feedstocks such as coal, biomass and waste products from different thermochemical processes is a possible solution. The use of these fuels for ICE applications is limited by its auto-ignition tendency due to its high concentration of hydrogen and carbon monoxide. The MN represents the antiknock capacity of gaseous fuels, similar to the concept of octane number for liquids fuels. Leiker et al.(1972) used the standard ASTM octane number determination method as a reference to measure the MN of different gaseous fuels composed of methane, hydrogen, carbon monoxide, propane, butane etc. Later, Ryan et al. (1993), and Callahan et al. (1996) used this methodology to measure the MN of fuel blends of methane, ethane, propane, butane, pentane, and carbon dioxide. These data have been used to develop predictive equations that have been implemented in a computational program to estimate the MN of natural gas as a function of the fuel blend composition. The estimations of MN for gaseous fuels different from natural gas, were addressed by Malensek and Olsen (2009). The

MN measurements of eight fuels with typical compositions of coal, wood, digester, landfill and reformed natural gas were carried out in this project. The results obtained showed that the MN of these alternative fuels ranged from 24 to 140. Later, Arunachalam and Olsen(2012) and Wise, Olsen, and Kim (2013), measured MN of producer gases with different compositions from gasification process to know their knocking characteristics. The results obtained reveal that fuels from gasification process, have a MN ranging from 50 to 130 MN. In particular, MN variability of synthesis gas, i.e., synthesis gas compositions, is a critical concern due to the effect on engine efficiency and emissions. Depending on the nature of feedstock and production method used for producing the fuel, the combustion parameters such as auto-ignition, combustion duration, ignition delay, start and end of combustion are considerably impacted. The abnormal combustion phenomenon of auto-ignition limits the compression ratio; therefore, the engine efficiency. The connections between auto-ignition and combustion parameters must be evaluated to improve the understanding of this issue. A first step for understanding this phenomenon, was developed by Peschke and Spadaccini (1985) who reported low temperature ignition delay time for $CO/CO_2/H_2$ mixtures. The low temperature ignition delay time data reported in this research represent a valuable information to link with syngas auto-ignition in an ICE. Although significant amount of work has been dedicated to the use of syngas in compression ignition ICE(Sahoo et al., 2011; Sahoo, 2012),and spark ignited ICE (Boloy et al., 2005) under normal combustion, there is little published research on the utilization of syngas in ICE under knock operation. Engine knock and combustion parameters for H_2/CO mixtures were evaluated by Bika et al.,(2011) who concluded that the high concentration of CO in the binary fuel is beneficial due to its knock resistance.

In this chapter, syngas auto-ignition is explored. Binary H_2/CO mixtures diluted with CO_2 were tested in order to:

- ✓ To measure the MN of fuel blends of $H_2/CO/CO_2$.
- ✓ To develop an empirical correlation for determining the MN as a function of the fuel blend composition.
- ✓ To examine the relationship between MN, combustion parameters, engine operating conditions and KOCA.

3.2. EXPERIMENTAL SETUP

3.2.1. CFR Engine. The engine used in this thesis has been used previously by Malenshek and Olsen (2009), Arunachalam and Olsen (2012) and Wise et al., (2013) to measure MN of alternative gaseous fuels. Figure 3-1 shows the facility CFR engine used for MN measurements.

Figure 3-1 CFR facility used for MN measurements. Source: author

Originally, this single cylinder, un-throttled, four stroke, spark-ignited engine was designed by the Waukesha Motor Company in 1957 for Motor Octane Number measurements. It is coupled with a belt to a 5 horsepower AC synchronous motor, which serves to start and load the engine, as well as to maintain the engine speed at 900 rpm. The compression ratio can be changed during a test due to the design of the

cylinder-piston system, suitable for MN measurements. The modifications made for gaseous fuels testing are focuses on the ignition and the intake system. The original ignition system was upgraded to a solid state Altronic CD 200 electronic system, and the engine intake system was upgraded with a pulse width modulated injector (PWM), Clean Air Power Model SP-051 for gaseous fuel injection.

The air/fuel ratio control of the engine is based on a feedback control system using either a lambda sensor or air/fuel ratio computed from fuel and air flow measurements. The latter method was employed due to low heating values fuels were used. The lambda sensor was not suitable for controlling the equivalence ratio for these fuels. This configuration allows the engine to run over a wide range of equivalence ratios, depending on the test objectives. Additionally, thermocouples were installed for measuring the intake and exhaust gas temperature. The main characteristic of the engine are shown in Table 3-1

Table 3-1 Characteristic of the CFR facility used in this thesis

Item	Description
Compression ratio	Adjustable 4:1 to 18:1
Cylinder bore	3.25 in (8.255 cm)
Stroke	4.5 in (11.43 cm)
Displacement	37.33 in^3 (611.73 cm^3)
Piston	Cast iron, flat top
Ignition timing (deg bTDC)	Adjustable from 12 to 30
Connecting rod length	25.4 cm

3.2.2. Gas blending and intake air system setup. Compressed gas bottles of chemically pure (CP) CO, CO_2, H_2 and CH_4 were purchased to prepare the test fuels. Regulator valves were installed on each gas bottle for discharging gas into the fuel manifold. Pulse Width Modulated (PMW) injectors were used to meter the fuel blend average flowrate. The mixture flows toward a combination flame arrestor-check valve, mixing later with the intake air. Figure 3-2 shows the compressed gas bottles used in this project.

Figure 3-2 Compressed gas bottles of the fuel blending system

The combustion air is supplied by the building compressed air system, which is filtered and dehumidified. The air fuel mixture is heated by an electrical resistance installed just upstream of the engine intake port. Intake fuel air mixture temperature is controlled by LabView in a feedback loop to achieve the desired temperature. Figure 3-3 shows a detailed scheme of the test cell used in this research.

3.2.3. Knock detection method. The quantitative knock detection method used was developed previously by Wise (2007).This approach evaluates the Fast Fourier Transform (FFT) of the cylinder pressure readings in order to obtain pressure amplitudes in the frequency domain produced by abnormal combustion. A band pass filter was applied to the real-time pressure data to remove the noise and operating pressure and extract the peaks end gas auto-ignition. An advantage of this method is the detailed information obtained about the start, development and intensity of the knock in the engine. The method employed, is similar to the approach of Brunt et al., (1998) and Elmqvist et al.,(2003) who used FFT of filtered pressure signals to detect knock onset. In this chapter, the maximum FFT amplitude of a knocking engine cycle was used as reference to stablish the knock level thresholds. The knock index used is defined as the

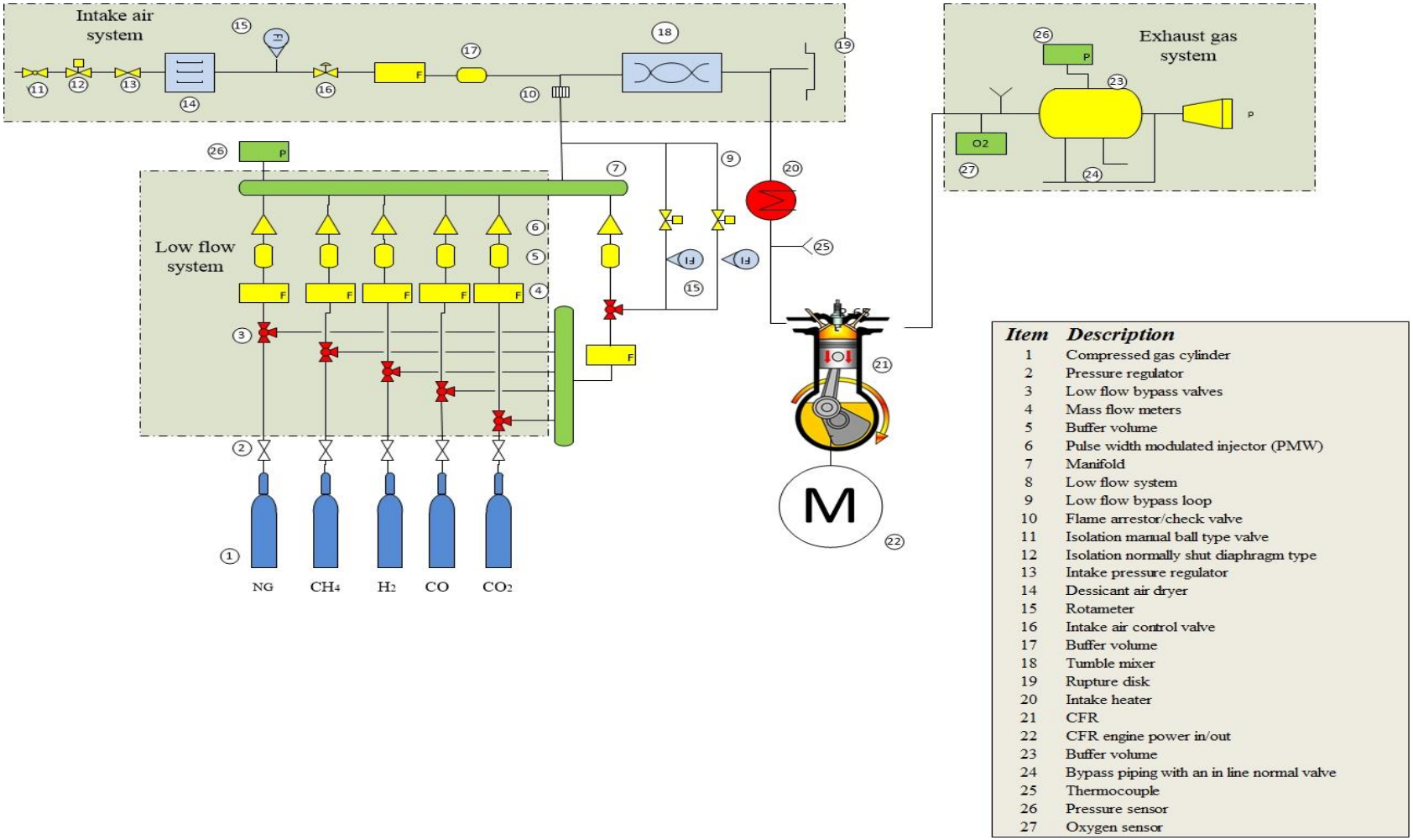

Item	Description
1	Compressed gas cylinder
2	Pressure regulator
3	Low flow bypass valves
4	Mass flow meters
5	Buffer volume
6	Pulse width modulated injector (PMW)
7	Manifold
8	Low flow system
9	Low flow bypass loop
10	Flame arrestor/check valve
11	Isolation manual ball type valve
12	Isolation normally shut diaphragm type
13	Intake pressure regulator
14	Dessicant air dryer
15	Rotameter
16	Intake air control valve
17	Buffer volume
18	Tumble mixer
19	Rupture disk
20	Intake heater
21	CFR
22	CFR engine power in/out
23	Buffer volume
24	Bypass piping with an in line normal valve
25	Thermocouple
26	Pressure sensor
27	Oxygen sensor

Figure 3-3 Engine test cell scheme

area under the curve of the maximum FFT amplitude of the first 200 engine cycles. After simplifications, the Knock Integral (KI) is defined as:

$$KI = KL(1) + KL(2) + \cdots + KL(n) \quad \text{Eq. 3-1}$$

where *KL(1), KL(2)* and *KL(n)* correspond the maximum FFT amplitude of the cycle 1, 2 and n respectively. This parameter is called Knock Integral (KI) and was found to be a stable and repeatable method for MN measurements (Wise D., 2007; Gomez J. et al., 2016). For more details on the Knock Integral methodology, see Wise (2007).

3.3. METHANE NUMBER MEASUREMENT

3.3.1. Test method. Although a standard method for MN measurement does not exist, the ASTM MON method has been used as reference. The first approach was performed by Leiker et al.,(1972) who measured MN for fuel blends with carbon monoxide, carbon dioxide, methane, propane, butane, hydrogen among other gases. The methodology developed by Leiker et al. (1972) was used by Wise (2007), Malenshek and Olsen (2009) and Gomez J.et al.,(2016) with some modifications in order to improve the accuracy of the method.

Initially, the standard CFR engine was fueled with the building natural gas supply to obtain stable and standard operation at 940 rpm and 15º bTDC of ignition timing. Once the engine was running at stable condition, the fuel was switched to the test gas. The compression ratio was adjusted to obtain the Knock Integral corresponding to light knock (KI~15-20). Then, the equivalence ratio was varied near to stoichiometric conditions until the KI was maximized, close to 25~30. This knock intensity range was used in this research. If sweeping the equivalence ratio is not enough to achieve the target KI, the compression ratio was slightly increased. This procedure was repeated until the desired KI was obtained. Data was recorded at desired KI. The data included fuel composition, compression ratio, ignition timing, cylinder pressure and ambient conditions. The test gas was switched to the reference mixture of methane and hydrogen while maintaining the same engine operating conditions. This was performed initially

with methane and then, adding hydrogen until knock integral of 30 was reached. The equivalence ratio was varied again in order to achieve maximum knock intensity followed by additional hydrogen adjustments if necessary. Once the desired Knock Integral was achieved, engine operating data was recorded. *By definition, the MN of the test gas is equal to the volume percent of methane in the binary reference blend.*

3.3.2. MN uncertainties. In this section an uncertainties analysis for MN testing was carried out. The uncertainties are caused mainly by three sources of errors: the error in the test method, test gas composition measurements, and reference gas composition measurements.

The error associated with the test method was previously evaluated by Malenshek and Olsen(2009), where MN of natural gas was measured ten times. The standard deviation was 0.3 MN, which was taken as the method uncertainty. Later, in order to evaluate consistency and repeatability of the knock measurement, Wise (2013) measured the MN of a fuel blend of 90 % of Methane (CH_4) and 10 % of ethane (C_2H_6) 21 times. The standard deviation of the method was 1.85 MN. For the current work, this standard deviation was used as the test method uncertainty since it was more recent and based on a larger number of data points. The uncertainty for preparing the composition of the test gas was neglected since the assigned MN depends only on the composition of the binary reference gas. This uncertainty comes from the flowmeters used to prepare the binary reference gas. For reference gas composition uncertainty determination, the methodology developed by Kline and McClintock (1953) was used. The flowmeters uncertainties come from two sources: the accuracy of the flowmeters given by the manufacturers and the calibration error. The accuracy of the Omega model FMA 1700 series flowmeters is 1.5% according to the manufacturer.

The error due to calibration was estimated by means of the calibration curve. The calibration curve for each flowmeter was built by using a GCA Precision Scientific Wet Test Meter. The MN uncertainty is the sum of test method and gas composition uncertainties. This procedure was used previously by Aparna Arunachalam (2010). Details of the methodology employed were described in Appendix A and B.

3.4. DESIGN OF EXPERIMENT AND FUEL SELECTION

The main objective of this section was to determine the MN of fuels blends of carbon monoxide (CO), carbon dioxide (CO_2) and hydrogen (H_2). For this purpose, a mixture design of experiment was carried out, with three factors and one response variable. Table 3-2 shows the factors and levels considered. The response variable was the test gases's MN. Figure 3-4 shows a graphical representation of the mixture design of experiment used in this research. The factor levels values were selected taking into account the average composition of the coal gas reported in the literature (Peschke and Spadaccini, 1985). A total of 19 completely randomized runs were performed.

Table 3-2. Factors and levels considered in the mixture design of experiment

Components	Low	High	Units
H_2	10	30	%
CO	20	40	%
CO_2	30	50	%

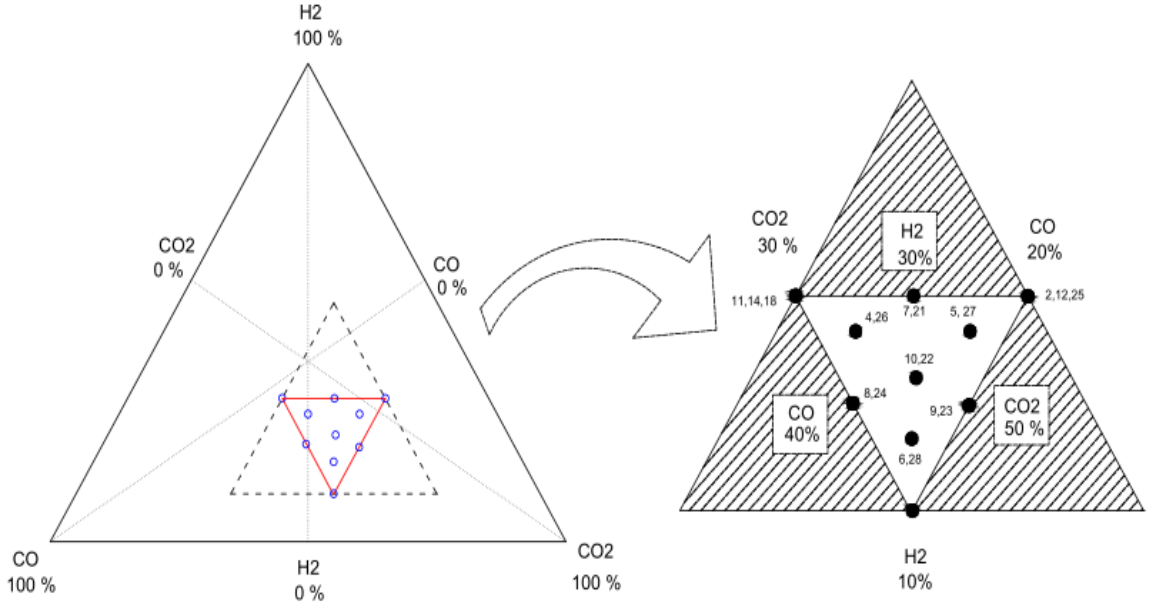

Figure 3-4 Graphical representation of the mixture design of experiment

Table 3-3 summarizes the results obtained. There were difficulties in the MN measurements of fuels with high concentration of carbon dioxide and low concentration of hydrogen as the knock intensity was very low. Also, the MN of the mixture 51.1%CO/ 10.3%CO_2/ 38.6% H_2 could not be measured due to the engine backfire. This fuel was used in Chapter 2 as reference fuel for evaluating the ignition chemistry.

Taking into account the results obtained in the experiment, a statistically validated second order regression model was proposed as shown in Eq. 3-2 :

$$MN = aH_2 + bCO + cCO_2 + dH_2 * CO + eH_2 * CO_2 + fCO * CO_2 \quad \text{Eq. 3-2}$$

where a, b, c, d, e and f are constants.

Table 3-3 MN measurements of H_2/CO/CO_2 mixtures

Run	*%H_2*	*%CO*	*%CO_2*	*Measured MN*	*Average MN*	*Predicted MN*	*AVL MN*	**δ MN**	*Average δ MN*
11	30.0	40.0	30.0	43.0	45.0	46.0	71.1	3.7	3.8
14				45.9				3.8	
18				46.1				3.8	
2	30.0	20.0	50.0	113.9	118.0	117.3	79.2	6.4	6.1
12				119.6				6.0	
25				120.5				6.0	
4	26.7	36.7	36.7	60.1	60.3	54.3	78.9	3.4	3.3
26				60.5				3.3	
5	26.7	26.7	46.7	92.0	91.9	93.6	83.2	3.2	3.2
27				91.8				3.3	
6	16.7	36.7	46.7	139.1	139.1	136.5	96.8	4.6	4.6
7	30.0	30.0	40.0	60.5	61.2	62.5	76.5	3.4	3.4
21				61.9				3.4	
8	20.0	40.0	40.0	81.2	85.5	87.7	88.7	3.3	3.3
24				89.7				3.2	
9	20.0	30.0	50.0	133.5	116.8	134.2	93.8	5.3	5.4
23				135.5				5.4	
10	23.3	33.3	43.3	81.5	81.9	83.7	86.3	3.3	3.3
22				82.3				3.2	

The regression model and the constants obtained were significant and explain the variability of the experimental data obtained. The values of the constants are $a = 17.7600,\ b = 6.1346,\ c = 11.0318, d = -0.3499, e = -0.4584, f = -0.1922.$

Figure 3-5 shows a comparison of the MN-guide line obtained in this research and those obtained in previous researches. Differences observed in the results are related to the knock detection method and knock intensity definition used.

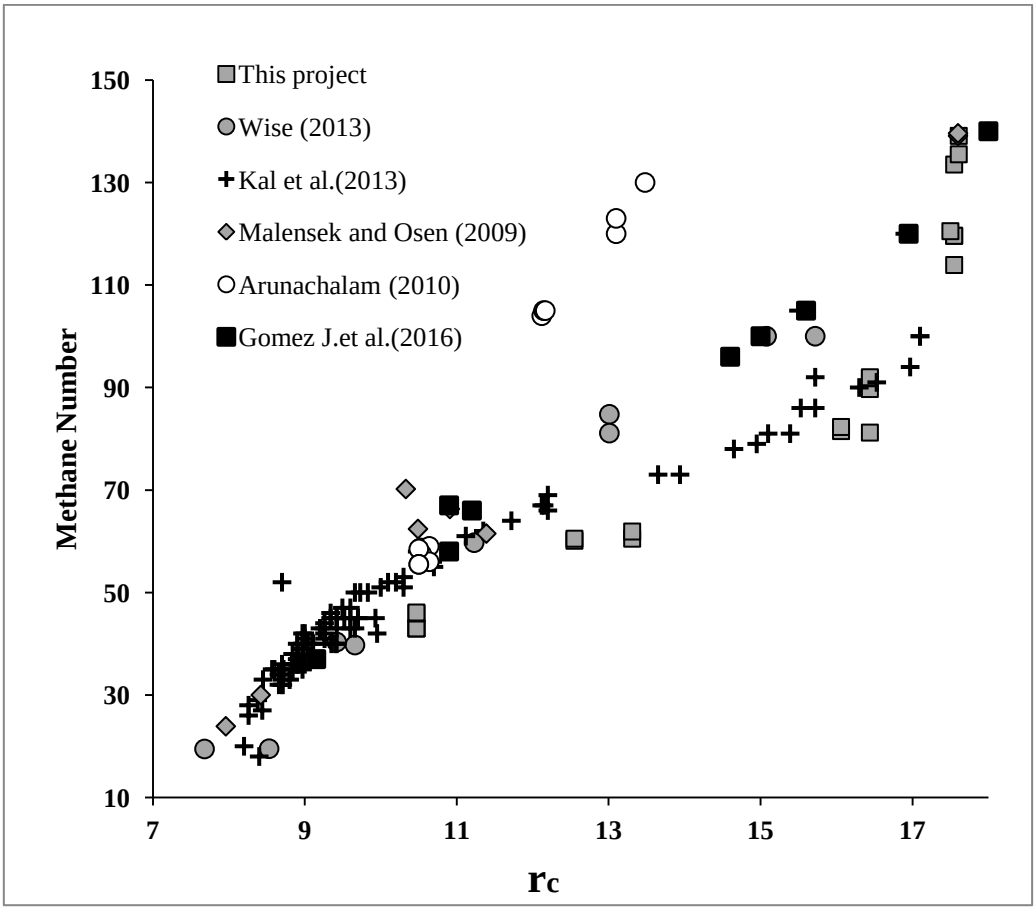

Figure 3-5 Comparison between the MN-guide line obtained in this thesis and those obtained previously by others researches

The MN measured in this thesis and those obtained by Kal et al. (2013) are close because the knock detection method and knock intensity definition was the same (KI ~ 25-30). Some MN measurements were obtained by using the detonation meter method and a knock intensity definition of 50 percent on the knock meter (Malenshek and

Olsen, 2009; Aparna Arunachalam, 2010), which was an arbitrary set point based on the audible detection of knock.

A response surface was built and plotted in Figure 3-56 based on the regression model. This surface relates the fuel blend compositions with the MN of the mixtures. It is evident that increments in the carbon dioxide concentration increase the MN of the mixture, and a high hydrogen concentration decreases the MN of the fuel blend. A graphical representation of the data summarized in Table 3-3 is shown in Figure 3-7. This figure shows a comparison between the experimental MN and those predicted by using the regression model and the AVL methane ® software. The strong deviation of the experimental MN from those obtained by using AVL is evident. This result contrasts with the predictions of the regression model developed in this research (Equation 3-2). The predictions in most of cases are within the uncertainties intervals.

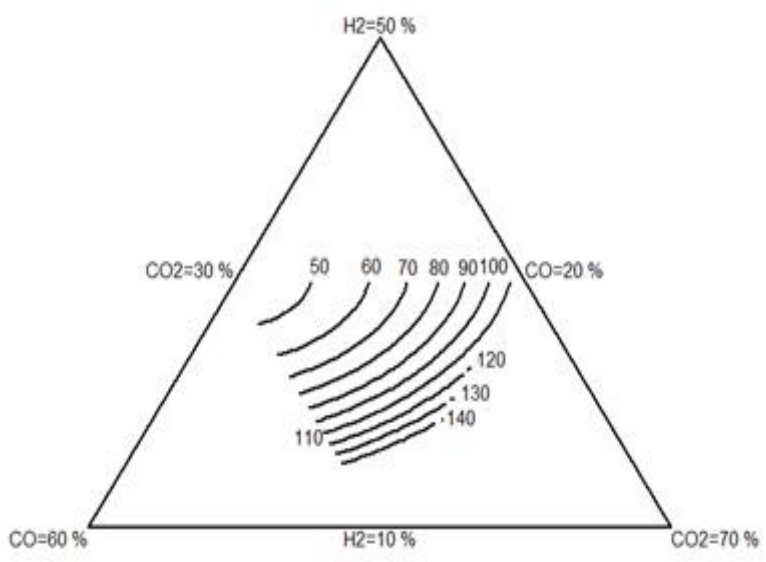

Figure 3-6 Response surface of the MN as a function of fuel blend composition

The importance of the regression model developed is that allows determining the MN of fuels with high concentration of carbon monoxide, carbon dioxide and hydrogen. The software AVL was developed for estimating the MN of natural gas, therefore, when it is used for estimating the MN of fuels with high concentration of these species the results do not agree with the experimental MN.

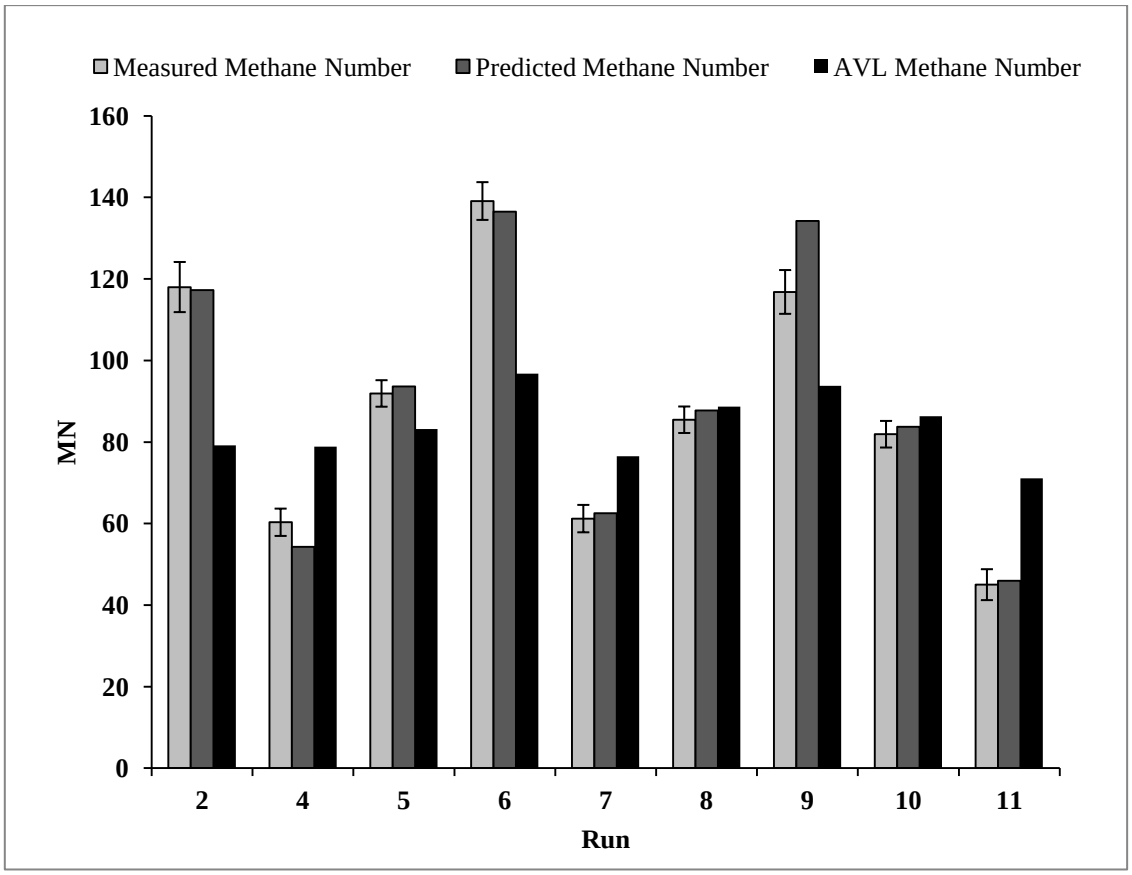

Figure 3-7 Comparison between experimental, predicted and AVL MN

3.5. KNOCK OCCURRENCE CRANK ANGLE DETECTION METHOD

This section describes the methodology employed to determine the KOCA in the CFR engine. This methodology was based on the research developed by Checkel and Dale, J.D,(1986), where the knock indicator algorithm was based on the third derivative of the pressure trace in the peak knock region. The numerical method is a central finite difference scheme defined in Eq. 3-3.

$$\frac{dP(\theta)}{d(\theta)} \approx \frac{[86 * (P_{i-4} - P_{i+4}) + 142 * (P_{i+3} - P_{i-3}) + 193 * (P_{i+2} - P_{i-2}) + 126 * (P_{i+1} - P_{i-1})]}{1188 * \Delta\theta} \quad \text{Eq. 3-3}$$

The derivative $dP(\theta)/d(\theta)$ represents the first derivative at crank angle , where $\Delta\theta$ is the crank angle interval, $P(\theta)$ is the pressure at crank angle θ and P_{i+1} and P_{i-1} are the succeding and preceding pressure values respectively. The crank angle interval used for this thesis was 0.1º .This differentiator includes an implicit filtering to smooth high

noise pressure signal from the combustion chamber. This equation is applied three times to the digitalized pressure signal to achieve the third derivative. The successive application of Eq. 3-3 amplifies the noise of the signal coming from the data acquisition system. A low pass filter was used on the second derivative prior to calculating the third derivative. This filter was defined as:

$$F(\theta) = \frac{[2 * (S_{i-4} + S_{i+4}) + 3 * (S_{i-3} + S_{i+3}) + 4 * (S_{i-2} + S_{i+2}) + 5 * (S_{i-1} + S_i + S_{i+1})]}{33} \quad \text{Eq. 3-4}$$

Figure 3-8 shows a pressure trace of an engine cycle with high knock. Knocking pressure peaks have significantly larger third derivatives than a non-knocking pressure peak in a normal combustion cycle. In this research, the crank angle with the most negative third derivative corresponds to the knock occurrence crank angle (KOCA) as shown in Figure 3-9. This methodology has been employed previously by Rodrigues and Shrestha (2006) and Wayne et al.,(1998). Moreover, an alternative definition of individual KI is presented. This approach uses the most negative third derivative to define the criterion. The advantage of this approach is its simplicity and the easy computational implementation. However, the discussion about the use of this criterion is out of the scope of this thesis; therefore the FFT approach was used in this thesis.

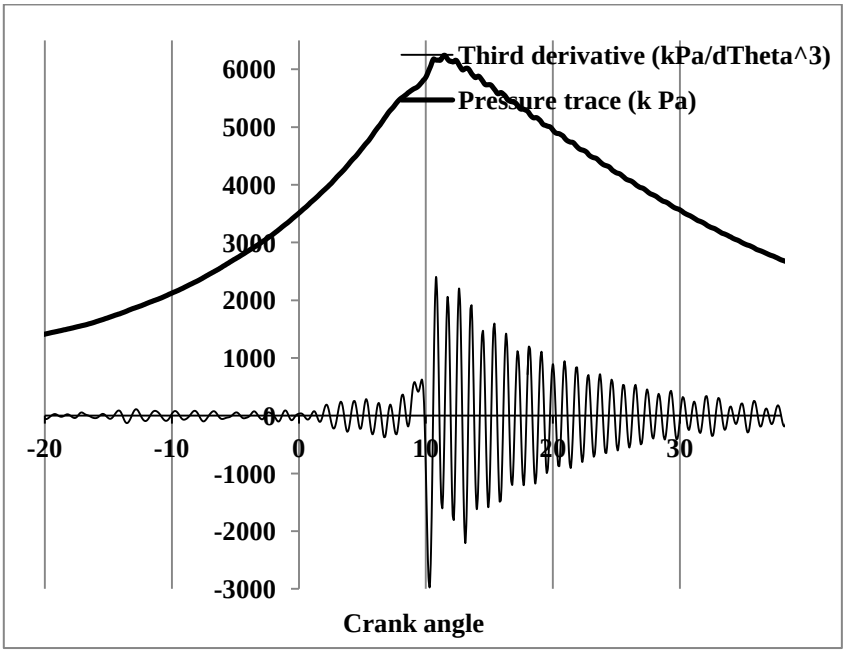

Figure 3-8 Pressure trace of a cycle with high knock and its third derivative

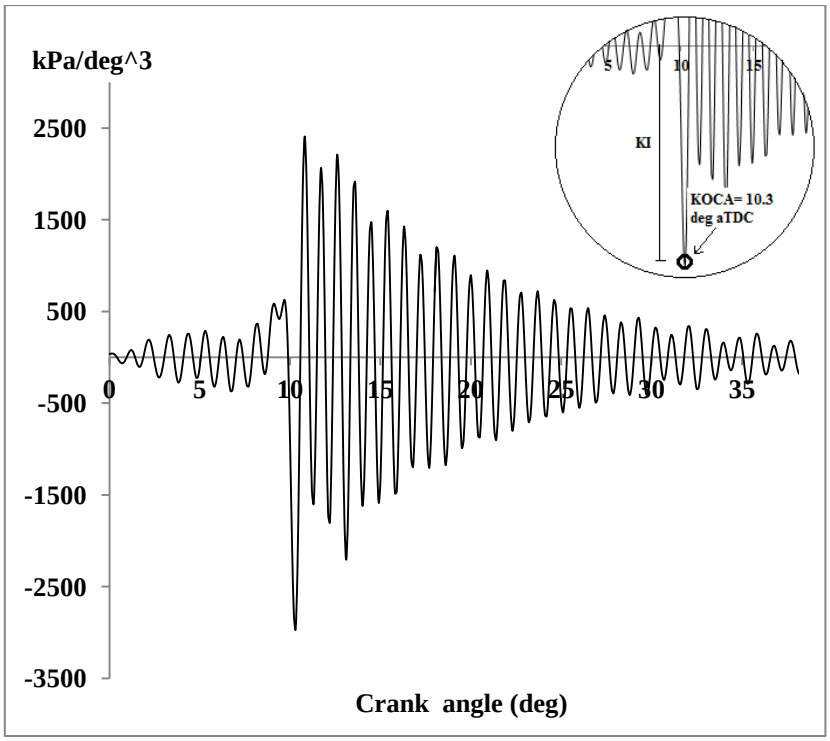

Figure 3-9 Filtered third derivative of pressure and the definition of an alternative knock intensity criterion and KOCA

3.6. EVALUATION OF EFFECTS OF INDIVIDUAL KNOCK INTENSITY ON INDIVIDUAL KOCA

To determine a representative KOCA corresponding to a particular engine operating conditions, an analysis of the influence of the cycle by cycle knock intensity on the cycle by cycle KOCA was carried out. High maximum FFT amplitude represents a high knock intensity cycle, while low maximum FFT amplitude corresponds to a low knock intensity cycle.

It is important to highlight the difference between the knock intensity (KI) defined in Section 3.4 and the individual knock intensity. KI is the reference knock intensity used for the MN measurements. The maximum FFT amplitude defines the individual knock intensity of each cycle in the engine. Figure 3-10 shows the individual knock intensity variability observed for the first 200 cycles. The maximum knock intensity reached is in the cycle number 59. The variability is caused by the random nature of the auto-ignition phenomenon.

To evaluate the effect a one-factor analysis of variance (ANOVA) was performed. The response variable was KOCA and the factor examined was the individual knock intensity represented by the maximum FFT amplitude of the cycle. The levels were defined as knock intensity ranges, which were equally spaced. The values were selected taking into account the maximum and minimum value of the maximum FFT amplitude obtained in the sample. Four replicas were performed for each knock intensity range to quantify the error of the experiment. The objective of the experiment was to determine if the average KOCA of four knock intensity ranges were equal or different, i.e., to determine whether individual cycle knock intensity affects the individual KOCA of each cycle. Taking into account the recommendation of Brunt et al.(1998), a sample of 1400 cycles was collected by using facility natural gas as reference fuel. Natural gas was selected to avoid the error of flowmeter measurements. The engine operating conditions and the maximum FFT variability of the first 200 cycles recorded are shown in Figure 3-10. The compression ratio was adjusted for achieving a stable KI ranging from 28 to 33. This KI guarantees high individual knock intensity values; therefore

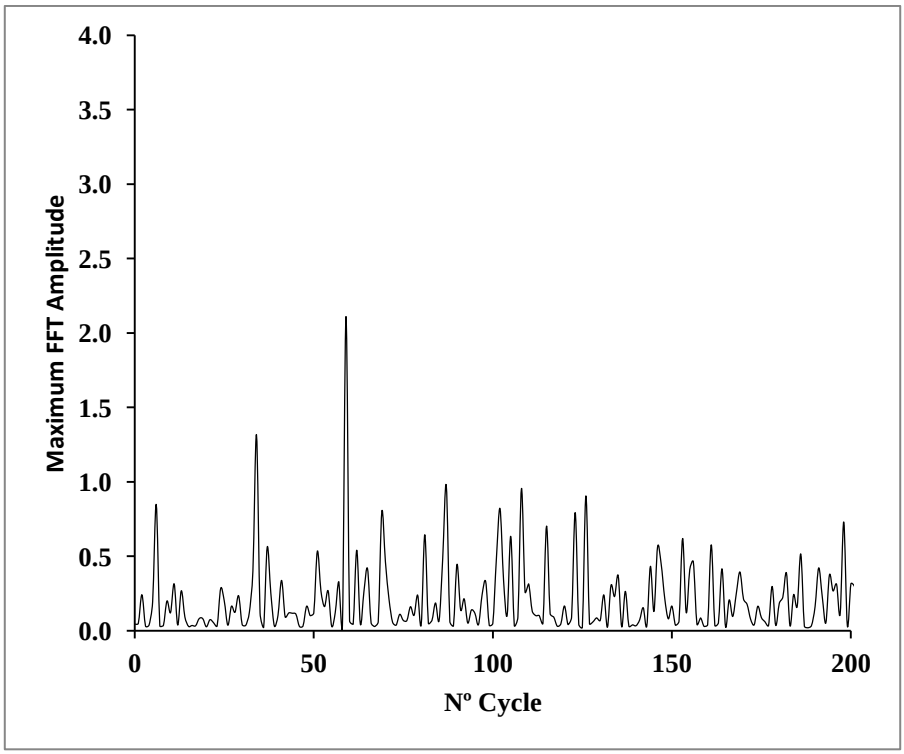

Figure 3-10 Cycle by cycle variability of the maximum FFT amplitude. Operating conditions in the experiment: stoichiometric operation; compression ratio: 11.54; Ignition Timing: 23.2º bTDC ; Inlet temperature: 40ºC ; Knock Index range :28-33; Fuel: facility natural gas.

more cycles with KOCA. The evaluation of the effect of KI on the characteristic KOCA of an engine operating conditions is out of the scope of this thesis.

A total of sixteen randomly cycles were selected per each level, grouped in four replicas (i.e., four KOCA values per replica). The averages of these values represent the characteristic KOCA value of each replica. Table 3-4 shows the KOCA measured for the different levels considered.

Table 3-4 The Analysis of Variance to determine the effect of individual knock intensity on KOCA of the cycle

KOCA (deg. aTDC)								
Maximum FFT Amplitude ranges	**Replica 1**		**Replica 2**		**Replica 3**		**Replica 4**	
0.25-0.49	5.69	8.19	10.8	8.1	7.19	9.89	7.5	10.8
	6.19	8.00	9.39	7.8	9.00	7.59	10.8	6.9
0.5-0.75	8.6	6.5	7.9	8.19	9.8	7.69	9.5	7.69
	6.8	8.19	9.1	8.89	8.69	9.89	7.9	8.6
0.76-1.0	9.8	9.8	8.3	8.1	8.3	10.00	8.6	7.8
	8.6	7.4	8.8	6.19	9.00	8.6	10.6	6.69
1.01>	9.8	7.00	10.1		8.3		7.9	
	9.8		6.9		5.5		10.3	

The sample did not contain very many cycles with knock intensity higher than 1.01; only nine data points were collected. The analysis performed revealed that there is not enough statistical evidence to conclude that averages KOCA of the levels considered were different. It is concluded that the individual knock intensity of each cycle does not affect the KOCA value of each cycle. This important result allows estimating KOCA as a function of the engine operating conditions by considering individual cycles regardless the individual knock intensity. The cycles with higher knock intensity were selected to quantify the characteristic KOCA. The representative KOCA for a given set of engine cycles is the average of KOCA of the individual cycles considered. This value depends on the operating engine conditions previously defined in the experiment.

3.7. RESULTS AND DISCUSSIONS

This section examines the relationship between KOCA and the engine operating conditions used in the MN measurement tests. For this analysis the reference fuels (CH_4/H_2 and CH_4/CO_2 fuel blends), and the test fuels ($CO/H_2/CO_2$ fuel blends) were considered. The unstretched laminar flame speeds of these mixtures were computed by using Gri-Mech. 3.0 (Smith G. et al., 1999) mechanism and the sub-routine PREMIX of Chemkin Pro® software. Figure 3-11 shows the correlations between the MN and laminar flame speed of the reference and test fuels. This high correlation is linked by the strong influence of the fuel composition on the MN and laminar flame speed of the fuels. The high concentration of the diluent both the reference fuels (CH_4/CO_2) and test fuels decrease the laminar flame speed and increases the MN of the fuels. A fuel with low MN has high concentration of hydrogen, which produces a high laminar flame speeds. According to Figure 3-12, there is no evidence of any relationship between KOCA and the laminar flame speed for both test fuels and reference fuels. This contrasts with the high relationship between MN and KOCA as shown in Figure 3-13. At constant MN the KOCA value is different for both reference fuels and test fuels. Both linear relationships have approximately the same slope. This trend is not present for fuels with MN greater than 100. These data points do not follow this trend due to the non-standard ignition timing was used. These data points are runs 2, 9 and 12 with MN of 135.5, 119.6 and 113.9 respectively. The ignition timing values used for these MN measurements were 21.2º, 25.0º and 22.0º bTDC respectively. These ignition timing values were used for two reasons: a) to achieve the reference knock intensity when compression ratio could not be further increased and, b) to obtain cycles with high knock to facilitate KOCA estimations. The ignition timing was often modified to obtain cycles with high knock for fuels with high knock resistance. For comparative purposes, only runs with the same ignition timing (15º bTDC) were considered. Most of the MN measurements were done by using the standard ignition timing as was originally propose by Leiker et al.,(1972). The strong influence of the ignition timing on KOCA is shown in Figure 3-14.

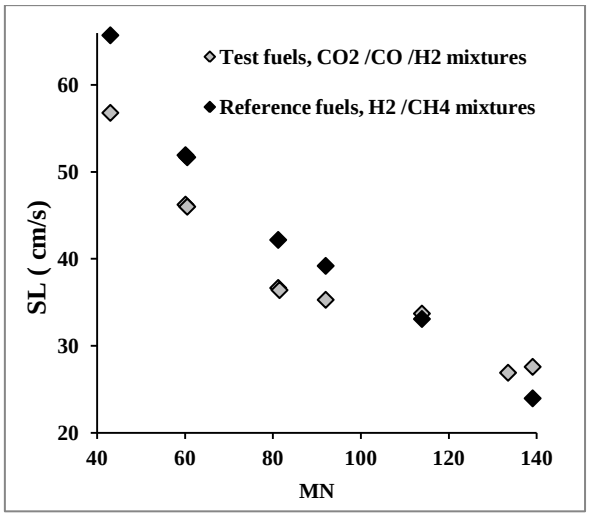

Figure 3-11 MNs vs laminar flame speeds for test and reference fuels used in the MN tests

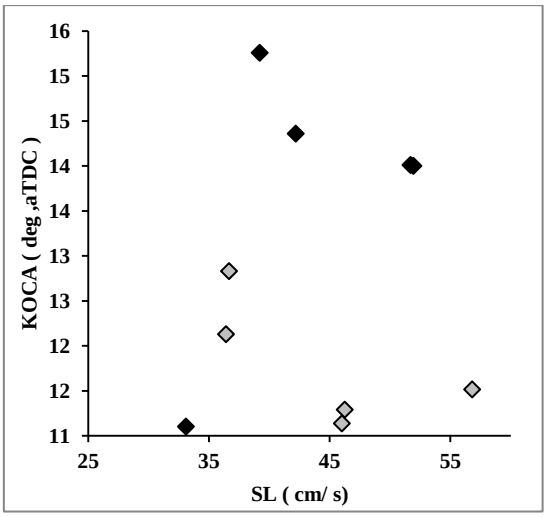

Figure 3-12 KOCA vs laminar flame speed of the reference and test fuel

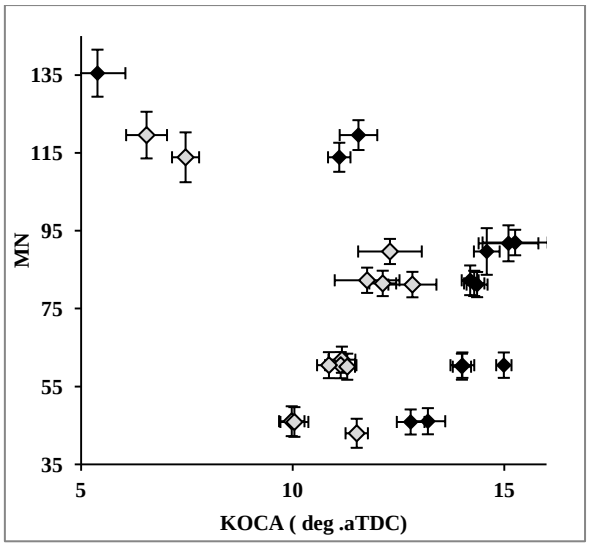

Figure 3-13 KOCA vs MN for both reference and test fuels

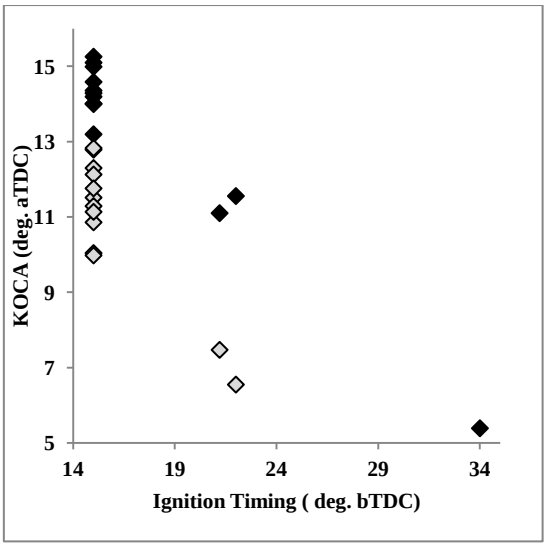

Figure 3-14 KOCA vs Ignition Timing for both reference and test fuels

This Figure shows that as ignition timing increases, (it advances with respect to the top dead center) KOCA value decreases following a linear trend. Similar results were obtained by Chun (1988) with 94 RON PRF at 1500 rpm and different equivalence ratios. Because the direct correlation between MN and critical compression ratio (CCR), it was observed that KOCA has the same trend with this parameter as it is observed in Figure 3-15.

In another hand, KOCA is influenced by the fuel composition as shown in Figure 3-16a, and Figure 3-16b. For the reference fuel blend, the high concentration of hydrogen (low CH_4/H_2 ratio) facilitates the auto-ignition phenomenon due to high auto-ignition

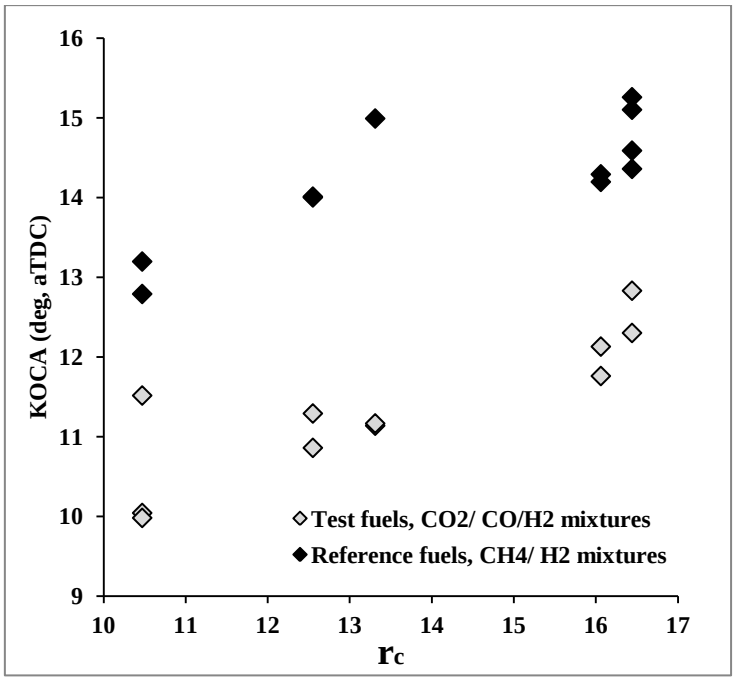

Figure 3-15 KOCA vs Critical Compression Ratio for both reference fuels and test fuels

tendency of hydrogen. The high concentration of hydrogen in the fuel increases the formation of critical intermediate species such as HO_2, OH, and H_2O_2 during the compression and combustion stages in the engine as was explained in detail in Chapter 2. In Figure 3-16-b the parameter $\alpha = H_2 * CO_2 * 100/CO$ was defined to take into account the effect of the composition of the test fuel on KOCA. The knock tendency is dominated by the hydrogen concentration in the fuel; in addition, there is a linear relationship between KOCA and the factor α.

Although KOCA values also depend on the CO concentration, the impact of H_2 concentration is stronger than CO concentration. An evaluation of the Pearson correlation coefficient between the fuel species and KOCA revealed a significant negative correlation between H_2 concentration and KOCA. If H_2 concentration increases in the fuel, KOCA decreases a factor of 0.82. The Pearson correlation coefficient between CO concentration and KOCA revealed that increasing CO concentration in the fuel, KOCA decreases by a factor of 0.04. High concentration of CO_2 in the fuel increases the MN of the fuel; in addition, KOCA moves away from the top dead center. According with Bika et al., (2011), when a binary fuel blend of H_2/CO is considered , CO concentration works as diluent, decreasing knock tendency of the fuels.

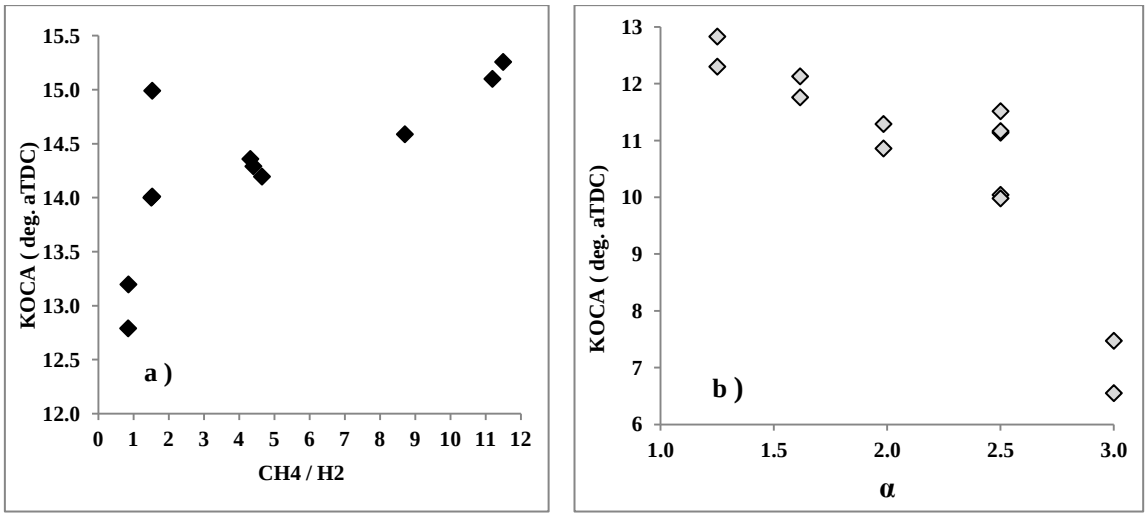

Figure 3-16 Effect of fuel composition on KOCA; a) reference fuels b) test fuels

The equivalence ratio was swept near to stoichiometric point in order to maximize the knock intensity and to achieve the desired KI. Theoretically maximum knock intensity is achieved at stoichiometric conditions; however, some runs required lean air fuels mixtures to achieve maximum knock intensity in the engine. The inhomogeneity of the air fuel mixture temperature and species concentration in the combustion chamber could explain this behavior. Figure 3-17-a shows the relationship between the equivalence ratio and KOCA, which was demonstrated in Chapter 4.

In this chapter, the combustion duration parameter (CD) was defined as the difference between the crank angle at 10 % of MFB corresponding to the start of the combustion and 90 % of MFB corresponding to the end of the combustion. According to the work developed by Rousseau et al.,(1999), the CD depends strongly on the boost pressure, equivalence ratio, ignition timing and fuel composition. However, there is not any relationship between CD and KOCA as shown in Figure 3-17-b. This result contrasts with the strong correlation between KOCA and the start of combustion (SOC) defined as 10% of MFB as shown in Figure 3-17-c. This behavior makes sense since KOCA depends on ignition timing and the unburned gas consumption is negligible during the ignition delay period. This linear correlation applies for fuels with different compositions and a constant ignition timing of 15º bTDC. Similar behavior was evidenced in the research develop by Chun (1988) with 94 RON PRF where KOCA has a linear correlation with 50% of MFB at constant ignition timing and equivalence ratio. The ignition delay or flame development period, is defined as the period of time between the ignition timing and the SOC in the engine. The relationship between

laminar flame speed and ignition delay is shown in Figure 3-17-d. Fuels with low laminar flame speed tend to start the combustion later than fuels with high laminar flame speed. Thus, fuels with high content of hydrogen have shorter ignition delay periods. According to the results obtained by Rousseau et al.,(1999), the effect of boost pressure on ignition delay is negligible and there are strong correlations of equivalence ratio and ignition timing with ignition delay.

Wobble index (WI) is a representation of the heating value of gaseous fuels. Relationship between the high heating value (HHV) of the fuels and KOCA was not found with the available data; however, when WI and KOCA were plotted an interesting trend was observed as shown in Figure 3-18-a. For the test fuels the trend is governed

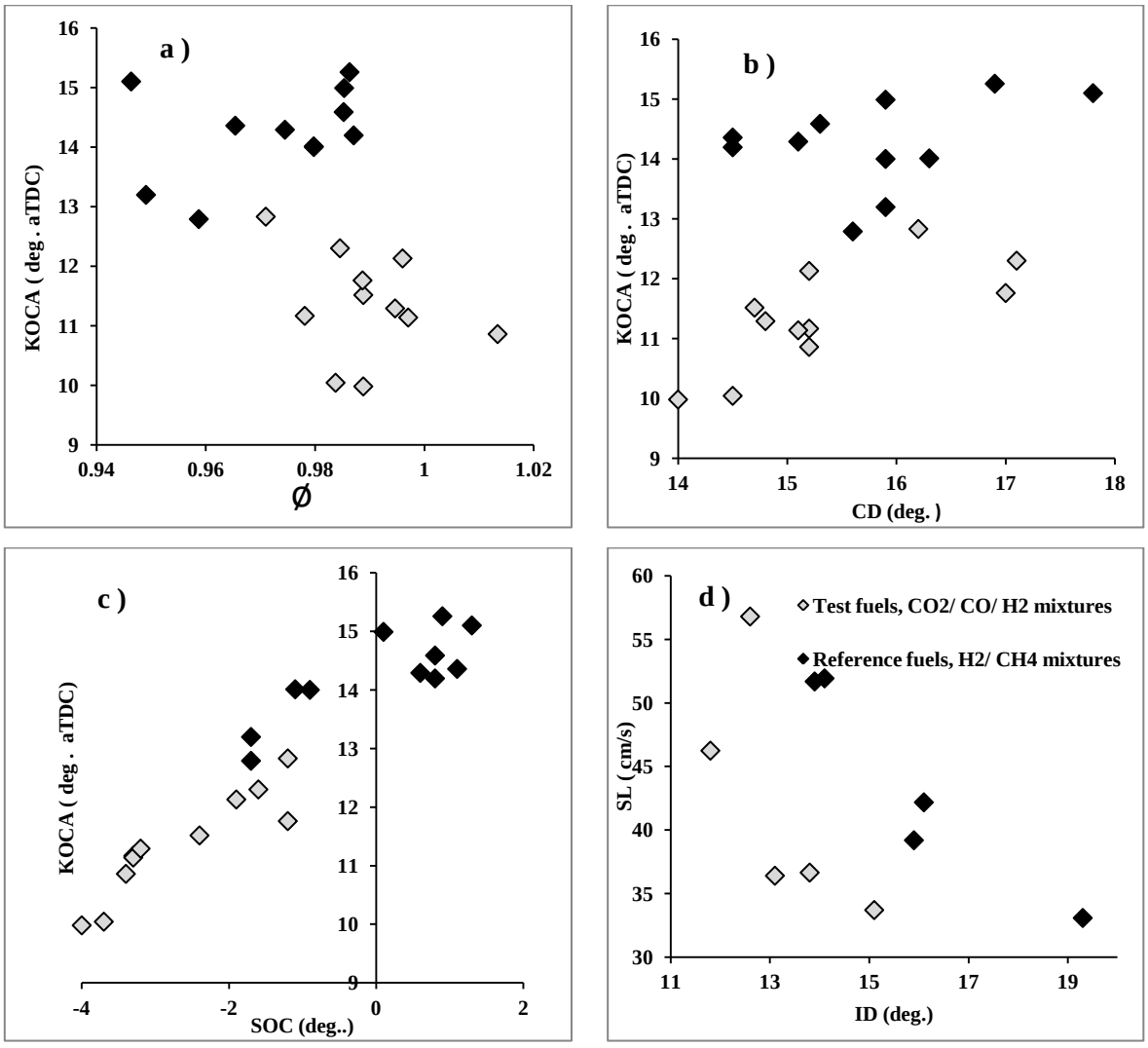

Figure 3-17 Effect of combustion parameters on KOCA both reference and test fuel. a) KOCA vs Ø; b) KOCA vs CD; c) KOCA vs SOC and d) SL vs ID

by the hydrogen concentration; the high hydrogen concentration in the fuel reduces KOCA. The WI of these fuels are almost the same according to the Figure 3-18-a.

For the reference fuels the high concentration of methane increases KOCA and the energy density of the fuels. The effect of the hydrogen moves KOCA toward the top dead center. This trend is governed by the fuel blend compositions; therefore for more general conclusion gaseous fuels with different compositions and WI values must be tested. The Net Mean Effective Pressure (NMEP) is linked with KOCA for both test fuel and reference fuel. According to Figure 3-18-b, KOCA increases as NMEP increases for all fuels tested. Reference fuels produce higher NMEP values in the engine due to the high HHV of the fuels.

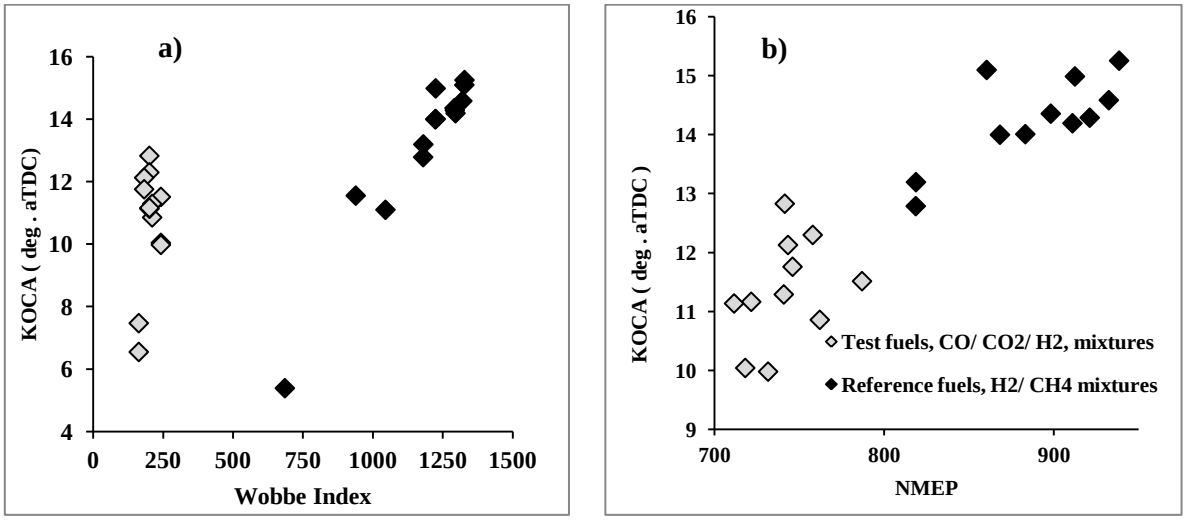

Figure 3-18 Trends between KOCA and a) Wobbe index b) NMEP

3.8. CONCLUSIONS

The most important conclusions derived from this chapter are described as follows:

- ✓ KOCA is not influenced by individual knock intensity. Therefore a characteristic KOCA can be computed as a function of a specific engine operating conditions.

- ✓ The MN of $CO/CO_2/H_2$ mixtures were measured experimentally. The MN predicted by using AVL software does not agree with the measured MN due to the high concentration of carbon dioxide and carbon monoxide. The regression model

developed is a good tool for MN estimation for fuels with high content of these species.

- ✓ There is a linear relationship between KOCA and MN regardless the fuel composition. The plotted data shows a linear trend for both reference fuels and test fuels. As MN increases, KOCA increases. This behavior is dominated by the hydrogen concentration in the fuels.

- ✓ Effects of ignition timing on KOCA are significative. This parameter controls the SOC in the combustion chamber and the KOCA value.

- ✓ There is a strong correlation between laminar flame speed and MN of the tested fuels. This relation is dominated by hydrogen concentration in the fuel. As MN increases, laminar flame speeds of the fuel decreases.

- ✓ Fuels with high concentration of hydrogen tend to decrease the values CD and KOCA. The SOC has a linear correlation with KOCA. The slope observed is positive both reference fuels and test fuels.

- ✓ Fuels with low laminar flame speed and high MN have large ignition delay when are used as fuels in an internal combustion engine.

Chapter 4

Auto-ignition Prediction in a CFR Fueled with CH_4/H_2 Mixtures by using a Detailed Chemical Kinetic Mechanism

4.1 INTRODUCTION

The engine knock phenomena and the use of chemical kinetic mechanism for auto-ignition modeling in spark ignited ICE fueled with gasoline and Primary References Fuels (PRF) have been widely studied in the recent decades (Stiebels et al., 1996; Russ,1996; Hajireza et al., 1997; Liu and Chen, 2009; Liu, 2010). These numerical predictions have been performed by considering different engine operating conditions and engine sizes by obtaining accurate results (Nakano et al., 1995). Accurate mechanisms have been developed and optimized with rapid compression machine data coming from experiments. This is the case of the well-known Shell mechanism, which is suitable for auto-ignition modeling of hydrocarbon fuels (Ho and Kuo, 1997). In contrast, few studies about auto-ignition modeling of gaseous fuels have been developed.

Alternative fuels coming from waste and renewable feedstock (Coal gas gasification,

Lignocellulosic gasification gas, Landfill gas, Biogas etc) are useful as fuel for ICE applications. The MN of these fuels can vary from 30 to 130 MN what requires some efforts oriented for understanding auto-ignition phenomena. A predictive knock model that uses a two steps mechanism for CH_4 oxidation modeling was coupled with a low temperature end gas thermodynamic model (Ho et al., 1996). The knock onset estimations were carried out for fuel blend mixtures of methane, propane and heptane. A more complex model was implemented by Trijselaar (2012) who used Gri-Mech 3.0 as reference mechanism to estimate onset of knock in a 150 kW four stroke natural gas engine. A good accuracy in the pressure trace estimation was achieved; however, there was not evidence of estimation of KOCA. The knock onset was detected by a knock criterion proposed by Karim and Gao (1992). Studies related to gaseous fuels auto-ignition have been focused in the knock resistance and MN measurements (Malenshek and Olsen, 2009; Ryan et al., 1993); however, the chemistry involved in the phenomenon has been not evaluated. Based on the foregoing, it is required to verify if there is a kinetic model that allows modeling auto-ignition of gaseous fuels with accuracy.

The objectives of this chapter are described as follows:

- ✓ To determine the effects of the engine operating conditions and the fuel MN on KOCA and,

- ✓ To verify the accuracy of a detailed chemical kinetic mechanism for auto-ignition crank angle prediction.

The observations done in Chapter 3 about the correlations of MN and engine operating conditions were evaluated through two designs of experiments. The reference mechanism used for auto-ignition modeling was selected after an exhaustive analysis developed in Chapter 2. This analysis evaluated the kinetic model performance for ignition delay time estimations. The kinetic model was coupled with a two-zone engine model for predicting the auto-ignition crank angle of CH_4/H_2 mixtures at different engine operating conditions. These mixtures were the primary reference fuels used for measuring the MN of gaseous fuels. The simulations were developed in the Close Internal Combustion Engine Simulator of Chemkin Pro® software. Moreover, a methodology was proposed to determine experimentally the input combustion

parameter required for simulations. A new set of equations based on the first law of thermodynamic and ideal gas law were developed for estimating the IVC unburned gas temperature, residual gas fraction and residual gas temperature.

4.2. EXPERIMENTAL SETUP

The engine feature description, the gas blending, exhaust gas and intake air system layout were described in detail in Chapter 3.

4.3. DESIGN OF EXPERIMENT

The aim of this section is to determine the effects of ignition timing, equivalence ratio and fuel compositions on KOCA. Also, the study of the effect of boost pressure on KOCA was a concern of importance due to the increment use of the gaseous fuels in turbocharged ICE. For these purposes, two design of experiment was carried out and described below. The binary fuel blends of CH_4/H_2 were selected as reference fuels due to two reasons: knock intensity stability under engine knocking conditions and the reduction of the effects of the flowmeters and methodology uncertainties on the conclusions obtained.

4.3.1 Effects determination of IT, ∅ and MN on KOCA. In Chapter 3 was evidenced some trends between engine operating parameters and KOCA, which were not studied from a statistical point of view. It is well known that engine operating conditions influence the auto-ignition tendency of fuels in the engine's combustion chamber. These tendencies were observed in a natural gas engines by Soylu and Van Gerpen, (2003), where the effect of ignition timing, compression ratio, propane addition, inlet pressure and temperature on auto-ignition were examined. Both the propane addition to natural gas and hydrogen addition to methane decrease the MN; therefore increase the auto-ignition tendency. Similar observations were found for compressed natural gas engine with addition of Liquefied Petroleum Gas (LPG). This addition modify the mixture MN, increasing or decreasing its auto-ignition tendency depending on the LPG concentration (Schiffgens et al., 1994). The variability of the

fuel's MN requires changes in the engine operating conditions. The effects of these modifications to improve the required MN of the engine were summarized in Table 4-1.

Although these effects have been evidenced, there have not been studies oriented to quantify them; especially the effects on the auto-ignition crank angle. In this chapter, these effects were quantified through a factorial 2^3 design of experiment with axial and central runs. The axial and central runs are suitable to detect curvature in the middle points of the factors selected (Montgomery, 2008). It is well known that the factors described in Table 4-1 influence the auto-ignition tendency of the fuels. However, only three controllable factors were considered: ignition timing, equivalence ratio, and MN. The other controllable factors were kept constant, i.e., boost pressure, air-fuel inlet temperature, knock intensity, output power and engine speed as shown in Figure 4-1. The variables of interest were KOCA and the critical compression ratio (CCR) required for achieving the desired knock intensity. Figure 4-2 shows a graphical representation of the experiment and the levels considered per each factor.

Table 4-1 Action and effect of engine operating conditions on knock tendency under stoichiometric and lean conditions

	EFFECT					
	Stoichiometric			***Lean***		
ACTION	***Tendency to knock***	***ή***	***NO_X***	***Tendency to knock***	***ή***	***NO_X***
Retarded ignition	++	--	o	++	-	++
Reduced load	+	--	o	+	-	+
Exhaust gas recirculation	++	o	+	++	o	++
Reduced mixture temperature	++	+	o	++	+	++
Reduced mixture cooling water temperature	+	o	o	+	o	+
Reduced speed	++	+	o	+	+	+
Reduced compression ratio	++	--	o	++	-	++

Nomenclature: (++) very effective/positive, (+) effective/positive, (o) no effect, (-) negative, (- -) very negative. Adapted from (schiffgens et al.,1994)

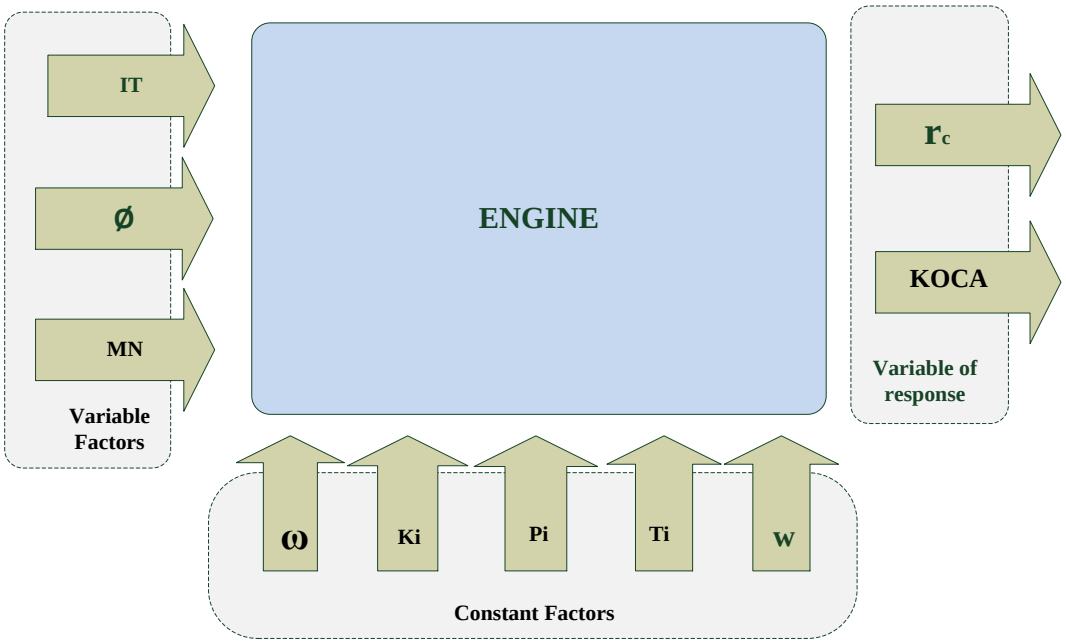

Figure 4-1 Constant , variable factors and variables of response considered in the factorial design of experiment

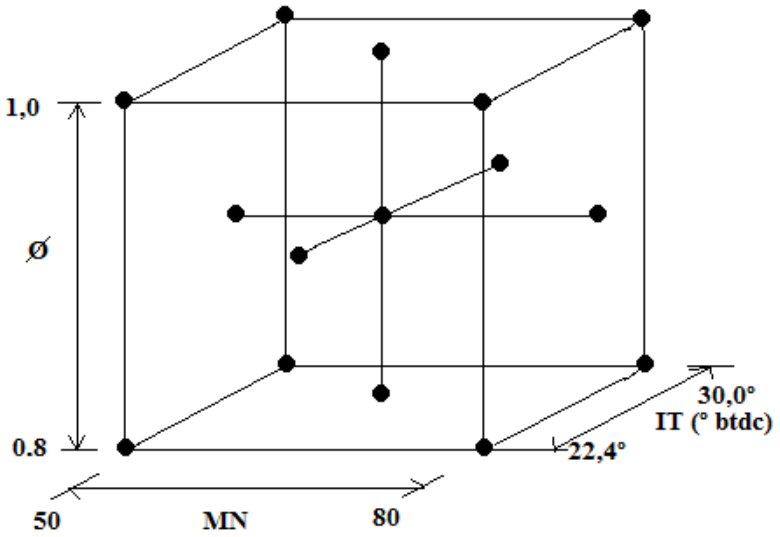

Figure 4-2 Graphical representation of the 2^3 factorial design of experiment with central and axial runs

Four replicas were run for the central points and two replicas for the remaining points. The runs were conducted randomly to mitigate the effect of hidden variables. Preliminary tests were performed in order to select suitable levels that allow having stable knock intensity and free backfiring engine operations.

4.3.2 Influence of boost pressure on KOCA. Effect of Boost pressure on KOCA was evaluated through a one-factor analysis of variance (ANOVA). The variable of response was KOCA and the levels were the typical boost pressure of natural aspirated and turbocharged spark ignited ICE. These values were: 80, 110, 135 and 160 kPa. Two replicas of the experiment were performed. The other factors were kept constant, including the knock intensity. The fuel composition was kept constant to reduce the flowmeters uncertainty at stoichiometric conditions where maximum knock intensity was reached. The compression ratio was increased until achieve the desired reference knock intensity in the engine. This methodology was employed in each point of the experiment. Table 4-2 shows the engine operating conditions and the general test information.

Table 4-2 Engine operating conditions and general test information

Test Parameters	Factorial 2^3	ANOVA
Fuel	Variable	65%CH_4/35%H_2
Equivalence ratio:	Variable	Stoichiometric
Boost Pressure (kPa):	101	Variable
Intake air temperature (°C):	40	40
Engine speed (rpm):	940	940
Compression ratio:	Variable	Variable
Knock Intensity :	30	30
Ignition Timing (^{o}bTDC):	Variable	22.4
Average time per test (min):	3	3
Output net power (kW):	2	2
Number of cycles:	1400	1400

4.4. TWO ZONE AUTO-IGNITION MODEL

In this section a detailed description of the two- zone auto-ignition model is performed. The auto-ignition model implemented is compounded for a two-zone ICE coupled with a detailed chemical kinetic mechanism. The objective of the model is to predict KOCA by using the actual operating engine conditions defined in the factorial design of experiments.

4.4.1. Chemical kinetic mechanism. The use of chemical kinetics mechanism for auto-ignition modeling has been widely studied for liquids fuels such as gasoline. As mentioned in Chapter 2, this thesis used Gri-Mech. 3.0 (Smith et al., 1999), a detailed chemical kinetics mechanism compound by 365 elementary reactions and 53 species. The thermochemical properties of the chemical species were estimated by using the Nasa polynomial coefficients.

4.4.2. Engine model. A set of energy, mass and species equations were solved simultaneously in order to model the engine. The input parameters that must be supplied to the software were: combustion chamber geometry, Wiebe function constants, compression ratio, combustion parameters, fuel composition, initial air-fuel temperature and pressure, residual mass fraction of burned gasses. The next section describes the methodology employed for estimating the combustion parameters of the test fuels.

4.4.3. Combustion parameter estimations. The estimations of the SOC and EOC crank angle in ICE is difficult (Heywood, 1988). Some authors have defined SOC as the crank angle corresponding the 1, 5 or 10% of MFB (Rousseau et al., 1999); however these percentages are arbitrary selections. In this chapter a method to estimate the SOC, ignition delay (ID) and combustion duration (CD) through the indicator diagram analysis was proposed. This technique takes advantage on the fact that there is a linear relationship between $\log_{10}(P)$ and $\log_{10}(V/V_{max})$ during the compression and expansion phase in the engine as shown in Figure 4-3. When the first derivative of $\log_{10}(P)$ with respect to $\log_{10}(V/V_{max})$ was calculated, it was observed that this value keeps constant until the combustion begins to change the slope as shown in Figure 4-4. The period of time between the ignition timing and the point where the combustion changes the linear trend was defined as Ignition Delay (ID) or flame development period. Mathematically, the ID was defined as:

$$ID = \theta_{soc} - \theta_{IT} \qquad \text{Eq. 4-1}$$

In this chapter, the crank angle at SOC (θ_{SOC}) was defined as the crank angle corresponding to the first change of slope as shown in Figure 4-4. This definition was based on the observations done to the first derivative of the indicator diagram of the

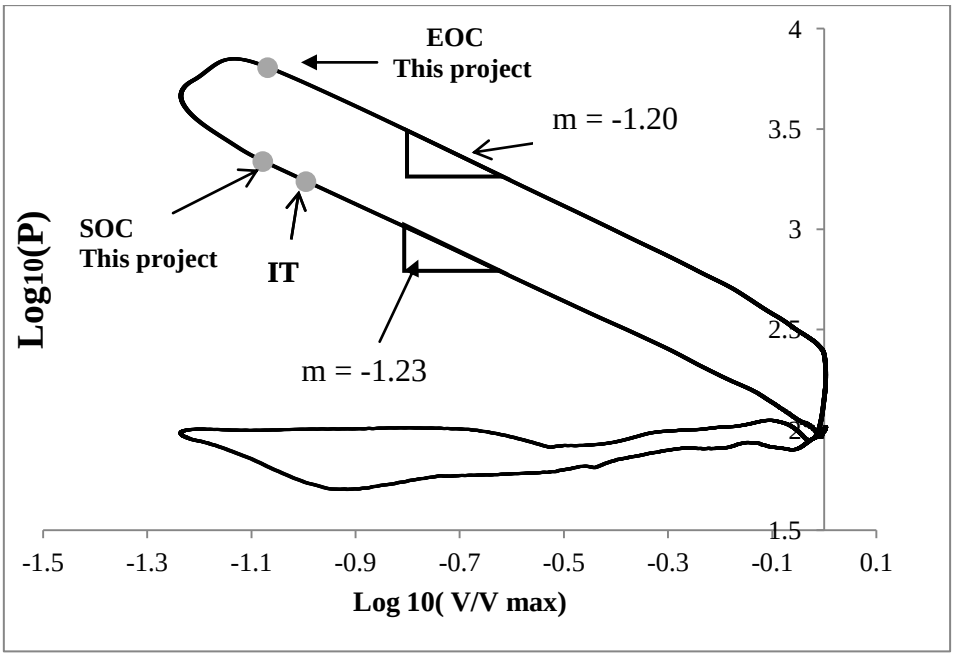

Figure 4-3 Indicator diagram with the estimated IT, SOC and EOC. Engine operating conditions: compression ratio:17.3 , Ø=0.8 , IT=22.4º bTDC, fuel: 80% CH_4 20%H_2

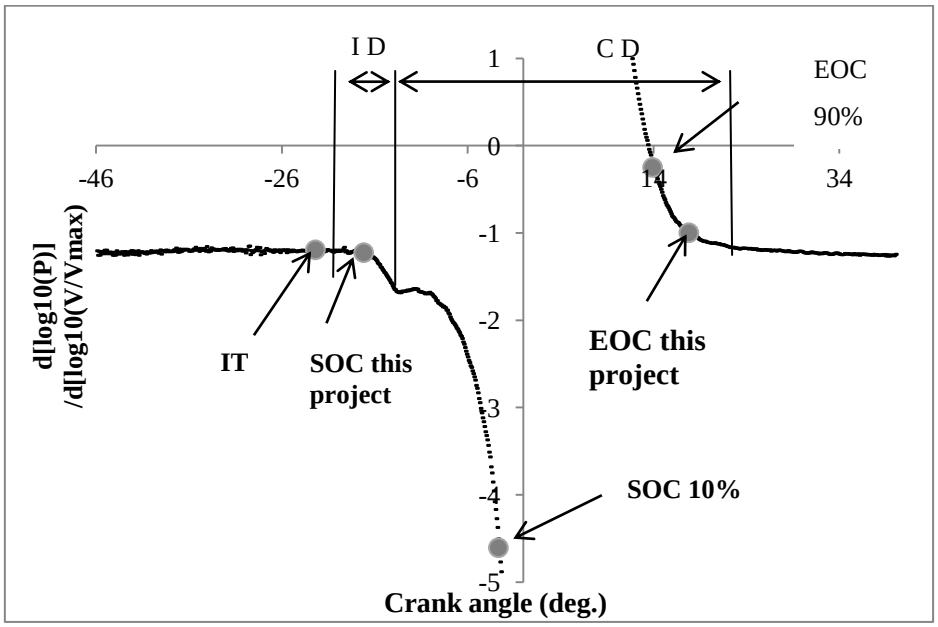

Figure 4-4 Graphical estimation of SOC, EOC, ID and CD from indicator diagram

engine at motoring operation, where there is not combustion. It was evidenced that near to TDC where maximum gas compression takes place, there is a change of slope because of the derivative tends to infinity near to this point. Because of the combustion, is concluded that the first change of slope corresponds to combustion effects and the

second due to proximity to the TDC and combustion effects. The end of combustion was defined as the crank angle where the product PV was maximum (Swarts, 2004), where V is the combustion chamber' volume and P is the in-cylinder pressure. The difference between EOC and SOC was known as Combustion Duration (CD). Mathematically, CD was defined as:

$$CD = \theta_{EOC} - \theta_{SOC} \quad \text{Eq. 4-2}$$

Figure 4-4 shows a comparative analysis of the SOC and EOC defined in this thesis and the SOC and EOC defined as 10 % and 90 % of MFB respectively. It is evident that actual values of these parameters are close to those defined in this chapter.

4.4.4. Polytropic constant estimations from indicator diagram. Additional information can be deduced from the indicator diagram. It can be demonstrated that:

$$\frac{d[log_{10}(P)]}{d\left[log_{10}\left(\frac{V}{V_{ref}}\right)\right]} \approx m \quad \text{Eq. 4-3}$$

where m is the negative of the polytropic coefficient n of the compression phase in the engine. This formulation is valid from any reference crank angle defined in the compression phase. In this chapter, the IVC crank angle was defined as the reference point. The linear correlation between $log_{10}(P)$ and $log_{10}(V/V_{ref})$ during the compression phase can be expressed in terms of :

$$log_{10}P = m * log_{10}\left(\frac{V}{V_{ref}}\right) + log_{10}(P_{ref}) \quad \text{Eq. 4-4}$$

where m is the slope of the line. To validate mathematically the Equation 4-4, it was considered the in-cylinder pressure in motoring operation, which can be modeled by means of the polytropic equation defined in equation Eq. 4-5 (Cuddihy, 2014):

$$P_m = P_{ref}\left(\frac{V_{ref}}{V}\right)^n \qquad \text{Eq. 4-5}$$

By replacing Equation 4-5 into the left of Equation 4-4 ($P = P_m$) , removing the logarithm from the equation and after of some algebraic calculations it is concluded that $n = -m$, i.e, the slope of the line represent the negative of the polytropic coefficient of the compression and expansion phase of the engine. This conclusion can be generalized for the combustion phase in the engine. The combustion phase of the engine can be modelled as isochoric process, therefore the polytropic coefficient must tend to infinity, $n \to \mp\infty$ (Moran, S. et al., 2010). This trend is observed in Figure 4-4 during the combustion process. Polytropic coefficient for compression and expansion of CH_4/H_2/Air mixture were 1.20 and 1.23 respectively. Similar observations can be found in (Heywood, 1988) for conventional fuels and (Pipitone et al., 2015) for gasoline propane mixtures. For improving accuracy in the estimation of this parameter, a filtered engine pressure trace is required due to the effect of the signal noise could affect its estimation.

4.4.5. MFB estimation from the in-cylinder pressure data. To improve the accuracy of the engine model, MFB was estimated by using the in-cylinder pressure data and the combustion chamber's volume at ignition timing as reference (Zhu et al., 2003). The pressure difference resulting from combustion between two crank angles can be estimated as:

$$\Delta P' = P_{(i+1)} - P_{(i)}\left(\frac{V_{(i)}}{V_{(i+1)}}\right)^n \qquad \text{Eq. 4-6}$$

where $P_{(i+1)}$, $V_{(i+1)}$, $P_{(i)}$ and $V_{(i)}$ are the succeeding and preceding pressure and volume values and n is the polytropic coefficient determined experimentally. The net pressure without any change of volume from ignition timing can be estimated by multiplying the pressure difference defined in Equation 4-6 by a factor $V_{(i)}/V_{(IT)}$:

$$\Delta P(i) = [\Delta P'] \left[\frac{V_{(i)}}{V_{(IT)}}\right] \quad \text{Eq. 4-7}$$

The net pressure at each crank angle was defined as:

$$P_{NET(i)} = P_{NET(i-1)} + \Delta P_{(i)} \quad \text{Eq. 4-8}$$

where $P_{NET(i)}$ and $P_{NET(i-1)}$ are the evaluated and the preceding net pressure respectively. Once established the EOC, the experimental MFB can be calculated from Equation 4-9.

$$X_b = \frac{P_{(i)NET}}{P_{(EOC)NET}} \quad \text{Eq. 4-9}$$

This methodology can be validated by estimating the MFB through the methodology developed by Rassweiler and Withrow (Heywood, 1988), who postulated that MFB can be estimated as:

$$X_b = \frac{P^{1/n}V - P_{IT}^{1/n}V_{IT}}{P_{soc}^{1/n}V_{soc} - P_{IT}^{1/n}V_{IT}} \quad \text{Eq. 4-10}$$

where P_{IT} , P_{soc}, V_{IT}, and V_{soc} are the pressure and volumes at ignition timing and EOC respectively.

MFB profiles as a function of crank angle can be modelled by means of the Wiebe function. The Chemkin Pro® software requires as input data the a and m constants and the combustion parameters determined by using the methodology proposed in this chapter. The Wiebe function is defined as (Heywood, 1988):

$$X_b = 1 - exp\left[-a\left(\frac{\theta - \theta_{SOC}}{CD}\right)^{m+1}\right] \quad \text{Eq. 4-11}$$

where a and m are adjustable constants that define the shape of the curve. When the ignition timing is considered as SOC time, the constants a, b and the CD value change. It was observed a correlation between these constants and those defined in this thesis. The Wiebe function defined with IT as SOC was defined as:

$$X_b = 1 - exp\left[-a'\left(\frac{\theta - \theta_{IT}}{CD'}\right)^{m'+1}\right] \quad \text{Eq. 4-12}$$

where $a'$and b' are the shape constants of the function. The correlations founded between the constants and combustion duration parameters are:

$$m' = m + 1 \quad \text{Eq. 4-13}$$

$$a' = a + \varphi \quad \text{Eq. 4-14}$$

$$CD' = ID + CD \quad \text{Eq. 4-15}$$

In equation 4-14, φ is a tuning parameter, which value is approximately between $0{\sim}0.3$. Figure 4-5 illustrates a comparison between the experimental MFB and the two approaches considered. The former approach is the MFB curve deduced by considering that SOC is equal to the ignition timing. The latter approach is the curve deduced from Wiebe function with the constants estimated with the methodology proposed in this thesis. Although the constants used in both methods were accurate, the one developed in this project is more representative of the combustion process. In Figure 4-6 was compared the SOC and EOC of a mixture of 80% CH_4 20%H_2 at two different engine operating conditions. It was observed that the combustion parameters estimated by using the methodology proposed is more accurate than those estimated by considering the percentages of MFB.

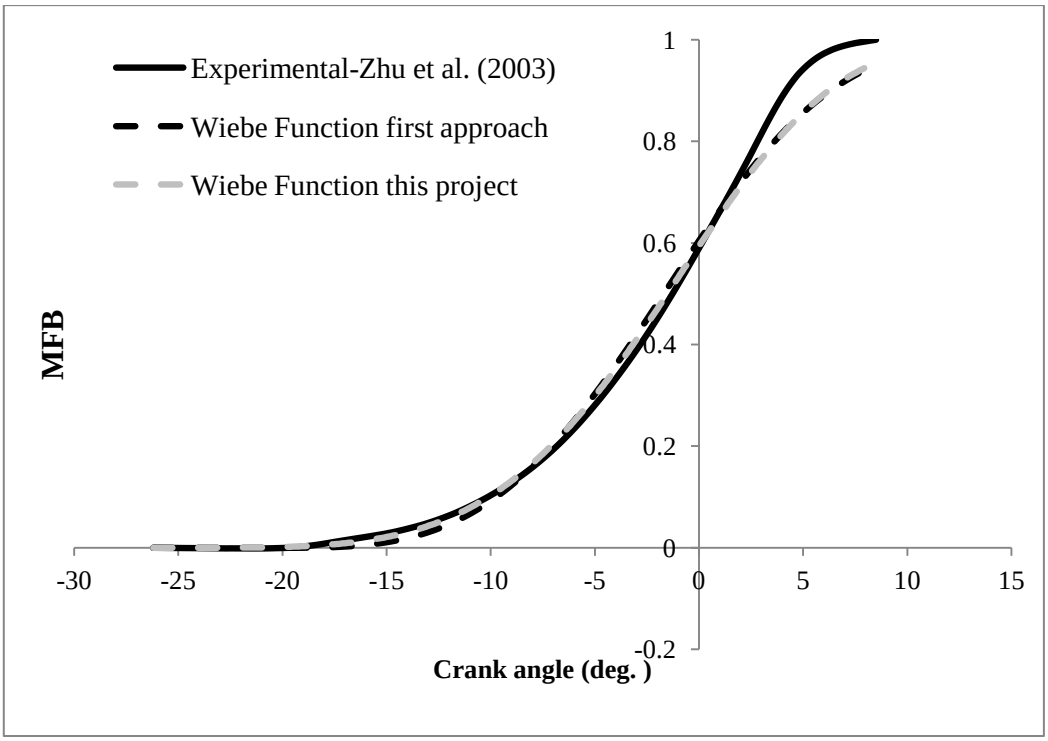

Figure 4-5 MFB estimated by using Wiebe function. First approach consider SOC equal to IT. Engine operating conditions: compression ratio: 10.4; Ø=0.9 ; IT=26.2º bTDC; fuel: 50% CH_4 50%H_2

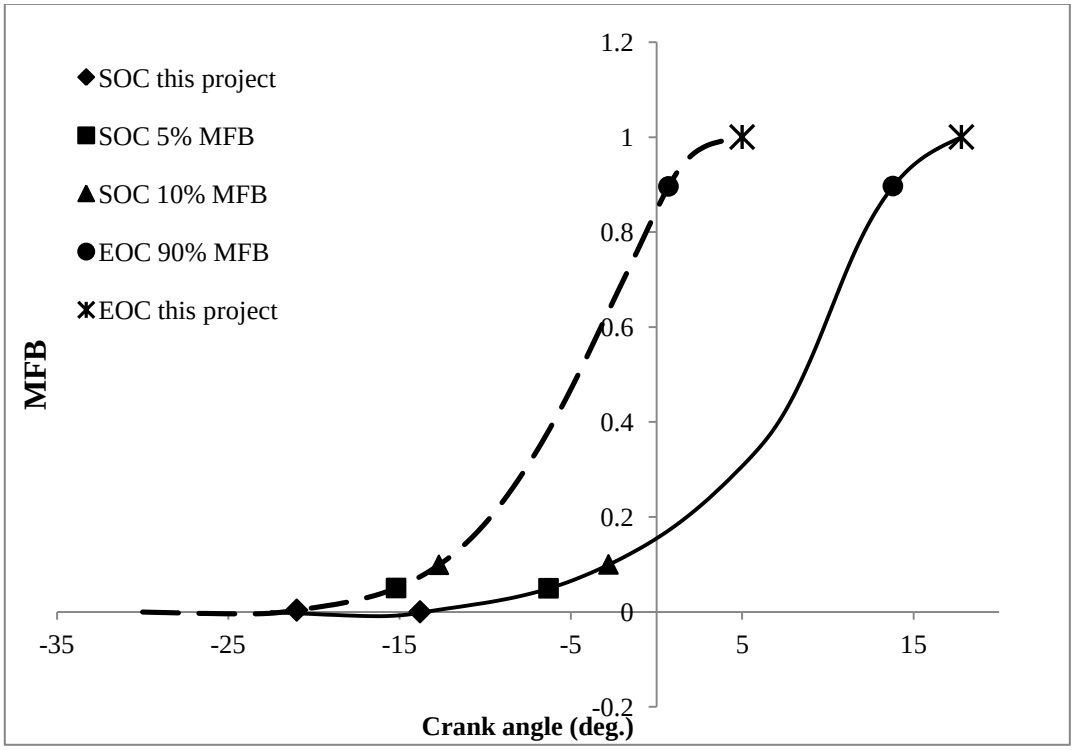

Figure 4-6 SOC, EOC estimation of 80% CH_4 20%H_2 mixture. Dashed lines: IT: 30° bTDC; Compression ratio:11.2 ; stoichiometric mixture. Solid line: Compression ratio: 17.3; Ø=0.8; IT=22.4º bTDC

4.4.6. Residual mass fraction estimation. Residual mass influences the combustion characteristics of the fresh charge in the engine's combustion chamber due to its effects on the mass charge, temperature and laminar flame speed of the fuel. Its strong influence on auto-ignition is based on its capacity for increasing slightly the MN of the fuel. To take into account this effect, a residual mass fraction model was considered. The residual mass fraction was defined as (Fox, Cheng, and Heywood, 1993):

$$\mathrm{X_r} = \frac{1}{r_c}\left(\frac{P_e}{P_i}\right)^{\frac{1}{\gamma}} \emptyset \qquad \text{Eq. 4-16}$$

where r_c is the compression ratio of the engine, $\emptyset$ the equivalence ratio, and P_e/P_i is the exhaust and inlet gas pressure ratio in the engine. The residual mass fraction in the model was considered as carbon dioxide. This equation has been used previously by Cuddihy, (2014) for predicting the engine performance.

4.4.7. Inlet Valve Close air fuel temperature estimation. In this section, a thermodynamic model to estimate the unburned gas temperature at IVC was developed. It was considered a transient filling process, with heat transfer coming from the wall cylinder. Residual gas from the exhaust process was considered. The intake gas pressure was considered constant along of the process. The homogeneous air fuel mixture was assumed to be ideal gas with homogenous properties in the combustion chamber. Kinetic and potential energy effects were negligible. The intake process begins at 10º aTDC and ends at 34º aBDC. The volumetric efficiency was assumed to be equal to 1, i.e., the air fuel mixture fills the entire volume cylinder during the intake process. Taking into account these assumptions, the energy balance was defined as:

$$Q - W + m_i h_i = m_2 u_2 - m_r u_r \qquad \text{Eq. 4-17}$$

where $m_i h_i$ is the enthalpy of the fresh mixture, $m_2 h_2$ is the final enthalpy of mixture and $m_r u_r$ is the residual gas internal energy . The heat transfer Q was considered to come from the cylinder wall. The work made by the fresh air fuel mixture on the piston head was defined as:

$$W = \int_{V_1}^{V_2} pdV \qquad \text{Eq. 4-18}$$

where $V_1$and V_2 are the initial and final combustion chamber volume respectively. The mass balance was defined as:

$$m_i = m_2 - m_r \qquad \text{Eq. 4-19}$$

From ideal gas law and constant specific heat capacity assumption, the enthalpy and internal energy were defined as:

$$h(T) = \int_0^T c_p dT = \tilde{c}_p \int_0^T dT = \tilde{c}_p T \qquad \text{Eq. 4-20}$$

$$u(T) = \int_0^T c_v dT = \tilde{c}_v \int_0^T dT = \tilde{c}_v T \qquad \text{Eq. 4-21}$$

where the reference point has been establish to be 0K where $h(0) = 0\,kJ/kg$ (Moran et al., 2010). In addition, it is well known that specific heat capacity at constant volume is related with heat specific ratio as:

$$\frac{\tilde{c}_p}{R} = \frac{1}{\gamma - 1} \qquad \text{where} \qquad \boldsymbol{\gamma = \frac{\tilde{c}_p}{\tilde{c}_v}} \qquad \text{Eq. 4-22}$$

The ideal gas relation of specific heat capacity $\tilde{c}_p = R + \tilde{c}_v$ was employed. Equation 4-18, Eq.4-19, Eq. 4-20, Eq.4-21 and Eq. 4-22 were replaced in Equation 4-17 to obtain after of some simplifications the following equation:

$$\frac{Q}{PV_{IVC}} - \frac{\gamma}{\gamma - 1}\left[1 + (x_r - 1)\frac{T_i}{T_{IVC}} - \frac{x_r}{\gamma}\frac{T_r}{T_{IVC}}\right] + \frac{V_{IVO}}{V_{IVC}} = 0 \qquad \text{Eq. 4-23}$$

It was observed that the end and the start of the process are the end and the start of the intake process in the engine. This equation relates heat transfer coming from cylinder wall, residual mass fraction, the fresh air fuel temperature and the temperature at IVC

time. Moreover, it takes into consideration actual valve time events. This equation can be validated by considering the following assumptions a) the start and the end of the intake process occur in the top dead center and the bottom dead center respectively and b) the process is adiabatic. Table 4-3 shows a comparative analysis between the equations that are deduced from Equation 4-23 and those that are deduced by considering the above assumptions. The latter equations agree with those reported by Heywood (1988) by considering gasoline as fuel: In these equations Q_{LHV} represents the fuel's low heating value and p_e/p_i is the exhaust and inlet gas pressures ratio.

It is important to highlight that the relation V_{IVO}/V_{IVC} in Equations 4-25 and 4-27 becomes into the compression ratio when valve events occur at top dead center and bottom dead center. Also in Equation 4-24 the expression V_{IVC}/V_2 becomes into compression ratio as V_2 is the clearance volume of the combustion chamber. In the same equation the expression V_{EVO}/V_2becomes to be equal to 1.

Table 4-3 Comparison between the equations developed in this thesis and those reported by Heywood (1988)

(Heywood,1988)	This thesis	
$x_r = \frac{1}{r_c}\frac{(p_e/p_i)^{1/\gamma}}{\left[1+\frac{Q_{LHV}}{\alpha(A/F)\check{c}_v r_c^{(\gamma-1)}}\right]^{\frac{1}{\gamma}}}$	$x_r = \left(\frac{p_e}{p_i}\right)^{\frac{1}{\gamma}}\left(\frac{V_{EVO}}{V_{IVC}}\right)\left[1+\frac{Q_{LHV}}{\alpha(AFR)c_v(V_{IVC}/V_2)^{\gamma-1}}\right]^{-\frac{1}{\gamma}}\left(\frac{V_{EVO}}{V_2}\right)^{-1}$	**Eq. 4-24**
$\frac{T_i}{T_{IVC}} = \frac{1-\left[\frac{1}{\gamma r_c}\right]\left[\frac{p_e}{p_i}+\gamma-1\right]}{1-x_r}$	$\frac{T_i}{T_{IVC}} = \frac{1-\frac{1}{\gamma}\left[\frac{V_{IVO}}{V_{IVC}}\right]\left[\frac{p_e}{p_i}+\gamma-1\right]}{1-x_r}$	**Eq. 4-25**
$\frac{T_r}{T_{IVC}} = \left(\frac{p_e}{p_i}\right)^{\frac{\gamma-1}{\gamma}}\left[1+\frac{Q_{LHV}}{\alpha(A/F)\check{c}_v r_c^{\gamma-1}}\right]^{\frac{1}{\gamma}}$	$\frac{T_r}{T_{IVC}} = \left(\frac{p_e}{p_i}\right)^{\frac{\gamma-1}{\gamma}}\left[1+\frac{Q_{LHV}}{\alpha(AFR)c_v(V_{IVC}/V_2)^{\gamma-1}}\right]^{\frac{1}{\gamma}}$	**Eq. 4-26**
Where $\alpha = \frac{T_i}{1-\left[\frac{1}{\gamma r_c}\right]\left[\frac{p_e}{p_i}+\gamma-1\right]}$	Where $\alpha = \frac{T_i}{1-\frac{1}{\gamma}\frac{V_{IVO}}{V_{IVC}}\left[\frac{p_e}{p_i}+\gamma-1\right]}$	**Eq. 4-27**

The unburned gas temperature at IVC time is influenced by heat coming from the cylinder wall, compression ratio, exhaust and inlet pressure ratio, equivalence ratio and the inlet temperature of air fuel mixture. When compression ratio was increased, the residual gas mass decreased in the combustion chamber. The resulting air- fuel- residual

gas mixture temperature at IVO time decrease leading to low gas temperature at the beginning of the compression phase. In contrast, the increment of exhaust gas pressure and equivalence ratio increases the residual gas fraction in the mixture. High concentration of residual gas in the fresh air fuel mixture produces high temperature in the mixture leading to high temperature at points near to the beginning of the compression phase. Figure 4-77 and Figure 4-68 shows these trends by considering CH_4/H_2 mixtures. In these figures were assumed adiabatic condition and the valve events occur at top dead center and bottom dead center.

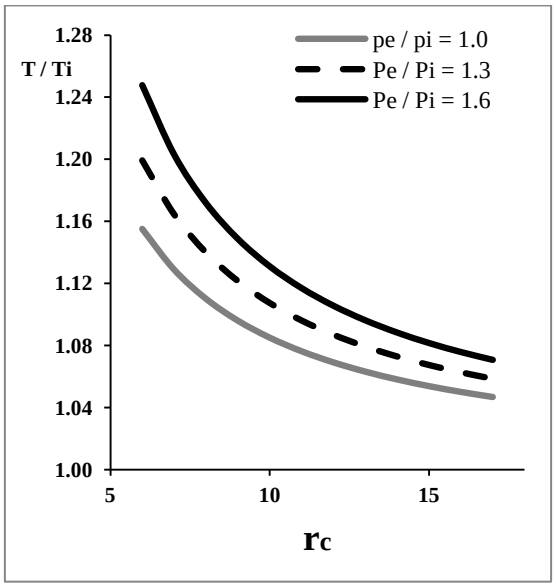

Figure 4-7 Effect of compression ratio and exhaust and inlet gas pressure ratio on temperature at points near to BDC. Mixture: 50% CH_4 50% H_2. Engine operating conditions: inlet temperature 313 K, Ø =0.93, specific heat ratio: γ=1.28

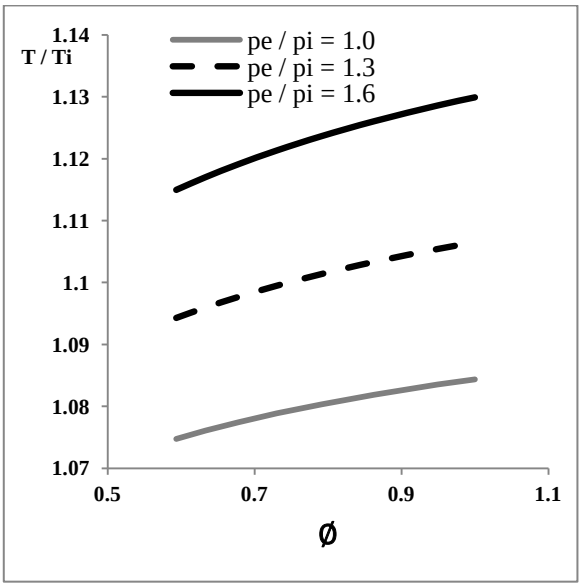

Figure 4-8 Effect of equivalence ratio and exhaust and inlet gas pressure ratio on temperature at points near to BDC. Mixture: 50% CH_4 50% H_2. Engine operating conditions: inlet temperature 313 K, rc=10.2, specific heat ratio: γ=1.28

4.5. HEAT RELEASE ANALYSIS

The knock onset, individual knock intensity and maximum heat release rate have an special relationship that has been studied by Kalghatgi et al., (1995) for PRF, alkylate, toluene/n-heptane mixtures among other fuels. Their observations also include gaseous fuels as butane and propane. In this section, a heat release analysis was performed to verity if $CO/CO_2/CH_4/H_2$ mixtures follow this trend. It is well known that heat release

in the combustion process can be estimated by means of the volume's combustion chamber and the in-cylinder pressure as (Gatowski et al., 1984) :

$$\frac{dQ}{d\theta} = \frac{1}{V}\frac{1}{\gamma - 1}\frac{dP}{d\theta} + \frac{1}{P}\frac{\gamma}{\gamma - 1}\frac{dV}{d\theta} \qquad \text{Eq. 4-28}$$

where γ is the specific heat ratio at constant pressure and volume respectively. Equation 4-28 is valid when pressure is uniform and cannot be used once auto-ignition has been developed (Bradley et al., 1996). However; due to auto-ignition period is small compared with combustion phase, and the period previous to auto-ignition is an important concern in this thesis, it was concluded that this approach was suitable. Figure 4-9 shows the heat release of two CH_4/H_2 mixtures at different engine operating conditions. The heat specific ratio γ used in Equation 4-28, was estimated by using Chemkin Pro ® software.

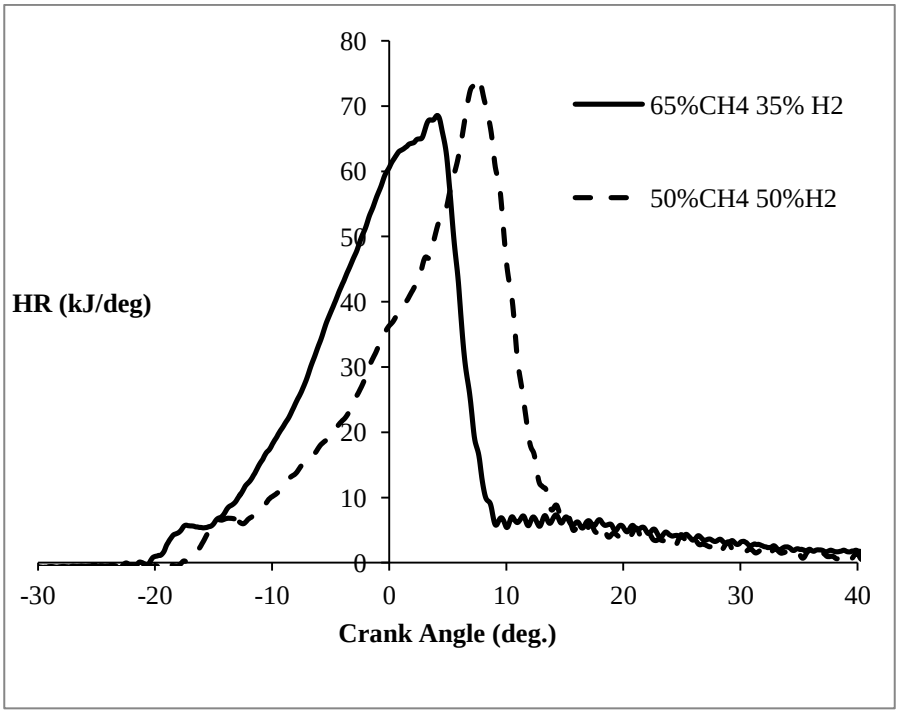

Figure 4-9 Heat release at different engine operating conditions. Solid line; IT=26.2 bTDC , Ø=0.9 , rc=10.9 ,T_i=313 K , p_i=101 kPa , 900 rpm, KOCA=4.45 º aTDC. Dashed line; IT=22.4 bTDC , Ø=0.8 , rc=13 ,Ti=313 K , pi=101 kPa , 900 rpm, KOCA=8.84 º aTDC

4.6. ANALYSIS AND DISCUSSION OF RESULTS

In this section a description of the methodology employed for modeling auto-ignition of CH_4/H_2 mixtures was carried out. In addition, it was described the results of the experiments. A brief discussion about the relationship between auto-ignition and heat released was presented.

4.6.1. Results of the experiments. In Chapter 3 a qualitative analysis of the relationship between the engine operating conditions and KOCA was carried out. In this section, the effects of equivalence ratio, MN and ignition timing on KOCA and CCR were evaluated. The statistical analysis of the data was carried out in Statgraphic ® software. As general conclusion, the engine operating conditions considered have a remarkable influence on the auto-ignition of the fuels tested and CCR values. The second order interactions between these factors were not significative for KOCA. This result was evidenced in the regression model derived from the experimental data obtained. Equation 4-29 is a tool for estimating KOCA as a function of MN, IT and ∅.

$$KOCA = 35.57990 + 0.064967MN - 11.05\emptyset - 0.93645IT \qquad \text{Eq. 4-29}$$

Figure 4-10 shows the effects considered on KOCA. When ignition timing was retarded, both a lean mixture and a high MN fuel were required; therefore, the auto-ignition tendency in the engine decreases. The following engine operating conditions were sensitive to produce high knock intensity: MN=50, IT = 30° bTDC and Ø=1. With these factor levels, the KOCA values were always the minimum as shown in Figure 4-10. The increment of hydrogen concentration in the fuel decreases the KOCA value. When the engine runs at stoichiometric conditions, KOCA decreases; in addition, if ignition timing was advanced, the KOCA value also decreases. As conclusion, when high auto-ignition tendency takes place, KOCA values are close to the TDC point. There is a linear correlation between engine operating conditions and KOCA since there was not evidence of curvature in Figure 4-9. This contrasts with the curvature in the effects of engine operating conditions on CCR as shown in Figure 4-11. The experimental CCR measured was obtained increasing compression ratio until achieve

the desired knock intensity (KI=30). This correlation was represented by the regression model shown in Equation 4-30. The factors and second order interactions were statistically significant. In all cases, the regression models and its coefficients were also significant.

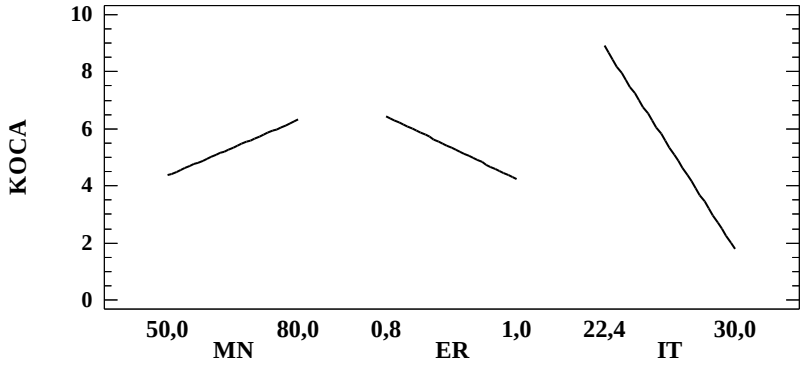

Figure 4-10 Effects of MN, Øand IT on KOCA at Knock Intensity of 30

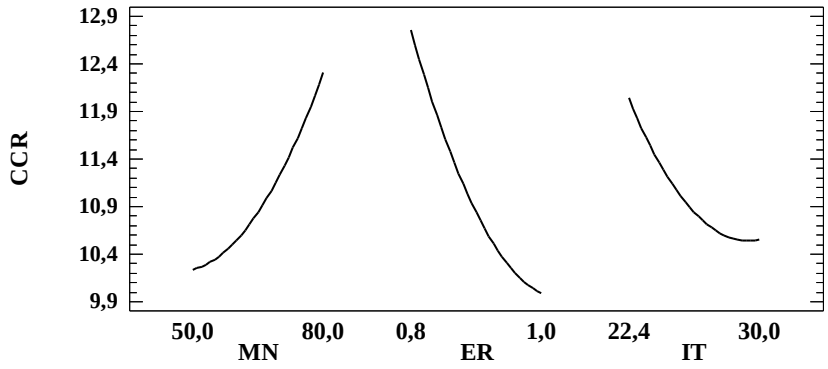

Figure 4-11 Effects of MN, Ø and IT on CCR at Knock Intensity of 30

$$CCR = 112.98 + 0.19319MN - 140.56\emptyset - 2.94861IT + 1.91 \times 10^{-3}MN^2 - 0.2125MN\emptyset - 6.91 \times 10^{-3}MN * IT + 52.931\emptyset^2 + 1.7270IT\emptyset + 3.1462 \times 10^{-2}IT^2 \quad \text{Eq. 4-30}$$

In another hand, the effects of boost pressure on KOCA were evaluated through a one-factor analysis of variance (ANOVA). As previously mentioned, if boost pressure increases, the fuel auto-ignition tendency also increases as shown in Figure 4-12.

However, an inflection point was observed when boost pressure was between 130 and 140 kPa. The hypothesis raised to explain this inflection point is the increment of residual gas coming from the exhaust process. Because of residual gases depend on the inlet/exhaust pressure ratio and compression ratio, it was expected a substantial influence of these gases. The low compression ratio and the high inlet/exhaust pressure ratio used in the experiment, increase the residual gases concentration in the fresh air-fuel mixture. It was observed in Chapter 3 (Figure 3-126 b) that addition of inert gases to the fuel decrease the KOCA value. The increment of residual gases in the mixture could have the same effect in this experiment. Although this trend was observed in Figure 4-12, the results of the experiments concluded that there is not statistical evidence that the average KOCA corresponding to each level were different, i.e., boost pressure increment does not affect KOCA in the engine.

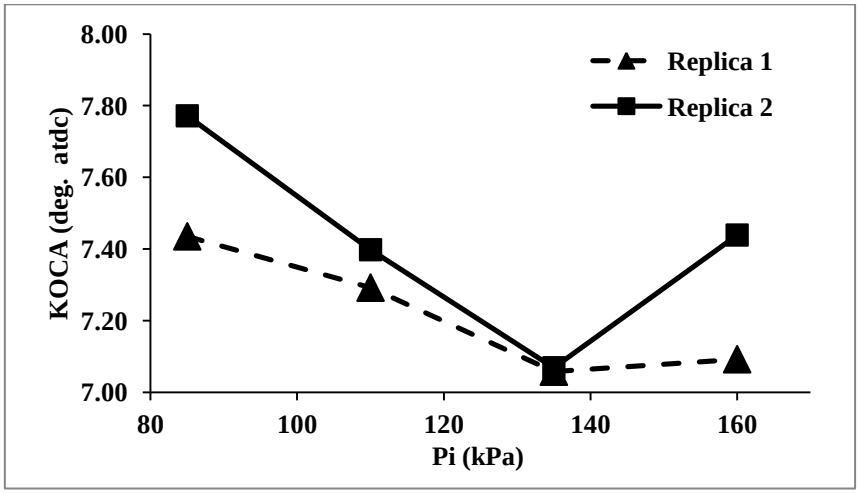

Figure 4-12 Variation of KOCA with boost pressure at stoichiometric mixture. Engine operating conditions: IT= 22.4° bTDC , Ti=40°C. Fuel : 65% CH_4 35%H_2

4.6.2. Combustion parameters estimation. In this section a description of the combustion parameter and polytropic coefficient determined at different engine operating conditions is presented. These parameters are: SOC, ID and CD. The results corresponding to the first replica of the factorial experiment are summarized in Table 4-3. Similar combustion parameters and Wiebe function constants were determined for the second replica.

Table 4-3 Resume of KOCA, SOC EOC, Wiebe function constants and polytropic coefficient (n) as a function of the engine operating conditions

Run	MN	Ø	IT (deg.bTDC)	CCR	KOCA (deg.aTDC)	SOC (deg.bTDC)	EOC (deg.aTDC)	ID (deg)	CD (deg)	a	m	n
1	80	0.8	22.4	17.3	11.20	-16.7	17.8	5.7	34.5	23	2.3	1.21
2	50	0.9	26.2	10.4	4.19	-20.6	8.5	5.6	29.1	3.0	2.4	1.24
3	65	0.9	26.2	10.9	5.18	-20.9	9.8	5.3	30.7	3.1	2.4	1.24
4	80	0.8	30.0	13.1	4.69	-23.0	9.9	7.0	32.9	2.8	2.4	1.22
5	80	1.0	30.0	11.2	1.27	-24.6	5.0	5.4	29.6	2.8	2.4	1.23
6	65	0.9	30.0	11.1	0.29	-25.4	5.1	4.6	30.5	3.1	2.4	1.22
7	80	1.0	22.4	11.9	8.98	-18.1	12.8	4.3	30.9	2.8	2.6	1.23
8	50	0.8	22.4	13.0	8.71	-18.0	13.6	4.4	31.6	2.6	2.4	1.22
9	65	0.9	22.4	11.6	8.57	-18.5	12.7	3.9	31.2	2.8	2.6	1.23
10	65	1.0	26.2	10.4	3.06	-21.1	7.0	5.1	28.1	3.1	2.4	1.24
11	80	0.9	26.2	12.1	6.13	-21.3	10.9	4.9	32.2	2.7	2.4	1.23
12	65	0.8	26.2	12.3	6.04	-21.3	11.7	4.9	33.0	2.7	2.4	1.22
13	65	0.9	26.2	11.0	5.07	-20.6	9.0	5.6	29.6	2.4	2.4	1.22
14	50	1.0	30.0	9.8	3.57	-21.1	7.5	8.9	28.6	2.9	2.4	1.25
15	50	0.8	30.0	11.5	0.86	-25.1	5.3	4.9	30.4	2.8	2.4	1.23
16	50	1.0	22.4	10.2	6.78	-17.7	10.8	4.7	28.5	3.0	2.4	1.25

Taking into consideration the MFB determined per each experimental point, it was concluded that the SOC calculated by using the methodology proposed in this thesis corresponds to approximately 0.42% of MFB. This result reveals that the most suitable SOC definition for CH_4/H_2 mixtures is 1% of MFB. This result agrees with the observations done by Rousseau et al., (1999) for natural gas engines. An explanation to this is the high hydrogen concentration that causes high flame front speed. The average Wiebe constant parameter for these fuels are different from those recommended by Heywood (1988) ($a = 5.0$ and $m = 2.0$) . Actual mass fraction burned have been fitted with $a = 2.8$ and $m = 2.4$.

In another hand, it was evidenced a strong correlation between the compression ratio and the polytropic coefficient. This correlation is influenced by the heat transfer inside

the combustion chamber during combustion phase. The polytropic coefficients determined are ranging from 1.21 to 1.25. This wide range of values represent different heat transfer regime, which depends on the engine operating conditions. Polytropic coefficient near to 1.25 and 1.21 represent low and high heat loss during combustion process respectively. During the tests, high heat loss was observed at high compression ratio, which is shown in Figure 4-13 where the polytropic coefficients decrease at high compression ratios. These conclusions agree with the thermodynamic theory (Moran et al., 2010). If the combustion process is assumed to be adiabatic, the average polytropic coefficient becomes into specific heat ratio γ, which is equal to 1.28 for these fuels. When there is high heat loss regime in the combustion phase, this coefficient tends to 1, which is the value of the coefficient for isothermal process. The specific heat ratio was calculated by using Chemkin Pro ® software during the simulations by considering adiabatic combustion chamber.

According to the results of the experiment, the engine operating conditions affect the CD and ID of the fuels inside the combustion chamber; in particular, the CD is influenced by MN, IT, and $\emptyset$. If MN decrease (hydrogen concentration increases in the fuel), it is expected that CD increases because of the high flame speed of the air fuel mixture.

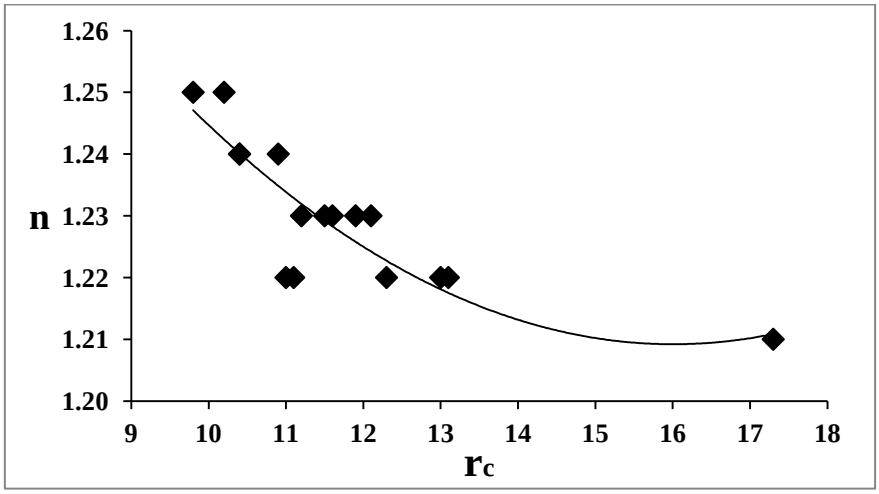

Figure 4-13 Correlation between compression ratio and polytropic coefficient for mixtures of H_2/CH_4 at engine operating conditions defined in Table 4-3

At lean conditions where nitrogen concentration increases with respect to stoichiometric conditions, the CD increases as was expected. Figure 4-14 illustrates the effects of significant engine operating conditions on CD.

Ignition delay, which represents the flame development period is affected by IT as shown in Figure 4-15. This observation was evaluated by Rousseau et al. (1999) for natural gas engines who found the same trend. This is caused by the reduction of the unburned gas temperature and pressure when ignition timing is advanced. This operating condition is unfavorable for the flame development in the combustion chamber.

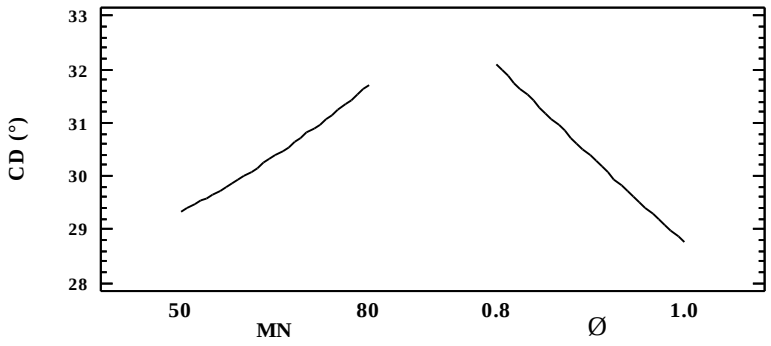

Figure 4-14 Effects of MN and Equivalence ratio on Combustion Duration (CD)

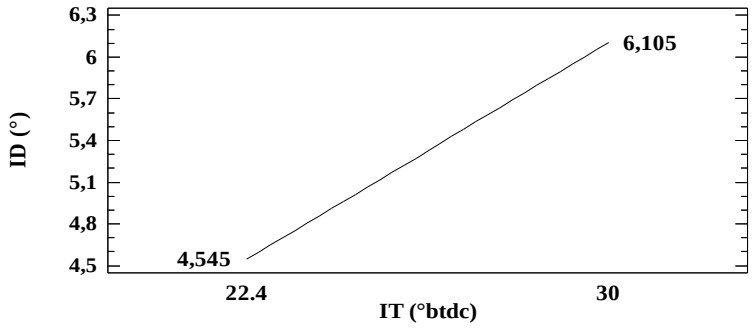

Figure 4-15 Effect of IT on Ignition delay (ID)

4.6.3. Correlation between KOCA and Maximum Heat Release Rate (MHRR)

There is a strong correlation between KOCA and MHRR (maximum heat release rate) in a cycle with auto-ignition. Figure 4-16 shows the equivalence line, which represents

the correlation between these parameters. Before the auto-ignition takes place, there is an increment of the unburned gas temperature produced by the high concentration of intermediate species, which promote auto-ignition. This concentration increment is reflected through the MHRR in the combustion chamber. Similar observations were done by Kalghatgi et al.,(1995) for PRF 90 (90% Iso octane and 10 % n-heptane). It is important to highlight that Figure 4-16 was plotted by considering different CH_4/H_2 mixtures, equivalence ratio, compression ratio and IT. It is concluded that same pattern was observed for gaseous fuels and PRF fuels, which indicate that there is a common factor that govern the chemistry of auto-ignition for both PRF of liquids and gaseous fuels. Another conclusion derived from Figure 4-16 are focused in the time of the events. It is observed that the MHRR occurs first that the auto-ignition; therefore, KOCA is greater than MHRR. This is caused by the heat released by the elementary reactions that promotes the formation of the active radical species.

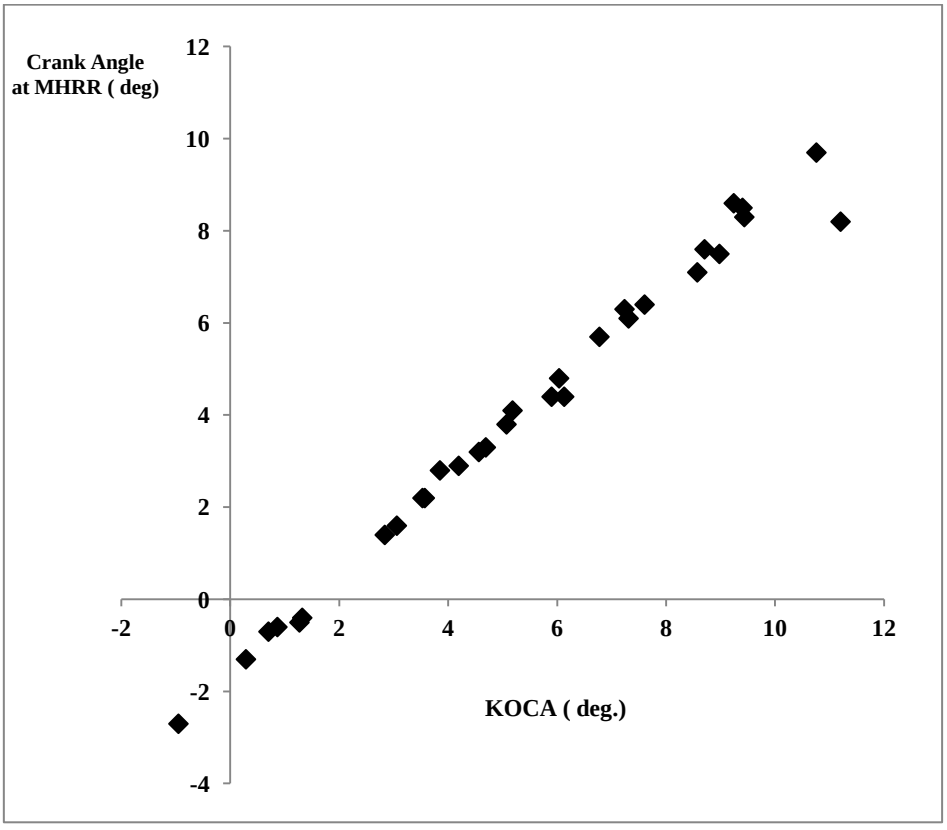

Figure 4-16 Correlation between KOCA and MHRR for CH_4/H_2 mixtures

.

4.6.4. Auto-ignition estimation by using a Detailed Chemical Kinetic Mechanism.

The objective of this section is to verify the thesis's hypothesis. It was evaluated if the reference chemical model is suitable for predicting the auto-ignition of CH_4/ H_2

mixtures; these predictions involve determining with accuracy the KOCA values at different engine operating conditions. The sensitive elementary reactions evaluated in Chapter 2 were examined in the two-zone engine model. The experimental pressure trace and KOCA were used to compare with numerical estimations. Although heat loss is an important factor that influences auto-ignition, an adiabatic combustion chamber was considered in the model as a first approximation. This assumption was considered for two reasons: the former to induce auto- ignition due to lack of accuracy of the mechanism; the latter to isolate the heat transfer effects on auto-ignition. The set of equations of energy, mass and species were solved by using the Closed Internal Combustion Engine Simulator of Chemkin Pro® software. The engine operating conditions, fuel compositions and combustion parameters estimated previously were used as input data of the two-zone auto-ignition model. The initial state (pressure and temperature) of the fresh air fuel mixture defines the pressure and temperature gas path during the compression and combustion phase. The estimations of pressure trace and KOCA were sensitive to the residual gas fraction, pressure and temperature at IVC. Equations 4-16 and 4-25 were used to estimate the residual mass fraction and the IVC temperature. The initial air-fuel mixture temperature was assumed to be 300 K for all points evaluated.

The engine operating conditions defined in the factorial design of experiment were defined to promote auto-ignition of the fuels during the tests. However, auto-ignition was not observed in the engine model when actual engine conditions were considered. These results were examined by considering both the reference kinetic model and the reference kinetic model with the modification III defined in Chapter 2. It was observed that the assumption of adiabatic combustion chamber was not enough to induce the auto-ignition. The computed unburned gas temperature did not increase the reaction rate required to produce the active radicals. Based on the above observation, it was concluded that the lack of accuracy of the reference chemical kinetic mechanism was evident. To promote the auto-ignition of the mixtures, an increment of the unburned gas temperature at IVC timing was used. This hypothetical condition contributes to the concentration increment for both the radicals OH, HO_2 and the intermediate specie H_2O_2, which promote auto-ignition. The IVC temperature was used as a tuning parameter, which was increased until the estimated KOCA matches with the experimental KOCA. This increment compensated the lack of accuracy of the kinetic

model used. A similar methodology was employed by Gersen et al., (2016) who increase the initial temperature 46K to induce auto-ignition in the model for Liquefied Natural Gas (LNG), Natural Gas (NG) and H_2/CO mixtures.

To verify the accuracy of the estimations, a relative error was defined as:

$$\varepsilon = \left| \frac{\left[\int_{IVC}^{EVO} P(\theta)d\theta\right]_{exp} - \left[\int_{IVC}^{EVO} P(\theta)d\theta\right]_{numerical}}{\left[\int_{IVC}^{EVO} P(\theta)d\theta\right]_{exp}} \right| \times 100 \qquad \text{Eq. 4-31}$$

where each integral correspond to the area under the experimental and numerical pressure trace. These errors were estimated per each run and are shown in Figure 4-17. The difference between the numerical and experimental pressure traces are caused by two sources: the former due to the inaccuracy of the kinetic model used and the latter due to the adiabatic assumption. The heat transfer between cylinder gases and the cylinder wall, cylinder head and piston during compression and combustion phase are significative at high compression ratio. It was observed that at lean conditions the error decrease considerably.

The unburned gas temperature at IVC estimated with Equation 4-25 was used by assuming an inlet air-fuel mixture temperature of 300K. For these estimations actual valve timing events were considered where the inlet valve opens at 350 º bTDC and closes at 146° bTDC. These estimations are an approximation of the actual unburned gas temperature and were considered as the baseline case. The additional increment of temperature with respect to the obtained with Equation 4-25, is an indicator of the inaccuracy of the kinetic model used as reference. When compression ratio was increased, the average unburned gas temperature inside the combustion chamber was also increased. This high temperature improves the accuracy of the mechanism, which has been optimized at intermediate and high temperature. This trend is observed in Figure 4-18 where engine operating point with low compression ratio required a high increment of the computational IVC temperature. The same trend observed in Figure 2-2 of Chapter 2 was examined in Figure 4-18. As the IVC unburned gas temperature decreases (low compression ratio), the inaccuracy of the mechanism increases for predicting KOCA in the auto-ignition model.

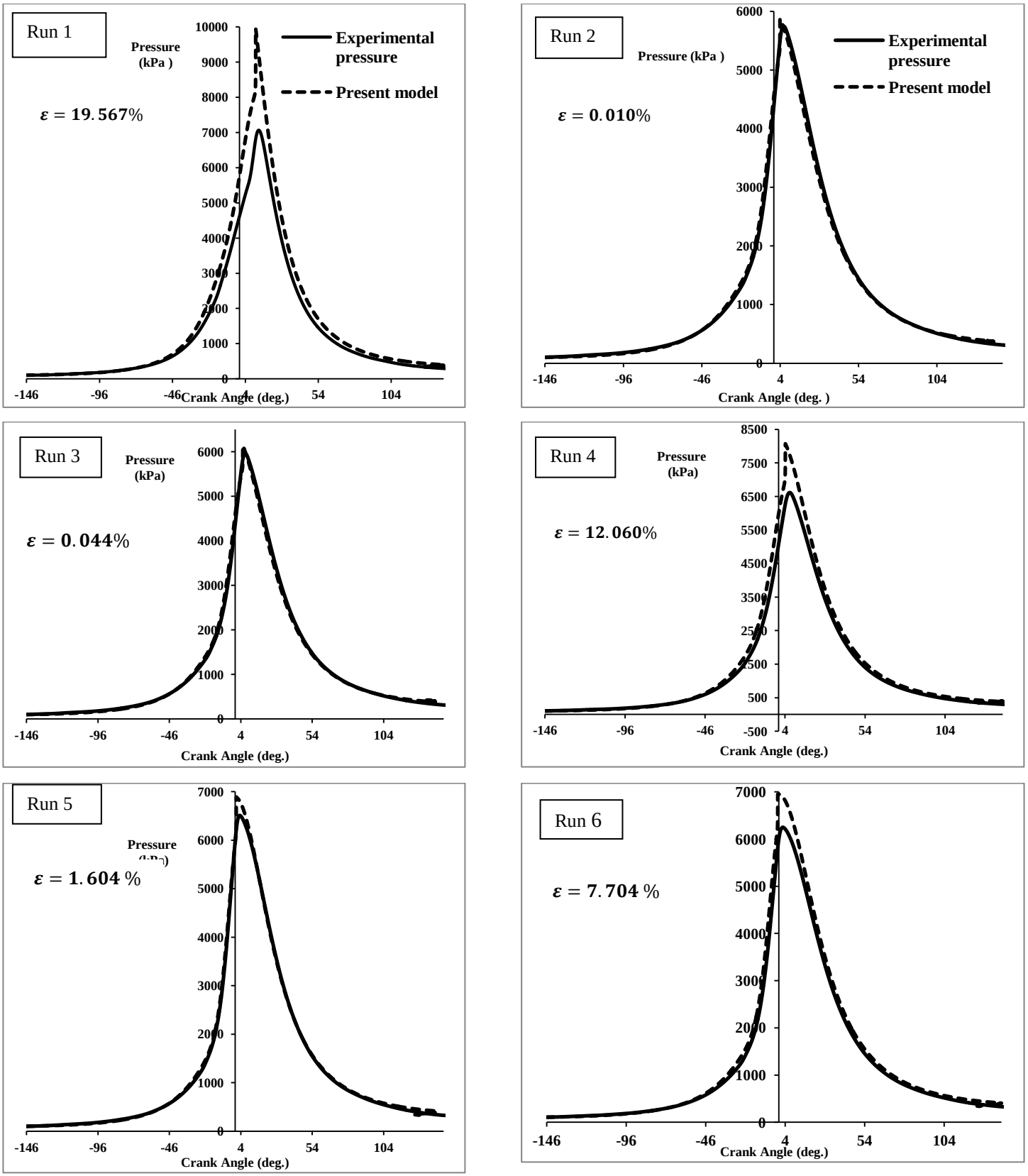

Figure 4-17 Experimental and numerical pressure trace and KOCA at different engine operating conditions and CH4/H2 mixture.

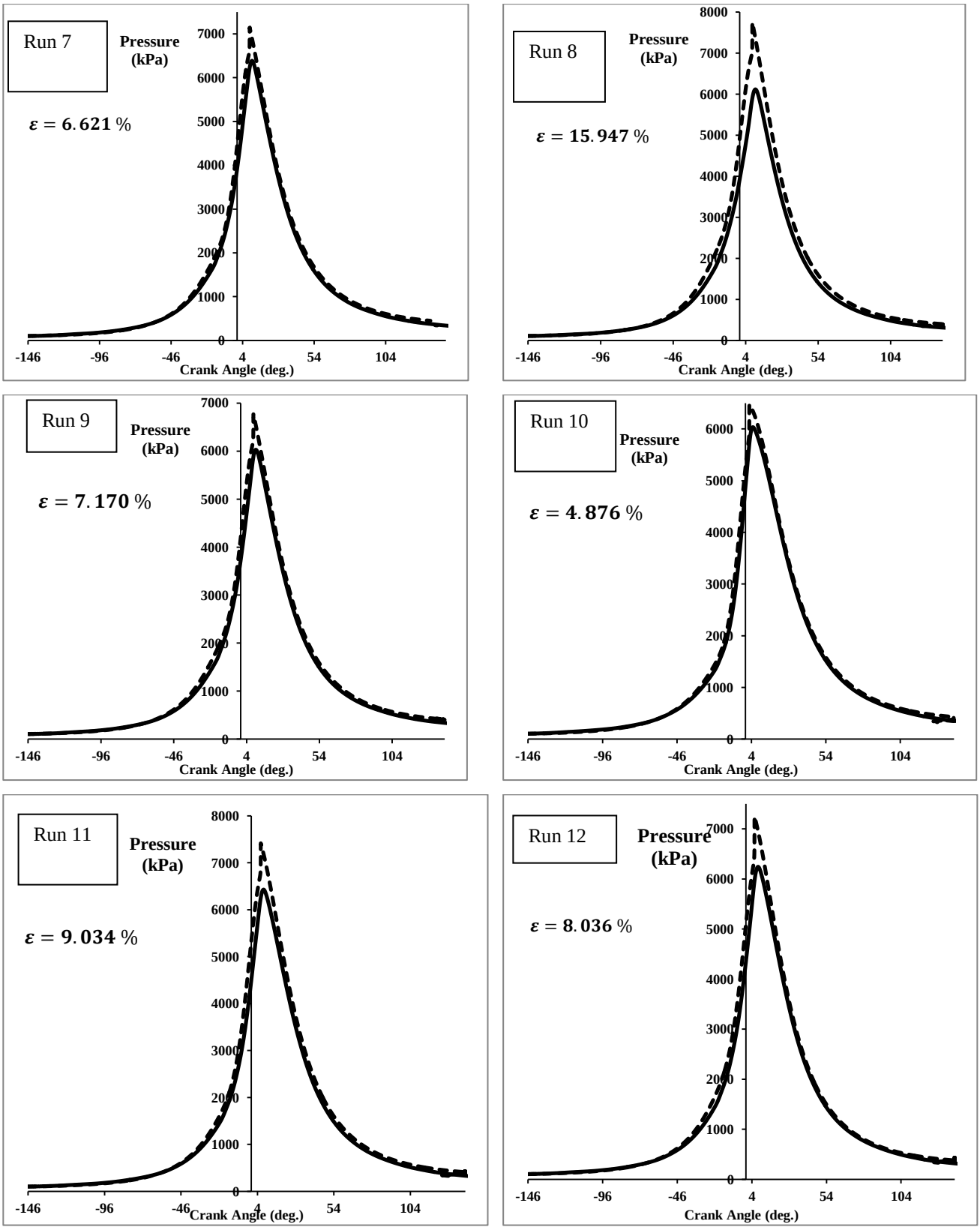

Figure 4-17 Continuation

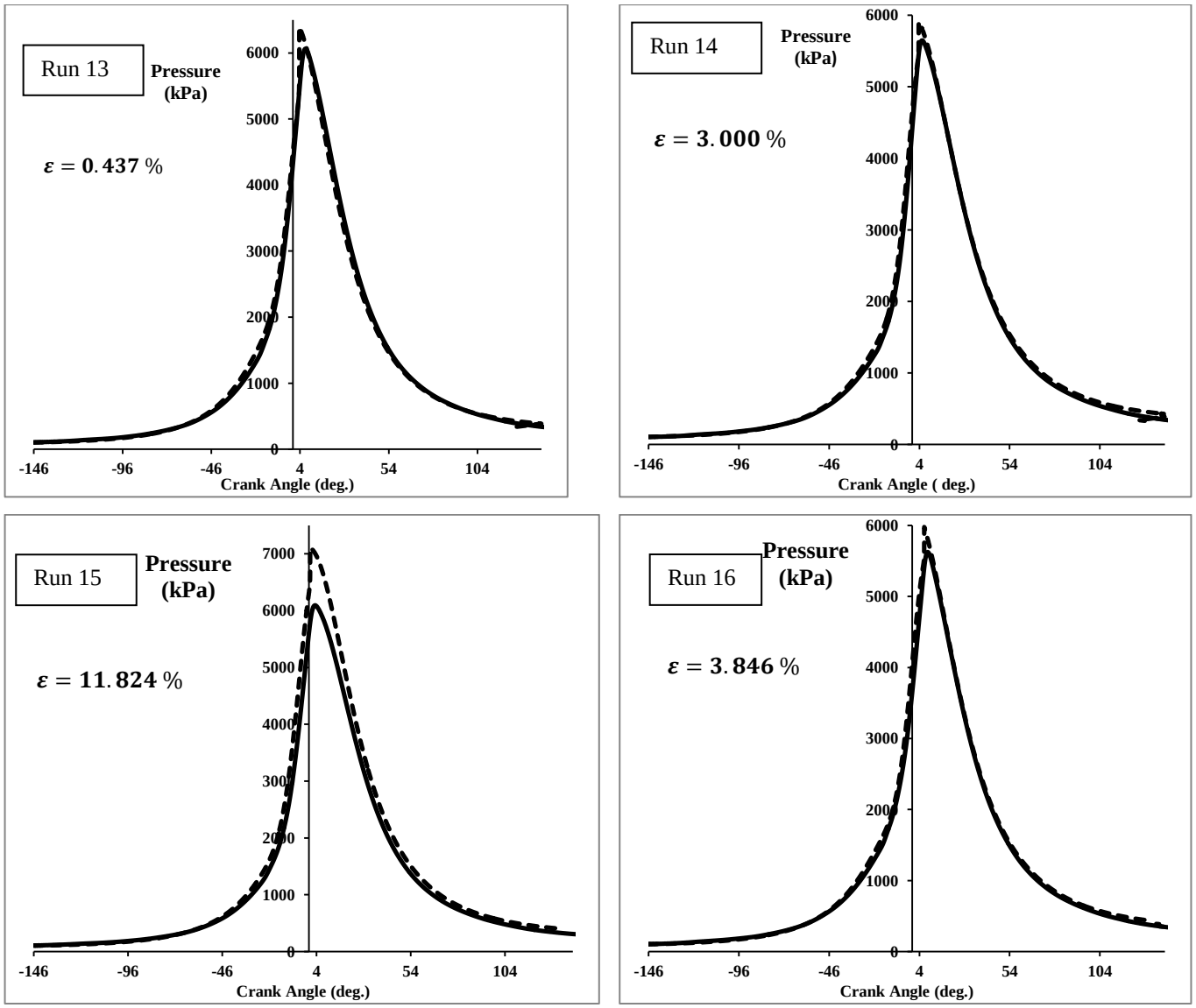

Figure 4-17 Continuation

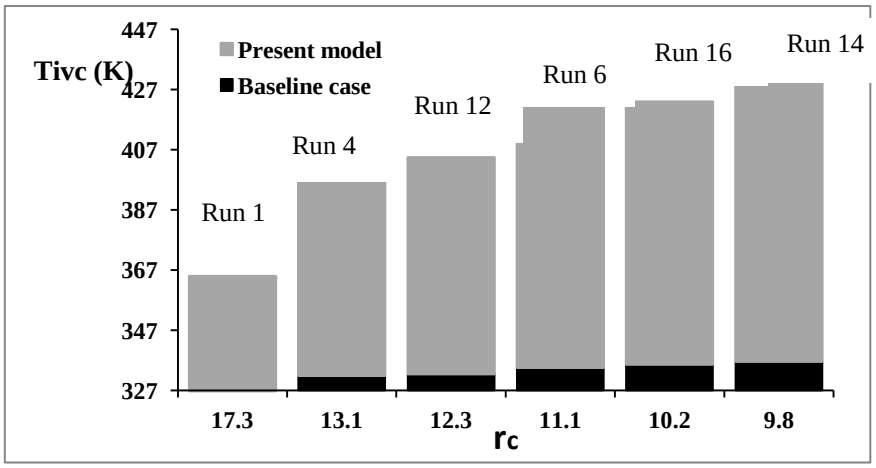

Figure 4-18 Unburned gas temperatures at IVC time as a function of compression ratio for CH4/H2 mixtures

4.7. CONCLUSIONS

The most important conclusions derived from this chapter are described as follows:

- ✓ The MN, equivalence ratio and ignition timing at constant inlet temperature and output power have a remarkable influence on KOCA and CCR.

- ✓ According to an-one analysis of variance (ANOVA), the boost pressure does not influence KOCA. If boost pressure increases, KOCA slightly decreases.

- ✓ A method was proposed to estimate SOC, EOC and CD of CH_4/H_2 mixtures from indicator diagram. This method allows estimating representative combustion parameters, which depends strongly on the fuel compositions, equivalence ratio and ignition timing.

- ✓ A correlation for estimating IVC unburned gas temperature, residual gas fraction and residual gas temperature were developed. These expressions match with those reported by Heywood (1988) by considering that the valve events occur at top dead center and bottom dead center. The results are consistent with theory.

- ✓ Combustion parameters determined by using the methodology employed in this thesis are suitable for Mass Fraction Burned modeling through Wiebe function. The Wiebe function' constants for CH_4/H_2 mixtures are a=2.8 and m=2.4. These values are different of those recommended in the literature for hydrocarbon fuels, which values are a=5.0 and m=2.0.

- ✓ It was demonstrated that polytropic coefficient of compression and expansion phase of the engine cycle is equal to the negative of slope of the linear region observed in the indicator diagram. Average polytropic coefficient for CH_4/H_2 mixtures at lean and stoichiometric conditions (Ø=0.8-1) are 1.23. As the polytropic coefficient decreases, the compression ratio increases. This is caused by the heat transfer from cylinder gas to head and wall cylinder of the engine.

✓ There is a linear correlation between KOCA and MHRR for CH_4/H_2 mixtures. This result agrees with results obtained for liquids fuels (PRF 90).

✓ The accuracy of the detailed chemical kinetic mechanism used as reference decreases when engine runs at low compression ratio. This lack of accuracy is evidenced when ignition delay time was estimated at low temperature in an adiabatic constant volume reactor.

Chapter 5

Development of an Empirical Model for Predicting KOCA Based on Integral Approach

5.1 INTRODUCTION

The development of empirical models for predicting auto-ignition in ICE is a progress for understanding the combustion of gaseous fuels different of Natural Gas. As was evidenced in the technical literature, the integral method has been employed for modeling auto-ignition of PRF(Douaud and Eyzat, 1978; Pipitone et al., 2015; Song and Song, 2016), Gasoline and Natural gas auto-ignition (Soylu and Van Gerpen, 2003). Although there are kinetic models for modeling the auto-ignition of PRF and gasoline, the empirical auto-ignition models are intresting due to its simplicity and easy computational implementation. The lack of accuracy of chemical kinetic mechanisms are compensated through the implementation of these models to the multi-dimensional, and zero-dimensional engine models (Rostampour and Toosi, 2015).

In this chapter, a method for predicting the Knock Occurrence Crank Angle (KOCA) through an empirical knock model based on integral approach was developed. The state time-path of unburned gas inside the combustion chamber was obtained by combining experimental in-cylinder pressure data and a thermodynamic model for unburned gas temperature estimation. The Integral Mean Value Theorem approach was used to

simplify the model. This approach was initially mentioned by Douaud and Eyzat, (1978) for PRF and gasoline fuels. The factorial design of experiment 2^3 with axial and central runs described in Chater 4 was used to provide the required experimental data.

5.2. INTEGRAL MODEL APPROACH

Once the ignition delay time correlation for a specific air-fuel mixture is determined, the Livengood and Wu Integral Method to predict knock is used. This method establishes that auto-ignition takes place if the integral of the function $\boldsymbol{1/\tau(P,T)}$ reaches the unity. The function $\boldsymbol{\tau(P,T)}$ is the ignition delay function that depends on the unburned gas temperature and pressure. An adapted version of the Livengood and Wu Integral Method as a function of crank angle is defined as (Soylu and Van Gerpen, 2003):

$$\int_{\theta_{ref}}^{KOCA} \frac{1}{\tau(\theta)}\, d\theta = 1 \qquad \text{Eq.5-1}$$

where KOCA is the Knock Occurrence Crank Angle and θ_{ref} is the reference crank angle used for calculations. Some authors define this reference crank angle as the start of the gas compression stroke (Hernandez, Serrano, and Perez, 2006); however, in this thesis the IVC crank angle was selected as the reference timing. The inlet valve close crank angle of the CFR engine was 146º bTDC.

5.3. UNBURNED GAS TEMPERATURE ESTIMATION

Unburned gas temperature is the most important thermodynamic property that defines the ignition delay time and the auto-ignition of fuels in ICE. The rate of production of reactive radicals depends on the unburned gas temperature. Some experimental techniques have been implemented for measuring this property, which have helped to validate the different thermodynamic approaches (Bood et al., 1997). These thermodynamic models have demonstrated to be a suitable and reliable approximation for computational implementation (Pipitone et al., 2015). In this chapter, three approaches to estimate the unburned gas temperature were considered. It was described in detail the mathematical formulation and assumptions considered for their

development. These approaches are called as: single zone approach, two-zone approach and single step model.

5.3.1. Single zone approach. In this approach the combustion chamber was considered adiabatic with homogeneous gas properties. The energy equation was defined as:

$$\frac{dQ}{d\theta} - \frac{dW}{d\theta} = \frac{dU}{d\theta} \qquad \text{Eq. 5-2}$$

where each expression of Equation 5-2 were defined as:

$$\frac{dU}{d\theta} = mC_v \frac{dT}{d\theta} \qquad \text{Eq.5-3}$$

$$\frac{dW}{d\theta} = P\frac{dV}{d\theta} \qquad \text{Eq.5-4}$$

and

$$\frac{dQ}{d\theta} = \frac{\gamma}{\gamma - 1}\, P\frac{dV}{d\theta} + \left(\frac{1}{\gamma - 1}\right) V\frac{dP}{d\theta} \qquad \text{Eq.5-5}$$

Equation 5-5 is the Net Heat Release of the air-fuel mixture inside the combustion chamber. This equation is suitable due to the elementary reactions that produce the radical species (OH, HO_2) release heat during the compression phase in the engine. Multiplying Equation 5-5 with the inverse of the gas constant and by replacing Equations 5-3, 5-4 and 5-5 in Equation 5-2, the following expression was obtained:

$$\frac{1}{R}\left[\frac{\gamma}{\gamma - 1}\, P\frac{dV}{d\theta} + \left(\frac{1}{\gamma - 1}\right) V\frac{dP}{d\theta}\right] - \frac{P}{R}\frac{dV}{d\theta} = \frac{m}{R}\, C_v \frac{dT}{d\theta} \qquad \text{Eq.5-6}$$

According to ideal gas law is well known that:

$$PV = mRT \implies \frac{1}{R} = \frac{mT}{PV} \qquad \text{Eq.5-7}$$

and:

$$C_v = \frac{1}{\gamma - 1} \qquad \text{Eq.5-8}$$

By replacing Equation 5-7 and Equation 5-8 in Equation Eq.5-6 and after of some mathematical operations was obtained:

$$\left[\frac{T}{V}\left(\frac{\gamma}{\gamma-1}\right)\frac{dV}{d\theta} + \frac{T}{P}\left(\frac{1}{\gamma-1}\right)\frac{dP}{d\theta} - \frac{T}{V}\frac{dV}{d\theta}\right] = \left(\frac{1}{\gamma-1}\frac{dT}{d\theta}\right) \qquad \text{Eq.5-9}$$

This equation can be simplified by multiplying both sides of Equation 5-9 by $(\gamma - 1)$:

$$\frac{T}{V}\frac{dV}{d\theta} + \frac{T}{P}\frac{dP}{d\theta} = \frac{dT}{d\theta} \qquad \text{Eq.5-10}$$

Equation 5-10 is equivalent to the following linear differential equation, which can be solved by using the integrating factor method:

$$\frac{dT}{d\theta} - \left(\frac{1}{V}\frac{dV}{d\theta} + \frac{1}{P}\frac{dP}{d\theta}\right)T = 0 \qquad \text{Eq.5-11}$$

After some mathematical manipulations the integrating factor obtained is:

$$FI = \frac{1}{PV} \qquad \text{Eq.5-12}$$

By using the integrating factor, the solution of Equation 5-11 is:

$$\frac{d}{d\theta}\left(\frac{1}{PV}\,T\right) = 0 \implies \frac{1}{PV}\,T = C \implies T(\theta) = CPV \qquad \text{Eq.5-13}$$

The initial conditions were defined as:

$$T(\theta) = T_{IVC} \quad \text{Eq.5-14}$$

$$P(\theta) = P_{IVC} \quad \text{Eq.5-15}$$

$$V(\theta) = V_{IVC} \quad \text{Eq.5-16}$$

where P_{IVC} and V_{IVC} are measured experimentally. The temperature at inlet valve close crank angle (T_{IVC}) is determined through Equation 4-25 defined in Chapter 4. By using the initial conditions defined in Equations 5-14 – 5-16 the constant was found to be:

$$C = \frac{T_{IVC}}{P_{IVC}V_{IVC}} \quad \text{Eq.5-17}$$

Taking into account the constant value, it was concluded that the single zone temperature is defined as:

$$T(\theta) = \frac{T_{IVC}}{P_{IVC}V_{IVC}}\, P(\theta)\, V(\theta) \quad \text{Eq.5-18}$$

This results is similar to those obtained by Ganestam (2010), who considered the following assumptions: a) the air fuel mixture behaves as ideal gas and b) the product of the mass trapped in the combustion chamber and the gas's constant during the compression and combustion phase keep constant ($mR = K$ where K is a constant).

5.3.2. Two-step model approach. This approach was derived from the two-zone model proposed by Ganestam (2010). The unburned gas temperature was estimated through two steps: the first step considered the unburned gas temperature before the ignition timing; and the second step considered the unburned gas temperature after of the ignition timing. The unburned gas temperature before ignition timing can be

estimated through Equation 5-18. The temperature of unburned gas after the ignition timing was estimated by considering a polytropic compression:

$$PV^n = C \qquad \text{Eq.5-19}$$

where n is the polytropic coefficient in the compression phase. This coefficient was determined experimentally in Chapter 4 as a function of the operating engine condition. According to this assumption, the volume of the unburned gas inside the combustion chamber can be estimated as:

$$\left(\frac{V_u}{V_{IT}}\right) = \left(\frac{P_{IT}}{P}\right)^{\frac{1}{n}} \qquad \text{Eq.5-20}$$

where V_u and P are the unburned gas volume and in-cylinder pressure respectively. From ideal gas law and considering the ignition timing crank angle as the reference crank angle, it was concluded that unburned gas temperature, combustion chamber's volume and pressure are related as:

$$\frac{T_{IT}}{T_u} = \frac{V_{IT}}{V_u}\frac{P_{IT}}{P} \qquad \text{Eq.5-21}$$

By replacing Equation 5-21 in Equation 5-20 was concluded that the unburned gas temperature is defined as:

$$T_u = T_{IT}\left(\frac{P}{P_{IT}}\right)^{\frac{n-1}{n}} \qquad \text{Eq.5-22}$$

where

$$T_{IT} = \frac{T_{IVC}}{P_{IVC}V_{IVC}}\, P_{IVC}(\theta)V_{IVC}(\theta) \qquad \text{Eq.5-23}$$

As conclusion; the unburned gas temperature can be estimated as:

$$T_u(\theta) = \begin{cases} \dfrac{T_{IVC}}{P_{IVC}V_{IVC}}\, P(\theta)V(\theta) & \theta < \theta_{IT} \\ T_{IVC}\left(\dfrac{P}{P_{IVC}}\right)^{\frac{n-1}{n}} & \theta > \theta_{IT} \end{cases} \qquad \text{Eq.5-24}$$

This formulation was used by Pipitone et al.,(2015) for estimating the unburned temperature of gasoline-propane mixtures.

5.3.3. Single step model approach. This approach is based on the ideal gas law assumption. It was proposed that unburned gas temperature can be estimated as:

$$T_u = \frac{PV_u}{m_u R} \qquad \text{Eq.5-25}$$

The objective is to determine the unburned gas mass and volume, and then replace this value in Equation 5-25. From ideal gas law is deduced that:

$$\frac{P_{IVC}V_{IVC}}{PV_u} = \frac{m_{IVC}T_{IVC}}{m_u T_u} \qquad \text{Eq.5-26}$$

To obtain Equation 5-26, it was assumed that molecular weight of the trapped gas is constant during the compression phase. By considering a polytropic compression process, it was possible to define the ratio T_{IVC}/T_u as:

$$\frac{T_{IVC}}{T_u} = \left(\frac{P}{P_{IVC}}\right)^{\frac{1-n}{n}} \qquad \text{Eq.5-27}$$

The Equation 5-26 and Equation 5-27 were combined and after of some mathematical manipulations, it was concluded that unburned gas volume can be estimated as:

$$V_u = V_{IVC}\left(\frac{m_u}{m_{IVC}}\right)\left(\frac{P}{P_{IVC}}\right)^{-\frac{1}{n}} \quad \text{Eq.5-28}$$

Later, Equation 5-25 and Equation 5-28 were combined. It was concluded that unburned gas temperature is equal to:

$$T_u = \frac{P}{R}\left[\frac{V_{IVC}}{m_{IVC}}\left(\frac{P}{P_{IVC}}\right)^{-\frac{1}{n}}\right] \quad \text{Eq.5.29}$$

The trapped mass, which is the initial charge in the combustion chamber of the engine, can be estimated as:

$$m_{IVC} = \frac{P_{IVC}V_{IVC}}{RT_{IVC}} \quad \text{Eq.5-30}$$

Finally, the unburned gas temperature can be calculated as:

$$T_u = T_{IVC}\left(\frac{P}{P_{IVC}}\right)^{\frac{n-1}{n}} \quad \text{Eq.5-31}$$

In this thesis, the unburned gas temperature in the compression phase was estimated by using Equation 5-31. There are two reasons to justify this selection: a) their easy implementation in computational codes and b) the estimations of the polytropic coefficients that were carried out in Chapter 4. Figure 5-1 shows a comparison of the unburned gas temperature estimated by using the different deduced models.

Two steps approach also uses the polytropic coefficient; however, in the combustion phase this coefficient begins to change dramatically tending to infinity. The third approach instead, considers a polytropic compression process, which are suitable for this analysis. It was evidenced that the single zone approach and the Chemkin Pro® estimations overpredicted the unburned gas temperature. It is important to highlight that Chemkin Pro ® predictions consider an adiabatic combustion chamber and the single-zone approach is an average temperature of the burned and unburned gases in the

compression and combustion phase. In each case, the temperature at inlet valve close crank angle (146º bTDC) was estimated through Equation 4-25.

Figure 5-2 shows a comparison between the unburned gas temperature estimated for different fuel blends and engine operating conditions. The polytropic coefficient depends on the heat transfer regime in the combustion chamber, which is influenced by the initial thermodynamic state of the air-fuel mixture. However, it was observed that polytropic coefficient did not change much despite of the different fuel compositions and engine operating conditions considered. With the same polytropic coefficient, the temperature trace follows different path due to the strong influence of engine operating conditions. For example, the operating point with high compression ratio and methane concentration (run 1) shows a high unburned gas temperature peak. The run 8 shows the lower unburned gas temperature peak due to its moderate compression ratio and low concentration of methane. The third approach was used in the next section for determining the constants of the ignition delay model proposed. The engine operating conditions of run 1, 2, 4 and 8 were described in Chapter 4.

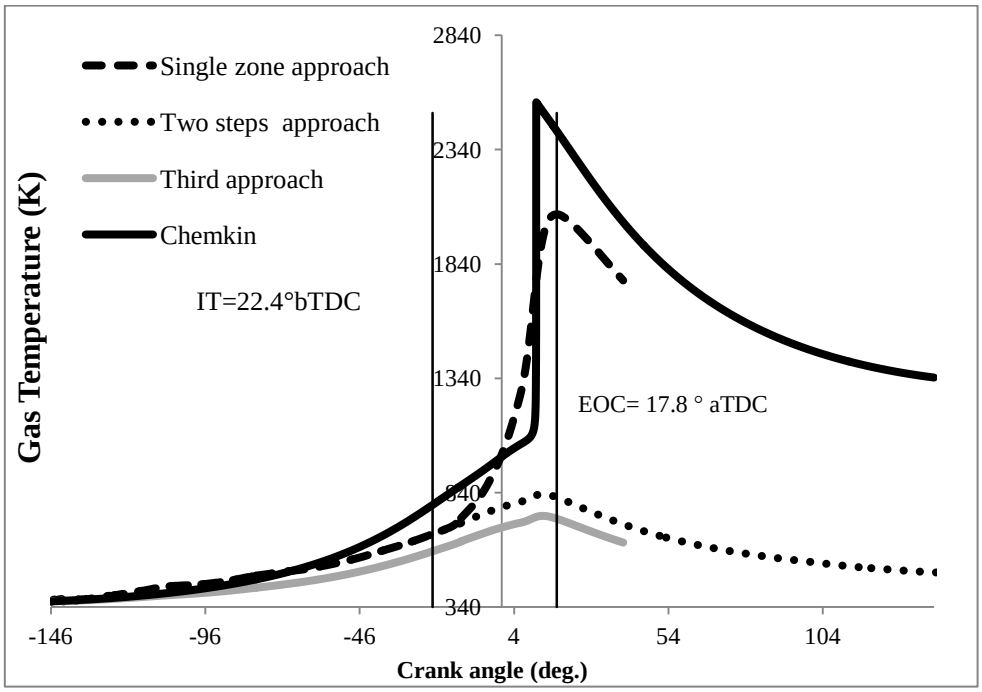

Figure 5-1. Unburned gas temperature by using the three approaches for 80% CH_4 20%H_2. Engine operating conditions: Ø=0.8, Compression ratio: 17.3 , IT= 22.4º bTDC, Inlet temperature: 40ºC, 900 rpm.

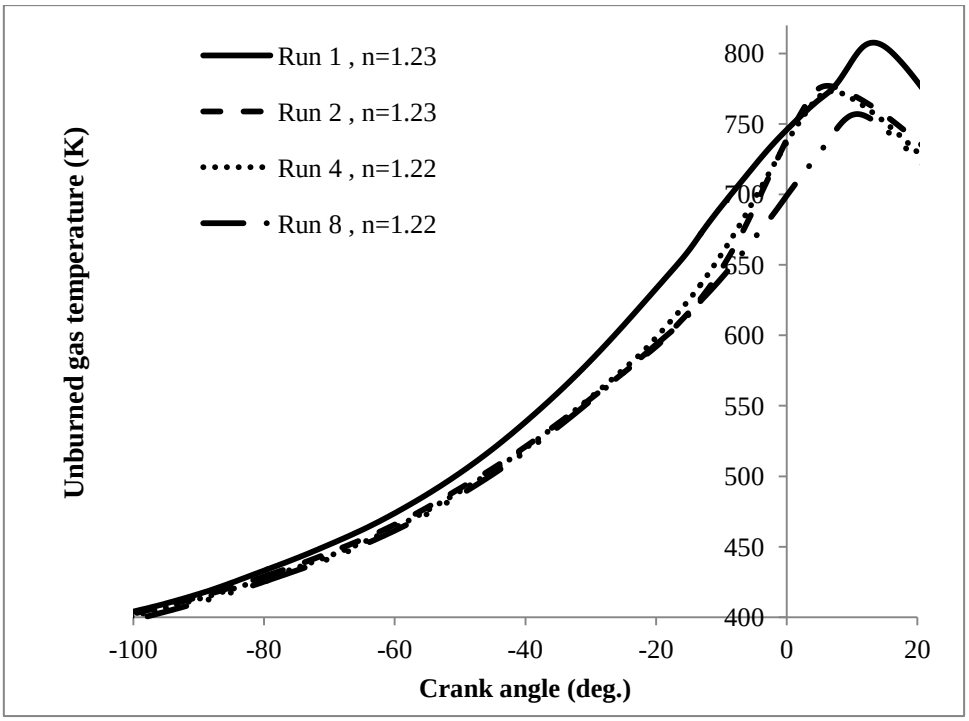

Figure 5-2 Unburned gas temperature estimated for run 1, Run 2 , Run 4 and Run 8 by considering different polytropic coefficients

5.4. DETERMINATION OF EMPIRICAL MODEL PARAMETERS

This section describes the methodology employed to determine the constants of the auto-ignition model. For this purpose, an optimization technique was performed similar to that employed by Douaud and Eyzat (1978) and Soylu and Van Gerpen, (2003). The cycle by cycle KOCA and the in-cylinder pressure collected from the factorial experiment at different engine operating conditions and CH_4/H_2 mixtures were used as input data. The knock detection method employed was explained in detail in Chapter 3. The statement of the optimization problem is described as follow:

To find the parameters:

$$X = [X_1\ X_2\ X_3]^{-1}$$

which minimize the cost function:

$$SS(X) = \sum_{k=1}^{m} \left[\int_{\theta_{IVC}}^{KOCA_k} \frac{d\theta}{\tau_k(X_1\, X_2\, X_3)} - 1 \right]^2 \qquad \text{Eq.5-32}$$

where m is the number of cycles with knocking at KI=30, $KOCA_k$ is the knock occurrence crank angle of the cycle k and X_1, X_2 and X_3 are the set of constants that will be determined. The value of these constants are used to deduce an ignition delay time function that depends on the engine operating conditions and MN of the fuel as shown in Equation 5-33:

$$\tau = X_1 p^{-X_2} exp\left(\frac{EX_3}{R_u T}\right) \qquad \text{Eq.5-33}$$

5.4.1. A modified formulation of the integral model. In this section, a modified formulation of the integral model for determining KOCA is described. The new formulation is based on the first mean value theorem. This theorem states that if $f(\theta)$ is a continuous function on the interval$[\theta_{ref}, \theta_{KOCA}]$, which is defined on R, and $g(\theta)$ is an integrable and positive semi-definite function on the interval $[\theta_{ref}, \theta_{KOCA}]$, then exist a $\tilde{\theta} \in [\theta_{ref}, \theta_{KOCA}]$ such that

$$\int_{\theta_{ref}}^{\theta_{KOCA}} f(\theta)g(\theta)d\theta = f(\tilde{\theta}) \int_{\theta_{ref}}^{\theta_{KOCA}} g(\theta)d\theta \qquad \text{Eq.5-34}$$

If it is assumed that $g(\theta) = 1$ for all θ in $[\theta_{ref}, \theta_{KOCA}]$ then exist a $\tilde{\theta} \in [\theta_{ref}, \theta_{KOCA}]$ such that:

$$\int_{\theta_{ref}}^{\theta_{KOCA}} f(\theta)d\theta = f(\tilde{\theta}) \int_{\theta_{ref}}^{\theta_{KOCA}} d\theta = f(\tilde{\theta})(\theta_{KOCA} - \theta_{ref}) = 1 \qquad \text{Eq.5-35}$$

where $f(\widetilde{\theta})$ correspond to the mean value of the function $f(\theta)$ on the interval $[\theta_{ref}, \theta_{KOCA}]$. Temperature and pressure trace history are both positive and completely known prior to calculation, thus the mean value theorem for integrals can be applied. Figure 5-3 shows schematically the function $f(\theta)$ and its means value$f(\tilde{\theta})$. The integral of these functions along the interval $[\theta_{ref}, \theta_{KOCA}]$ is equal to one. According to the above, the mean value of the function $f(\theta)$ is defined as:

$$f(\tilde{\theta}) = \frac{1}{\tau(\tilde{\theta})} = \frac{1}{X_1 P(\tilde{\theta})^{-X_2} exp\left(\frac{EX_3}{R_u T(\tilde{\theta})}\right)} \quad \text{Eq.5-36}$$

Thus, it can be concluded that:

$$\frac{\theta_{KOCA} - \theta_{ref}}{X_1 P(\tilde{\theta})^{-X_2} exp\left(\frac{EX_3}{R_u T(\tilde{\theta})}\right)} = 1 \quad \text{Eq.5-37}$$

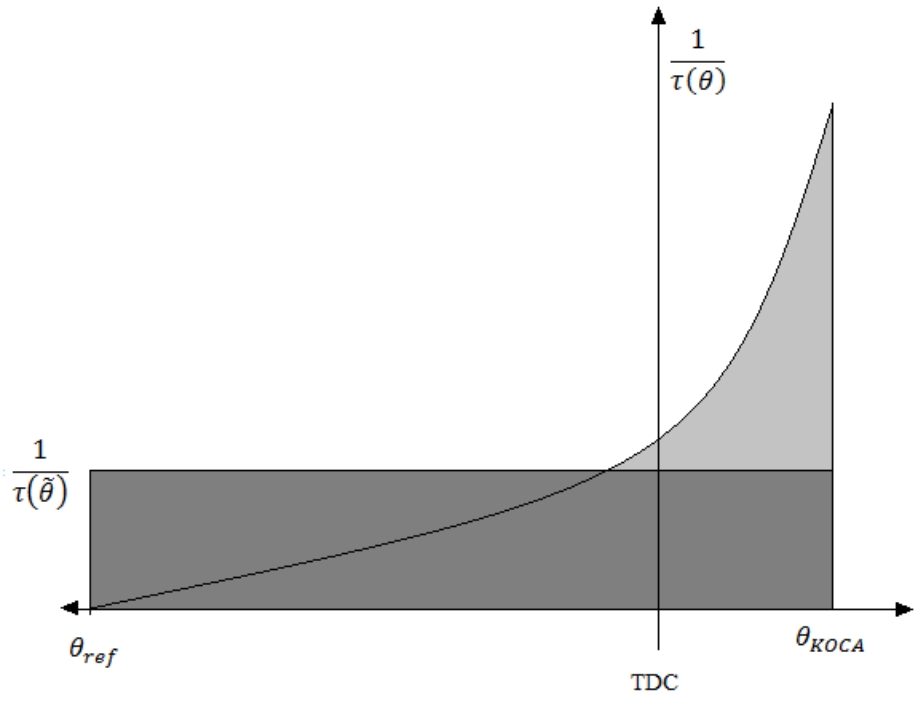

Figure 5-3 Graphical interpretation of the Integral mean Value theorem applied for KOCA estimation.

This expression allows estimating KOCA as a function of $P(\tilde{\theta})$ and $T(\tilde{\theta})$, which are defined as *characteristic pressure and temperature*. These parameters represent the temperature and pressure path of the unburned gas in the engine's combustion chamber.

A second optimization process was carried out in order to estimate these characteristic parameters. These parameters depend on the engine operating conditions, fuel composition and the initial state of the air-fuel mixture. The statement of the second optimization problem is defined as follow:

To find

$$P(\tilde{\theta}) \text{ and } T(\tilde{\theta})$$

which minimize the cost function:

$$\sigma\big(P(\theta), T(\theta)\big) = \left[\frac{\theta_{KOCA} - \theta_{ref}}{X_1 P(\theta)^{-X_2} exp\left(\frac{EX_3}{R_u T(\theta)}\right)} - 1\right]^2 \qquad \text{Eq.5-38}$$

The cost function was defined with the following constraints:

$$P(\theta_{IVC}) < P(\tilde{\theta}) < P(\theta_{KOCA})$$

$$T(\theta_{IVC}) < T(\tilde{\theta}) < T(\theta_{KOCA})$$

For a given engine operating conditions, this process was carried out per each cycle with high knock intensity. The characteristic pressure $P(\tilde{\theta})$ and temperature $T(\tilde{\theta})$ of each run is the average of the characteristic pressure and temperature of each cycle of the run. This methodology was applied to different engine operating conditions defined in the design of experiment.

5.5. RESULTS AND DISCUSSIONS

In this section a description of the results obtained in the optimization problem are described. The results were summarized in Table 5-1 and 5-2. From these data, regression models were developed to estimate the integral model constants. The models are reported as a function of the engine operating conditions and MN of the fuel. The best models that explain the variability of the process are:

$$X_1 = 1.131207 \quad \text{Eq.5-39}$$

$$X_2 = -0.623804 - 0.100836\emptyset - 9.89853 \times 10^{-3} IT + 3.84868 \times 10^{-3}\emptyset * IT + 1.3862 \times 10^{-4} IT^2 \quad \text{Eq.5-40}$$

$$X_3 = 1.769326 \times 10^{-3} MN + 0.1951718\emptyset + 6.339252 IT - 1.50478 \times 10^{-5} MN^2 - 6.280962 \times 10^{-3}\emptyset * IT \quad \text{Eq.5-41}$$

$$P(\tilde{\theta}) = 662.4288 + 0.34003 MN - 410.00349\emptyset + 13.54441\emptyset * IT - 1.023665 IT^2 + 1.93659 \times 10^{-2} IT^3 \quad \text{Eq.5-42}$$

The models proposed are significative and the assumptions of normality of the data, homoscedasticity and independence were validated. The parameter X_1 was established to be constant for simplicity. Moreover, accurate results were obtained by considering this approximation. The value selected for this constant was calculated as the average of the 32 values obtained in the optimization problem.

The characteristic temperature can be deduced by using the Equation 5-31 as a function of the characteristic pressure. Accurate results were obtained with this approach:

$$T(\tilde{\theta}) = T_{IVC}\left(\frac{P(\tilde{\theta})}{P_{IVC}}\right)^{\frac{n-1}{n}} \quad \text{Eq.5-43}$$

The temperature at IVC (T_{IVC}) crank angle can be estimated by using Equation 4-25. Because it was assumed adiabatic conditions for estimating unburned gas temperature, the polytropic coefficient n becomes the specific heat ratio ($\gamma = 1.28$). Nevertheless,

similar results were obtained by considering polytropic coefficient and specific heat ratio. This formulation requires prior knowledge of P_{IVC}, which correspond to the fuel-air mixture pressure at inlet valve close crank angle. This problem can be solved by considering that pressure is approximately equal to inlet boost pressure. This assumption can be assumed due to the few variation of pressure during the intake process and early stage of compression phase. A positive difference of 2 kPa between the air-fuel pressure from IVO to IVC crank angle was observed. These equations are valid within equivalence ratio, MN and IT levels considered in the experiments.

A strong correlation was evidenced between engine operating conditions and the optimal set of model parameters obtained in the optimization problem. Figure 5-4 illustrates the relationship between the model parameter X_2 and the CCR/IT ratio. This parameter defines the unburned gas pressure effect on auto-ignition of the fuel. The trend of X_2 is slightly affected by the increment of the compression ratio. This increment promotes auto-ignition of the fuel inside the combustion chamber, which is consistent with the observations. Similar observations can be deduced from the IT effects. An advance (or increment) of the IT increases the pressure effect on the auto-ignition of the fuel. Figure 5-5 shows a strong correlation between activation energy coefficient X_3 and CCR. This parameter describe the synergy that exist between the unburned gas temperature and CCR. Low activation energy coefficient represents high auto-ignition tendency of the fuel due to the ignition delay time function tends to decrease significantly. This observation matches with the high CCR effect, which is represented by a high unburned gas temperature in the combustion chamber.

The consistency of characteristic pressure $P(\tilde{\theta})$ and temperature $T(\tilde{\theta})$ were evaluated in Figure 5-6. This figure illustrates the relationship between CCR and $T(\tilde{\theta})/P(\tilde{\theta})$ ratio. These parameters represent the thermodynamic state of the air-fuel mixture when auto-ignition takes place. Therefore, it is expected that the effects of these parameters must be similar that the effects of the unburned gas pressure and temperature. When characteristic pressure increases, the ignition delay time function decreases drastically. This behavior promotes the auto-ignition of the fuel.

Table 5-1. Optimal constant coefficients of the integral model and characteristics temperature and pressure of the first round of the experiment

Run	MN	$\emptyset$	IT(°bTDC)	X_1	X_2	X_3	$\tilde{P}$ (kPa)	$\tilde{T}$ (K)	KOCA (deg.)
1	80	0.8	22.4	1.1279	-0.7870	0.2308	311.290	464.000	11.20
2	50	0.9	26.2	1.1318	-0.7870	0.2439	281.280	457.660	4.9
3	65	0.9	26.2	1.1320	-0.7882	0.2442	278.220	456.570	5.18
4	80	0.8	30.0	1.1302	-0.7846	0.2395	290.770	458.750	4.69
5	80	1.0	30.0	1.1287	-0.7728	0.2382	311.030	462.720	1.27
6	65	0.9	30.0	1.1306	-0.7793	0.2447	283.920	451.920	0.28
7	80	1.0	22.4	1.1303	-0.7884	0.2386	294.610	460.210	8.97
8	50	0.8	22.4	1.1291	-0.7850	0.2368	303.410	458.840	8.71
9	65	0.9	22.4	1.1306	-0.7881	0.2412	291.880	457.090	8.57
10	65	1.0	26.2	1.1310	-0.7828	0.2449	284.460	453.110	3.05
11	80	0.9	26.2	1.1304	-0.7866	0.2398	291.000	458.970	6.12
12	65	0.8	26.2	1.1305	-0.7859	0.2405	290.490	458.030	6.03
13	65	0.9	26.2	1.1318	-0.7877	0.2449	280.470	455.630	5.07
14	50	1.0	30.0	1.1319	-0.7855	0.2470	279.240	452.700	3.57
15	50	0.8	30.0	1.1309	-0.7812	0.2457	281.590	451.220	0.86
16	50	1.0	22.4	1.1314	-0.7875	0.2441	285.680	455.460	6.77

Table 5-2 Optimal constant coefficients of the integral model and characteristics temperature and pressure of the second round of the experiment

Run	MN	∅	IT(°bTDC)	X_1	X_2	X_3	$\tilde{P}$ (KPa)	$\tilde{T}$(K)	KOCA (deg.)
17	80	0.8	22.4	1.1284	-0.7876	0.2312	307.620	465.240	10.75
18	50	0.9	26.2	1.1314	-0.7850	0.2450	283.340	454.240	3.52
19	65	0.9	26.2	1.1330	-0.7895	0.2486	271.910	453.610	5.89
20	80	0.8	30.0	1.1307	-0.7863	0.2407	286.540	458.370	4.56
21	80	1.0	30.0	1.1319	-0.7849	0.2453	276.530	455.550	1.32
22	65	0.9	30.0	1.1315	-0.7822	0.2472	277.790	450.990	0.70
23	80	1.0	22.4	1.1321	-0.7940	0.2425	280.200	460.050	9.43
24	50	0.8	22.4	1.1300	-0.7889	0.2376	296.870	460.770	9.40
25	65	0.9	22.4	1.1322	-0.7936	0.2434	280.640	459.090	9.24
26	65	1.0	26.2	1.1333	-0.7906	0.2486	268.810	455.010	3.84
27	80	0.9	26.2	1.1322	-0.7923	0.2434	278.420	459.230	7.31
28	65	0.8	26.2	1.1314	-0.7908	0.2410	285.830	460.160	7.60
29	65	0.9	26.2	1.1330	-0.7896	0.2487	271.930	453.600	2.99
30	50	1.0	30.0	1.1332	-0.7849	0.2516	265.170	450.120	-0.95
31	50	0.8	30.0	1.1322	-0.7867	0.2462	275.510	455.120	2.83
32	50	1.0	22.4	1.1331	-0.7913	0.2489	273.910	453.360	7.23

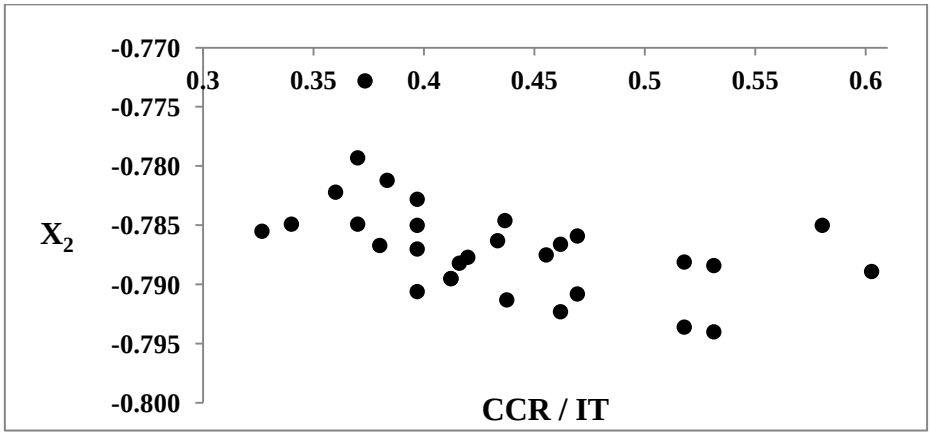

Figure 5-4 Correlation between CCR/ IT ratio and pressure coefficient of the empirical auto-ignition model

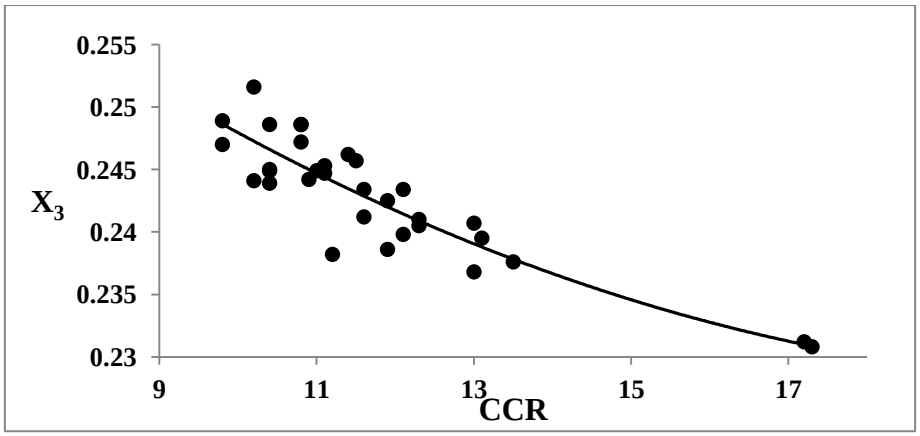

Figure 5-5 Correlation between CCR and activation energy coefficient of the empirical auto-ignition model

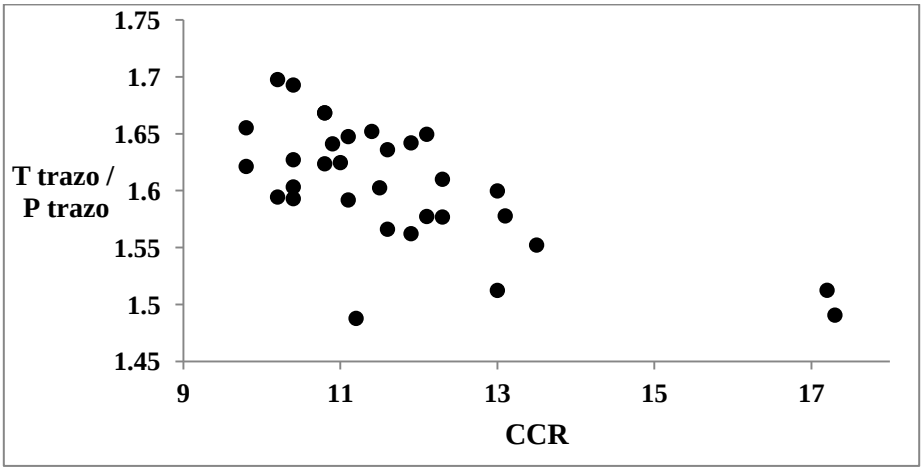

Figure 5-6 Effect of CCR on characteristic pressure and temperature

An increment in the CCR represents high auto-ignition tendency of the fuel, being consistent with the observations done.

To verify that the optimization technique used was appropriate, an error function was defined as:

$$I(KOCA) = \left\{ \int_{\theta_{IVC}}^{KOCA} \left[\frac{d\theta}{X_1 p^{X_2} \exp\left(\frac{EX_3}{T}\right)} \right] - 1 \right\}^2 \approx 0 \qquad \text{Eq.5-45}$$

If the model parameters are optimal, the error function must tend to zero at crank angles near to KOCA. To develop this analysis, an arbitrary selection of operating point in the experiment was carried out. The operating point selected were: Run 1,2,3 and 5. Figure 5-7 illustrates the error function for each operating point defined. It is observed that this function tend to zero when crank angle are near to KOCA. The experimental KOCA can be evaluated in Tables 5-1 and 5-2.

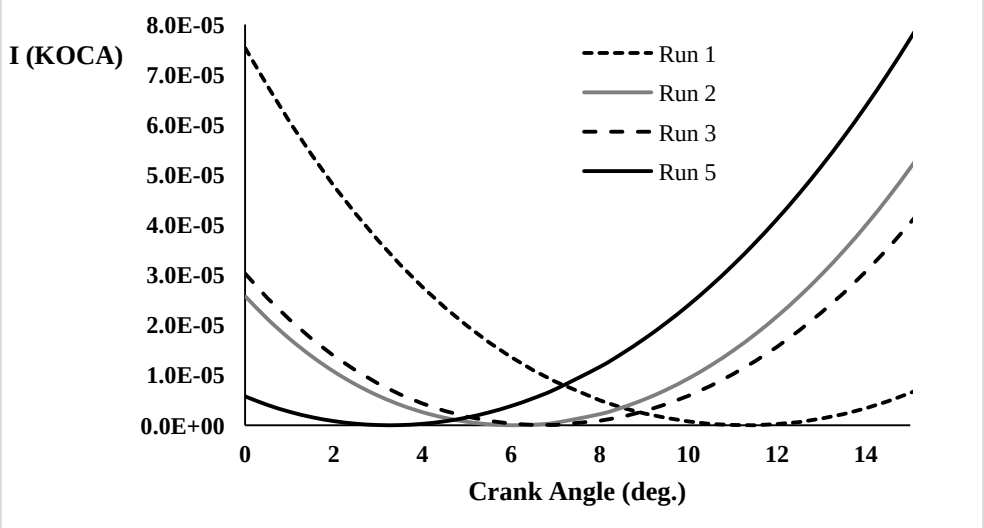

Figure 5.7 Error function defined for five operating points for CH_4/H_2 mixtures

5.5.1. Auto-ignition prediction and model validation. In this section an evaluation of the performance of the auto-ignition model was carried out. Figure 5-8 shows the experimental KOCA and those estimated by using the present model. The experimental

values of KOCA in Figure 5-8 are the average KOCA of each operating point of the experiment. The points used in this figure are those used for developing the present empirical model. These predictions are compared with the predictions done with Equation 4-29, which is an alternative tool for predicting KOCA.

$$KOCA = 35.57990 + 0.064967MN - 11.05\emptyset - 0.93645IT \qquad \text{Eq. 5-1}$$

It is observed that the models proposed follow the variability of the experimental data; in addition, accurate estimations were obtained.

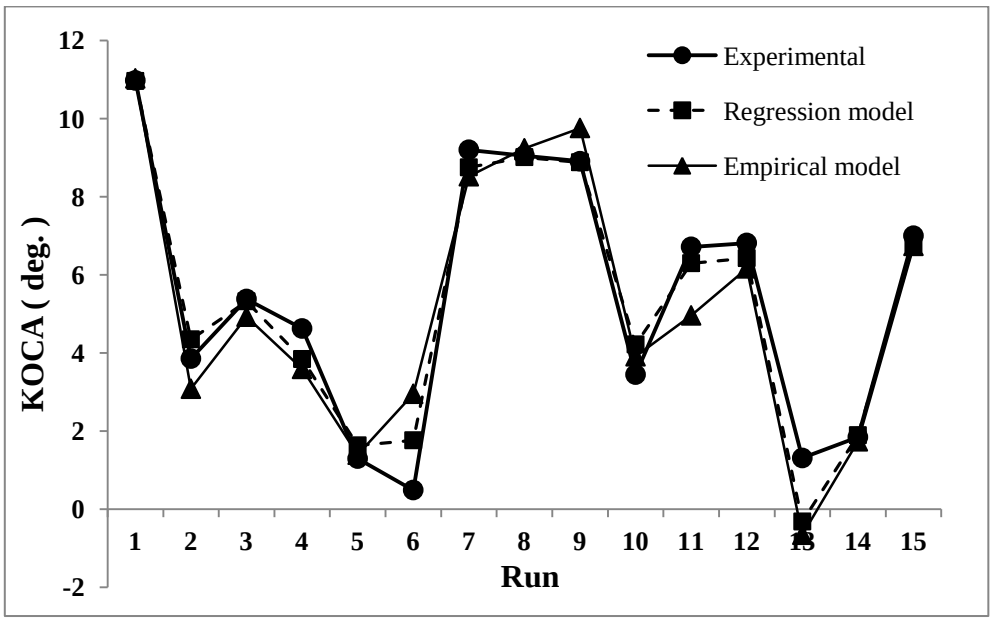

Figure 5-8. KOCA predictions by using the empirical model and the regression model

To validate the model proposed, additional runs were carried out. Table 5-3 shows eight intermediate operating points that are within the levels of the factors defined in the design of experiment. These intermediate points were obtained following the methodology employed in Chapter 4. Figure 5-9 shows the prediction done with both models. It is observed that these models follow the variability of the experimental data.

Table 5.3 Intermediate operating points for the validation of the models proposed

				KOCA (deg.)		
Run	**MN**	**ø**	**IT (ºbTDC)**	**Exp**	**Regression Model**	**This model**
1	55	0.85	24	7.1	7.3	8.0
2	68	0.86	28	1.5	4.3	5.1
3	78	0.98	29	1.5	2.7	3.0
4	52	0.95	23	6.2	6.9	7.4
5	78	0.84	28	3.4	5.1	5.3
7	50	0.9	30	-2.1	0.8	1.2

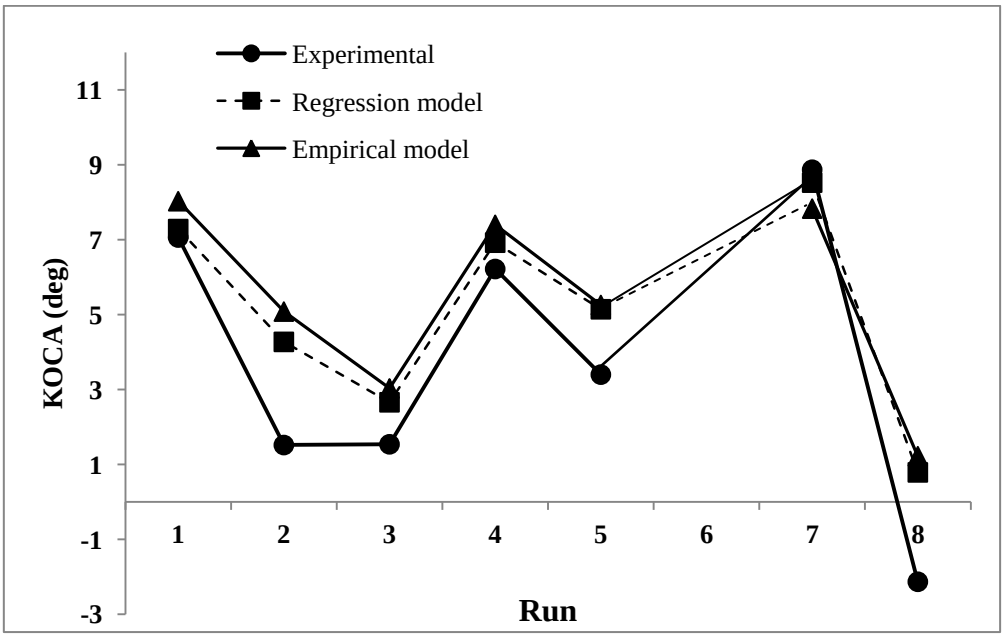

Figure 5-9 Prediction of KOCA for intermediate operating points

It is observed that the models overpredict KOCA in almost all cases. An explanation of this is the uncertainty of the equivalence ratio and the fuel composition since these parameters depend on the accuracy of the flowmeters used. Another explanation of this difference is the error propagation of the typical error of the regression models employed. However, the auto-ignition model is an interesting tool that can be implemented in zero and multi-dimensional models.

5.6. CONCLUSIONS

A comprehensive analysis of the influence of engine operating conditions and MN on the auto-ignition in a CFR was developed. Based on the results obtained, the following conclusions are described:

✓ Empirical auto-ignition model is a suitable approach to determine KOCA at different engine operating conditions and MN. This model is a contribution for understanding the auto-ignition phenomena of gaseous fuels with variable MN.

✓ There is a strong correlation between optimal model parameters and CCR since explains the observations about the effects of variation of the pressure and temperature of the unburned gas in the combustion chamber.

✓ Characteristic pressure $P(\tilde{\theta})$ and temperature $T(\tilde{\theta})$ are representative parameters of the thermodynamic state of air fuel gas inside the combustion chamber. They explain the effects of CCR and IT on the phenomenon.

✓ Single step model is a suitable approach for estimating unburned gas temperature due to polytropic coefficient is known previously.

Chapter 6

Conclusions Future works and Recommendations

6.1 CONCLUSIONS

The most important conclusions derived from this thesis are described as follows:

✓ Strong deviation with respect to the experimental ignition delay time data was obtained at low temperature for $CO/CO_2/H_2$ mixtures. This thesis demonstrated that these deviations are also followed for H_2/CH_4 mixtures and natural gas.

✓ The most sensitivity elementary reactions, which govern auto-ignition phenomena are $2OH\ (+M) \Leftrightarrow H_2O_2(+M)$ and $H+H_2O_2 \Leftrightarrow HO_2+H_2$. However, it was observed that another elementary reaction, which plays an important role for the estimations of ignition delay time of $CO/CO_2/H_2$ mixtures, is $HO_2+CO \Leftrightarrow OH+CO_2$; Good results were obtained with the first two elementary reactions described. When Cavaliere et al., (2010)'s modifications were applied, improvement on the ignition delay time estimations were obtained without decrease accuracy in the laminar flame speed estimations of $CO/CO_2/H_2$ and CH_4/H_2 mixtures.

✓ An important contribution of this thesis is the demonstration that values of individual KOCA is not affected by individual knock intensity. An- one factor analysis of variance (ANOVA) was used to evaluated this effect by considering constant engine operating conditions. For this test, facility natural gas as reference fuel was employed.

This result allows studying auto-ignition of a fuel without take into account the variability of individual knock intensity during a test.

✓ An empirical model for estimating MN of CO/CO2/H2 mixtures was proposed. The MN as a function of the fuel composition is given by:

$$MN = 17.76H_2 + 6.1346CO + 11.0318CO_2 - 0.3499H_2 * CO - 0.4584H_2 * CO_2 - 0.1922fCO * CO_2$$

Strong deviation between experimental MN and those predicted by using AVL software was evidenced, due to the high concentration of carbon dioxide and carbon monoxide in the fuel. The model proposed represents a good tool for MN estimation of fuels with high concentrations of these species.

✓ There is a linear relationship between KOCA and MN regardless of the fuel composition. As MN increases, KOCA also increases; this behavior is dominated by the hydrogen concentration in the fuels.

✓ The MN, equivalence ratio and IT influence KOCA and CCR. This conclusion is based on the assumption of constant inlet temperature and output power. There is not enough statistical evidence that increment of boost pressure affect KOCA. However, a slight effect was evidence since KOCA decreased when boost pressure increased.

✓ A contribution for estimating combustion parameters of gaseous fuels was developed in this thesis. This method is based on indicator diagram and allows estimating with accuracy SOC and EOC of fuels. It was demonstrated that the parameters obtained are consistent with the Wiebe function for modeling MFB. Typical values of the Wiebe function for these fuels are $a = 2.8$ and $= 2.4$.

✓ A set of equations for estimating unburned gas temperature at IVC crank angle, residual gas fraction and residual gas temperature were developed. These equations consider heat transfer (coming from cylinder wall, head cylinder during intake process) and residual gas effects. The general equation that relates this variables is given by:

$$\frac{Q}{PV_{ivc}} - \frac{\gamma}{\gamma - 1}\left[1 + (x_r - 1)\frac{T_i}{T_{ivc}} - \frac{x_r}{\gamma}\frac{T_r}{T_{ivc}}\right] + \frac{V_{ivo}}{V_{ivc}} = 0 \qquad \text{Eq. 4-23}$$

✓ It was demonstrated analytically that polytropic coefficient of compression and expansion phase of the engine cycle is equal to the negative slope of the linear region observed in the indicator diagram. Average polytropic coefficient for CH_4/H_2 mixtures at lean and stoichiometric conditions (Ø=0.8~1) is 1.23. The adiabatic polytropic coefficient, which is called the specific heat ratio, is equal to 1.28. The polytropic coefficient decreases as compression ratio increases. This is caused by the heat transfer from cylinder gas to head and wall cylinder of the engine.

✓ The lack of accuracy of a detailed chemical kinetic mechanism was quantified through a auto-ignition model. The observations are consistent with the observations done to the mechanism for predicting ignition delay times of gaseous fuels such as syngas and CH_4/H_2 mixtures. It was concluded that the accuracy of the mechanism used as reference increases when engine runs at high compression ratio.

✓ The empirical auto-ignition model developed in this thesis is a suitable tool to determine KOCA under different engine operating conditions and MN. This model is a contribution for understanding the auto-ignition phenomena of gaseous fuels with variable MN.

6.2. FUTURE WORKS AND RECOMMENDATIONS

To model auto-ignition of gaseous fuels by using detailed chemical kinetic mechanism in ICE is an active field of research. It is imperative to produce experimental data of ignition delay time of gaseous fuels at low temperature. This experimental data is required to optimize the currents chemical kinetic mechanism for modeling auto-ignition of gaseous fuels.

To improve the understanding of auto-ignition phenomena, it is required to consider heat transfer. Heat transfer influences significantly auto-ignition and must be determined experimentally in order to quantify its actual effect on KOCA.

The measurement of unburned gas temperature is important for developing accurate auto-ignition models. This measurement allows optimizing actual chemical kinetic mechanism by using KOCA as target data.

To generalize the use of the methodologies developed in this thesis, it is required to apply the methodologies by using engines of different sizes fueled with other fuels.

A linear trend was observed between MN of the fuel and KOCA. It is required to verify if this trend is the same with fuel blend that does not have hydrogen as component.

Although it was demonstrated that individual cycle by cycle KOCA is not affected by individual knock intensity, and extrapolation of this conclusion cannot be done for global knock intensity. It is required to design an experiment in order to verify if the average KOCA corresponding to an operating point of the engine is affected by the global knock intensity in the engine.

Bibliography

A

Aparna Arunachalam. (2010). *Experimental & analytical evaluation of knock characteristics of producer gas*. Colorado State University.

Arunachalam, A., & Olsen, D. B. (2012). Experimental evaluation of knock characteristics of producer gas. *Biomass and Bioenergy*, *37*, 169–176.

Attar, A. A., & Karim, G. A. (2003). Knock rating of gaseous fuels. *Journal of Engineering for Gas Turbines and Power*, *125*(2), 500–504.

B

Beccari, S., Pipitone, E., & Genchi, G. (2016). Knock onset prediction of propane, gasoline and their mixtures in spark ignition engines. *Journal of the Energy Institute*, *89*(1), 101–114.

Bika, A. S., Franklin, L., & Kittelson, D. B. (2011). Engine knock and combustion characteristics of a spark ignition engine operating with varying hydrogen and carbon monoxide proportions. *International Journal of Hydrogen Energy*, *36*(8), 5143–5152.

Blumenthal, R., Fieweger, K., Komp, K. H., Adomeit, G., & Gelfand, B. E. (1996). Self-ignition of H2-air mixtures at high pressure and low temperature. *Proc. 20th ISSW, World Scientific*, *2*, 935–940.

Boloy, R. A. M., Silveira, J. L., Tuna, C. E., Coronado, C. R., & Antunes, J. S. (2011). Ecological impacts from syngas burning in internal combustion engine:

Technical and economic aspects. *Renewable and Sustainable Energy Reviews*, *15*(9), 5194–5201.

Bood, J., Bengtsson, P.-E., Mauss, F., Burgdorf, K., & Denbratt, I. (1997). *Knock in spark-ignition engines: end-gas temperature measurements using rotational CARS and detailed kinetic calculations of the autoignition process*. SAE Technical Paper. Retrieved from http://papers.sae.org/971669/

Bouvet, N. (2009). *Experimental and numerical studies of the fundamental flame speeds of methane/air and syngas (H2/CO)/air mixtures*. Université d'Orléans. Retrieved from https://tel.archives-ouvertes.fr/tel-00473266/

Bradley, D., Kalghatgi, G. T., & Golombok, M. (1996). *Fuel blend and mixture strength effects on autoignition heat release rates and knock intensity in SI engines*. SAE Technical Paper. Retrieved from http://papers.sae.org/962105/

Brunt, M. F., Pond, C. R., & Biundo, J. (1998). *Gasoline engine knock analysis using cylinder pressure data*. SAE Technical Paper. Retrieved from http://papers.sae.org/980896/

C

Callahan, T. J., Ryan III, T. W., Buckingham, J. P., Kakockzi, R. J., & Sorge, G. (1996). *Engine knock rating of natural gases–Expanding the MN database*. American Society of Mechanical Engineers, New York, NY (United States). Retrieved from http://www.osti.gov/scitech/biblio/541054

Cavaliere, D. E., Joannon, M. de, Sabia, P., Sirignano, M., & D'Anna, A. (2010a). A comprehensive kinetic modeling of ignition of syngas–air mixtures at low temperatures and high pressures. *Combustion Science and Technology*, *182*(4–6), 692–701.

Chaos, M., & Dryer, F. L. (2008). Syngas Combustion Kinetics and Applications. *Combustion Science and Technology*, *180*(6), 1053–1096. https://doi.org/10.1080/00102200801963011

Checkel, M. D., & Dale, J.D. (1986). computerized knock detection from engine pressure records. No. 860028. *Society of Automotive Engineers*, 1–11.

Chen, L., Li, T., Yin, T., & Zheng, B. (2014). A predictive model for knock onset in spark-ignition engines with cooled EGR. *Energy Conversion and Management*, *87*, 946–955.

Cheng, S., Yang, Y., Brear, M. J., Kang, D., Bohac, S., & Boehman, A. L. (2016). Autoignition of pentane isomers in a spark-ignition engine. *Proceedings of the Combustion Institute*. Retrieved from http://www.sciencedirect.com/science/article/pii/S154074891630431X

Chun, K. M. (1988). *Characterization of knock and prediction of its onset in a spark-ignition engine*. Massachusetts Institute of Technology. Retrieved from http://dspace.mit.edu/handle/1721.1/14741

Cuddihy, J. L. (2014). *A User-friendly, Two-zone Heat Release Model for Predicting Spark-ignition Engine Performance and Emissions*.

da Silva, L. F. F., & Junior, A. R. N. (2011). On The Predictability of Chemical Kinetics for the Description of the Combustion of Simple Fuels, *33*. Retrieved from http://www.scielo.br/pdf/jbsmse/v33n4/a13v33n4.pdf

D

Davis, S. G., Joshi, A. V., Wang, H., & Egolfopoulos, F. (2005). An optimized kinetic model of H 2/CO combustion. *Proceedings of the Combustion Institute*, *30*(1), 1283–1292.

de Vries, J. (2005). *An Investigation of the Autoignition of Power Generation Gas Turbine Fuel Blends Using a Design of Experiments Approach*. University of Central Florida Orlando, Florida. Retrieved from http://purl.fcla.edu/fcla/etd/cfe0000817

Deutschmann, O., Schmidt, R., Behrendt, F., & Warnat, J. (1996). Numerical modeling of catalytic ignition. *Symposium (International) on Combustion*, *26*(1), 1747–1754. https://doi.org/10.1016/S0082-0784(96)80400-0

Douaud, A. M., & Eyzat, P. (1978). *Four-octane-number method for predicting the anti-knock behavior of fuels and engines*. SAE Technical Paper. Retrieved from http://papers.sae.org/780080/

E

Elmqvist, C., Lindström, F., \AAngström, H.-E., Grandin, B., & Kalghatgi, G. (2003). *Optimizing engine concepts by using a simple model for knock prediction*. SAE Technical Paper. Retrieved from http://papers.sae.org/2003-01-3123/

F

F. A. Williams. (2005). San Diego mechanism 2005/12/01. *Technical Report*.

Fox, J. W., Cheng, W. K., & Heywood, J. B. (1993). *A model for predicting residual gas fraction in spark-ignition engines*. SAE Technical Paper. Retrieved from http://papers.sae.org/931025/

Frenklach, M., Wang, H., & Rabinowitz, M. J. (1992). Optimization and analysis of large chemical kinetic mechanisms using the solution mapping method—combustion of methane. *Progress in Energy and Combustion Science*, *18*(1), 47–73. https://doi.org/10.1016/0360-1285(92)90032-V

G

Ganestam, P. (2010). Empirical Knock Model for Automatic Engine Calibration. *MSc Theses*. Retrieved from http://lup.lub.lu.se/student-papers/record/8847475

GASURE. (2011). Manual:Metodlogia para el calculo de la velocidad de deflagracion laminar y espesor de llama.

Gatowski, J. A., Balles, E. N., Chun, K. M., Nelson, F. E., Ekchian, J. A., & Heywood, J. B. (1984). *Heat release analysis of engine pressure data*. SAE Technical paper. Retrieved from http://papers.sae.org/841359/

Gersen, S., van Essen, M., Levinsky, H., & van Dijk, G. (2016). Characterizing Gaseous Fuels for Their Knock Resistance based on the Chemical and Physical Properties of the Fuel. *SAE International Journal of Fuels and Lubricants*, *9*(2015-01-9077), 1–13.

Gomez M. Juan, Amell Andres, & Olsen Daniel B. (2016). Prediction and measurement of the critical compression ratio and MN for blends of biogas with methane, propane and hydrogen. *Fuel*, *186*, 168–175.

H

Hajireza, S., Mauss, F., & Sundén, B. (1997). *Investigation of end-gas temperature and pressure increases in gasoline engines and relevance for knock occurrence*. SAE Technical Paper. Retrieved from http://papers.sae.org/971671/

Hassan, M. I., Aung, K. T., & Faeth, G. M. (1997). Properties of laminar premixed CO/H/air flames at various pressures. *Journal of Propulsion and Power*, *13*(2), 239–245.

Healy, D., Donato, N. S., Aul, C. J., Petersen, E. L., Zinner, C. M., Bourque, G., & Curran, H. J. (2010). n-Butane: Ignition delay measurements at high pressure and detailed chemical kinetic simulations. *Combustion and Flame*, *157*(8), 1526–1539.

Hernandez, J. J., Serrano, C., & Perez, J. (2006). Prediction of the Autoignition Delay Time of Producer Gas from Biomass Gasification. *Energy & Fuels*, *20*(2), 532–539. https://doi.org/10.1021/ef058025c

Heywood, J. B., & others. (1988). *Internal combustion engine fundamentals* (Vol. 930). Mcgraw-hill New York. Retrieved from http://www.sidalc.net/cgi-bin/wxis.exe/?IsisScript=LIBRO.xis&method=post&formato=2&cantidad=1&expresion=mfn=015556

Ho, S., Amlee, D., & Johns, R. (1996). *A comprehensive knock model for application in gas engines*. SAE Technical Paper. Retrieved from http://papers.sae.org/961938/

Ho, S. Y., & Kuo, T.-W. (1997). *A hydrocarbon autoignition model for knocking combustion in SI engines*. SAE Technical Paper. Retrieved from http://papers.sae.org/971672/

Hu, E., Huang, Z., He, J., Jin, C., & Zheng, J. (2009). Experimental and numerical study on laminar burning characteristics of premixed methane–hydrogen–air flames. *International Journal of Hydrogen Energy*, *34*(11), 4876–4888.

Huang, J., Bushe, W. K., Hill, P. G., & Munshi, S. R. (2006). Experimental and kinetic study of shock initiated ignition in homogeneous methane–hydrogen–air mixtures at engine-relevant conditions. *International Journal of Chemical Kinetics*, *38*(4), 221–233.

Hughes, K. J., Turanyi, T., Clague, A. R., & Pilling, M. J. (2001). Development and testing of a comprehensive chemical mechanism for the oxidation of methane. *International Journal of Chemical Kinetics*, *33*(9), 513–538.

K

Kalghatgi, G. T., Golombok, M., & Snowdon, P. (1995). Fuel effects on knock, heat release and “CARS” temperatures in a spark ignition engine. *Combustion Science and Technology*, *110*(1), 209–228.

Kalitan, D. M. (2007). *A Study of Syngas Oxidation at High Pressures and Low Temperatures*. ProQuest. Retrieved from http://books.google.es/books?hl=es&lr=&id=k4-UYFZmnl0C&oi=fnd&pg=PR13&dq=A+Study+of+Syngas+Oxidation+at+High+Pressures+and+Low+Temperatures&ots=-WiKZ9BLV4&sig=SI7BgcBCRKc15_Jg24AcJTRXIzU

Karim, G. A., & Gao, J. (1992). *A predictive model for knock in spark ignition engines*. SAE Technical Paper. Retrieved from http://papers.sae.org/922366/

Karim, G. A., & Liu, Z. (1992). *A predictive model for knock in dual fuel engines*. SAE Technical Paper. Retrieved from http://papers.sae.org/921550/

Kéromnès, A., Metcalfe, W. K., Heufer, K. A., Donohoe, N., Das, A. K., Sung, C.-J., … others. (2013). An experimental and detailed chemical kinetic modeling study of hydrogen and syngas mixture oxidation at elevated pressures. *Combustion and Flame*, *160*(6), 995–1011.

Kitada, T., Kuchita, M., Hayashi, S., Shirota, T., Sakai, Y., & Kawazoe, H. (2015). A Study on Knocking Prediction Improvement Using Chemical Reaction Calculation. *SAE International Journal of Engines*, *9*(2015-01-1905), 201–209.

Kline, S. J., & McClintock, F. A. (1953). Describing uncertainties in single-sample experiments. *Mechanical Engineering*, *75*(1), 3–8.

L

Leiker, M., K, C., W, C., Pfeifer, U., & Rankl, M. (1972). Evaluation of antiknocking property of gaseous fuels by means of MN and its practical application to gas engines. In *MECHANICAL ENGINEERING* (Vol. 94, p. 55). ASME-AMER SOC MECHANICAL ENG 345 E 47TH ST, NEW YORK, NY 10017.

Li, H., & Karim, G. A. (2005). Exhaust emissions from an SI engine operating on gaseous fuel mixtures containing hydrogen. *International Journal of Hydrogen Energy*, *30*(13), 1491–1499.

Li, J., Zhao, Z., Kazakov, A., Chaos, M., Dryer, F. L., & Scire, J. J. (2007). A comprehensive kinetic mechanism for CO, CH2O, and CH3OH combustion. *International Journal of Chemical Kinetics*, *39*(3), 109–136. https://doi.org/10.1002/kin.20218

Lieuwen, T., Yang, V., & Yetter, R. (2009). *Synthesis Gas Combustion: Fundamentals and Applications*. CRC Press.

Lifshitz, A., Scheller, K., Burcat, A., & Skinner, G. B. (1971). Shock-tube investigation of ignition in methane-oxygen-argon mixtures. *Combustion and Flame*, *16*(3), 311–321. https://doi.org/10.1016/S0010-2180(71)80102-5

Liu, Z. (2010). *Chemical kinetics modeling study on fuel autoignition in internal combustion engines*. \copyright Zhen Liu. Retrieved from https://dspace.lboro.ac.uk/dspace/handle/2134/6533

Liu, Z., & Chen, R. (2009). A zero-dimensional combustion model with reduced kinetics for SI engine knock simulation. *Combustion Science and Technology*, *181*(6), 828–852.

Livengood, J. C., & Wu, P. C. (1955). Correlation of autoignition phenomena in internal combustion engines and rapid compression machines. In *Symposium (International) on Combustion* (Vol. 5, pp. 347–356). Elsevier.

M

Malenshek, M., & Olsen, D. B. (2009b). MN testing of alternative gaseous fuels. *Fuel*, *88*(4), 650–656.

Marinov, N. M., Pitz, W. J., Westbrook, C. K., Vincitore, A. M., Castaldi, M. J., Senkan, S. M., & Melius, C. F. (1998). Aromatic and polycyclic aromatic hydrocarbon formation in a laminar premixed n-butane flame. *Combustion and Flame*, *114*(1), 192–213.

Metcalfe, W. K., Burke, S. M., Ahmed, S. S., & Curran, H. J. (2013). A hierarchical and comparative kinetic modeling study of C1- C2 hydrocarbon and oxygenated fuels. *International Journal of Chemical Kinetics*, *45*(10), 638–675.

Montgomery, D. C. (2008). *Design and analysis of experiments*. John Wiley & Sons. Retrieved from https://books.google.es/books?hl=es&lr=&id=kMMJAm5bD34C&oi=fnd&pg=PA1&dq=montgomery+design+of+experiments&ots=Kmq4Lw-LrD&sig=lYQ1VBmP-zWUrp-6nFYSIEpU4bI

Montoya, J. P. G., Amell, A. A., & Olsen, D. B. (2016). Prediction and measurement of the critical compression ratio and MN for blends of biogas with methane, propane and hydrogen. *Fuel*, *186*, 168–175.

Moran, M. J., Shapiro, H. N., Boettner, D. D., & Bailey, M. B. (2010). *Fundamentals of engineering thermodynamics*. John Wiley & Sons. Retrieved from https://books.google.es/books?hl=es&lr=&id=oyt8iW6B4aUC&oi=fnd&pg=PA21&dq=moran+shapiro+fundamentals&ots=9YM9yyi4GQ&sig=jO4mR8fPZWvTWhBUz7GUryCk3ms

Morganti, K. J., Brear, M. J., da Silva, G., Yang, Y., & Dryer, F. L. (2015). The autoignition of Liquefied Petroleum Gas (LPG) in spark-ignition engines. *Proceedings of the Combustion Institute*, *35*(3), 2933–2940.

N

Nakano, M., Nakahara, S., Akihama, K., Kubo, S., & Yamazahi, S. (1995). *Predictions of the knock onset and the effects of heat release pattern and unburned gas temperature on torque at knock limit in SI engines*. SAE Technical Paper. Retrieved from http://papers.sae.org/952408/

Noda, T., Hasegawa, K., Kubo, M., & Itoh, T. (2004). *Development of transient knock prediction technique by using a zero-dimensional knocking simulation with chemical kinetics*. SAE Technical Paper.

P

Pang, G. A., Davidson, D. F., & Hanson, R. K. (2009). Experimental study and modeling of shock tube ignition delay times for hydrogen–oxygen–argon mixtures at low temperatures. *Proceedings of the Combustion Institute, 32*(1), 181–188. https://doi.org/10.1016/j.proci.2008.06.014

Peschke, W. T., & Spadaccini, L. J. (1985). *Determination of autoignition and flame speed characteristics of coal gases having medium heating values*. The Institute.

Petersen, E. L., Davidson, D. F., & Hanson, R. K. (1999). Kinetics modeling of shock-induced ignition in low-dilution CH4/O2 mixtures at high pressures and intermediate temperatures. *Combustion and Flame, 117*(1–2), 272–290. https://doi.org/10.1016/S0010-2180(98)00111-4

Petersen, E. L., Kalitan, D. M., Barrett, A. B., Reehal, S. C., Mertens, J. D., Beerer, D. J., … McDonell, V. G. (2007a). New syngas/air ignition data at lower temperature and elevated pressure and comparison to current kinetics models. *Combustion and Flame, 149*(1), 244–247.

Pipitone, E., Beccari, S., & Genchi, G. (2015). A refined model for knock onset prediction in spark ignition engines fueled with mixtures of gasoline and propane. *Journal of Engineering for Gas Turbines and Power, 137*(11), 111501.

R

Reaction Design. (2013). Chemkin Theory Manual.

Reehal, S., T Hair, A Barrett, & EL Petersen. (2007). Ignition delay time measurements of synthesis gas mixtures at engine pressures. Presented at the In Proc. 5 th US Combustion Meeting.

Rodrigues, R., & Shrestha, S. B. (2006). *Knock Rating of Gaseous Fuels in the Presence of Diluents*. SAE Technical Paper. Retrieved from http://papers.sae.org/2006-01-3429/

Rostampour, A., & Toosi, A. N. (2015). Numerical Investigation of the Effect of Knock on Heat Transfer in a Turbocharged Spark Ignition Engine. *Journal of Engineering for Gas Turbines and Power*, *137*(12), 121502.

Rousseau, S., Lemoult, B., & Tazerout, M. (1999). Combustion characterization of natural gas in a lean burn spark-ignition engine. *Proceedings of the Institution of Mechanical Engineers, Part D: Journal of Automobile Engineering*, *213*(5), 481–489.

Russ, S. (1996). *A review of the effect of engine operating conditions on borderline knock*. SAE Technical Paper. Retrieved from http://papers.sae.org/960497/

Ryan, T. W., Callahan, T. J., & King, S. R. (1993). Engine Knock Rating of Natural Gases—MN. *Journal of Engineering for Gas Turbines and Power*, *115*(4), 769–776.

S

Sahoo, B. B., Saha, U. K., & Sahoo, N. (2011). Theoretical performance limits of a syngas–diesel fueled compression ignition engine from second law analysis. *Energy*, *36*(2), 760–769.

Sahoo, B. B., Sahoo, N., & Saha, U. K. (2012). Effect of H 2: CO ratio in syngas on the performance of a dual fuel diesel engine operation. *Applied Thermal Engineering*, *49*, 139–146.

Saxena, P. (2007). Numerical and experimental studies of ethanol flames and autoignition theory for higher alkanes. Retrieved from https://escholarship.org/uc/item/3bq724kg.pdf

Schiffgens, H.-J., Endres, H., Wackertapp, H., & Schrey, E. (1994). Concepts for the adaptation of si gas engines to changing MN. *Journal of Engineering for Gas Turbines and Power*, *116*(4), 733–739.

Shao, J., & Rutland, C. (2014). *Modeling Investigation of Auto-Ignition and Engine Knock by HO 2*. SAE Technical Paper. Retrieved from http://papers.sae.org/2014-01-1221/

Smith G., David M. Golden, Michael Frenklach, Nigel W. Moriarty, Boris Eiteneer, Mikhail Goldenberg, … Zhiwei Q. (1999). Retrieved from http://www.me.berkeley.edu/gri_mech/

Smith, G. P., Golden, D. M., Frenklach, M., Moriarty, N. W., Eiteneer, B., Goldenberg, M., … others. (1999). *GRI-Mech 3.0*.

Song, H., & Song, H. H. (2016). *Knock Prediction of Two-Stage Ignition Fuels with Modified Livengood-Wu Integration Model by Cool Flame Elimination Method*. SAE Technical Paper.

Soylu, S., & Van Gerpen, J. (2003). Development of an autoignition submodel for natural gas engines. *Fuel*, *82*(14), 1699–1707.

Stiebels, B., Schreiber, M., & Sakak, A. S. (1996). *Development of a new measurement technique for the investigation of end-gas autoignition and engine knock*. SAE Technical Paper. Retrieved from http://papers.sae.org/960827/

Sun, H., Yang, S. I., Jomaas, G., & Law, C. K. (2007). High-pressure laminar flame speeds and kinetic modeling of carbon monoxide/hydrogen combustion. *Proceedings of the Combustion Institute*, *31*(1), 439–446.

Swarts, A., Yates, A., Viljoen, C., & Coetzer, R. (2004). *Standard knock intensity revisited: Atypical burn rate characteristics identified in the CFR octane rating engine*. SAE Technical Paper. Retrieved from http://papers.sae.org/2004-01-1850/

T

Tanaka, H., Kobayashi, K., Sako, T., Kuwahara, K., Kawanabe, H., & Ishiyama, T. (2016). Factors Determining Antiknocking Properties of Gaseous Fuels in Spark-Ignition Gas Engines. *Journal of Engineering for Gas Turbines and Power*, *138*(10), 102806.

Taylor, S. C. (1991). *Burning velocity and the influence of flame stretch*. University of Leeds. Retrieved from http://etheses.whiterose.ac.uk/2099/

Thiessen, S., Khalil, E., & Karim, G. (2010). The autoignition in air of some binary fuel mixtures containing hydrogen. *International Journal of Hydrogen Energy*, *35*(18), 10013–10017.

Tougri, I., Colaço, M. J., Leiroz, A. J., & Melo, T. C. (2016). Knocking prediction in internal combustion engines via thermodynamic modeling: preliminary results and comparison with experimental data. *Journal of the Brazilian Society of Mechanical Sciences and Engineering*, 1–7.

Trijselaar, A. (2012). Knock prediction in gas-fired reciprocating engines. *Development of a Zerodimensional Two Zone Model Indicating Detailed Chemical Kinetics*, 20.

V

Vargas Salgado, C. A. (2012). *Estudio comparativo de la utilización de las tecnologías de gasificación Downdraft y lecho fluidizado burbujeante para la generación de energía eléctrica en aplicaciones de baja potencia*. Universidad Politécnica de Valencia. Retrieved from http://riunet.upv.es/bitstream/handle/10251/16379/tesisUPV3813.pdf?sequence=1

Vélez, J. F., Chejne, F., Valdés, C. F., Emery, E. J., & Londoño, C. A. (2009). Co-gasification of Colombian coal and biomass in fluidized bed: An experimental study. *Fuel*, *88*(3), 424–430. https://doi.org/10.1016/j.fuel.2008.10.018

W

Walton, S. M., He, X., Zigler, B. T., & Wooldridge, M. S. (2007). An experimental investigation of the ignition properties of hydrogen and carbon monoxide mixtures for syngas turbine applications. *Proceedings of the Combustion Institute*, *31*(2), 3147–3154.

Wang, Z., Li, F., & Wang, Y. (2017). A generalized kinetic model with variable octane number for engine knock prediction. *Fuel*, *188*, 489–499.

Wayne, W. S., Clark, N., & Atkinson, C. (1998). *A parametric study of knock control strategies for a bi-fuel engine*. SAE Technical Paper. Retrieved from http://papers.sae.org/980895/

Westbrook, C. K., & Pitz, W. J. (1990). Modeling of knock in spark-ignition engines. In *International Symposium COMODIA* (Vol. 90, p. 1). Retrieved from http://technovol.jsme.or.jp/esd/COMODIA-Procs/Data/002/C90_P011.pdf

Williams, F. A., & Li, S.-C. (2000). *Some basic considerations of pollutant emission and knock in internal combustion engines*. SAE Technical Paper. Retrieved from http://papers.sae.org/2000-01-0647/

Wise, D. M. (2007). *Investigation into producer gas utilization in high performance natural gas engines*. Colorado State University. Libraries. Retrieved from https://dspace.library.colostate.edu/handle/10217/78876

Wise, D. M., Olsen, D. B., & Kim, M. (2013). Characterization of MN for producer gas blends. In *ASME 2013 Internal Combustion Engine Division Fall Technical Conference* (p. V002T02A015–V002T02A015). American Society of Mechanical Engineers. Retrieved from http://proceedings.asmedigitalcollection.asme.org/proceeding.aspx?articleid=1837833

Y

Yavuz, I., Celik, I., & McMillian, M. H. (2001). *Knock Prediction in Reciprocating Gas-Engines Using Detailed Chemical Kinetics*. SAE Technical Paper. Retrieved from http://papers.sae.org/2001-01-1012/

Z

Zhu, G. G., Daniels, C. F., & Winkelman, J. (2003). *MBT timing detection and its closed-loop control using in-cylinder pressure signal*. SAE Technical Paper. Retrieved from http://papers.sae.org/2003-01-3266/

APPENDIX

Appendix A: Calibration curve determination

In this section a description of the methodology employed to determine the calibration curve of the flowmeters used in the MN test is described.

Wet Test Meter

Standard Operating Procedure (SOP)

Introduction:

A Wet Test Meter (WTM) measures a gas-volume flow by lifting rotating chambers out of water. The water provides the seal so that the gas cannot bypass the chambers. The chambers have a fixed volume. For example, in the Precision Scientific 3L Wet Test Meter, four chambers at 0.75L each give a total volume of 3L per full rotation. The only other variable is the water level, which must be set precisely.

Specifics about the Precision Scientific 3L Wet Test Meter:

Catalog Nr. 63126
Volume per rotation 3 L/min
Flow rate range: 0-13 L/min.

Note: **Above 13 L/min (~10 SLPM depending on temperature and pressure), gas bypasses the chambers and the result will be incorrect**

Preparation:

3L Model: Close the Wet Test Meter at the bottom with the 1/4" pipe plug. Use Teflon tape or grease on the plug to ensure proper sealing. For filling, use either the large

stainless cap on top of the glass tube, or open the 1/4 pipe plug on top of the meter. Use grease only at the top 1/4" pipe plug, so that no Teflon threads fall into the Wet Test Meter.

0.25cft Model: Close the Wet Test Meter at the bottom with the plug. A Viton washer provides a good seal. For filling, use the top opening that can hold a thermometer.

Level the Wet Test Meter and fill with distilled or deionized water up to the tip of the needle.

Note: **Never use tap water in the Wet Test Meter. Deposits will form and the meter will become inaccurate and passages will block over time.**

Close all plugs and connect the exhaust of the Wet Test Meter (upper fitting either on top or in the top of the back) to a vent, but do not put unnecessary back pressure or under pressure on the instrument. Connect the inlet (fitting in center of back) to your gas source. For hazardous gases, make sure the outlet is connected to a vent with nitrogen dilution and mild suction. Do not use gases that strongly absorb or react with water (ammonia).

Measurement:

Start the flow through the Wet Test Meter at a flow rate that you want to calibrate at. The pointer on the dial will start to rotate. Wait a few minutes, so that the Wet Test Meter can equilibrate by allowing it to absorb or desorb gases from the water. Always stop the Wet Test Meter for a short while to adjust the water level, by adding water to the glass tube.

During the actual measurement, it is recommended to measure the time it takes to complete several complete rotations. To gain a good precision, allow the meter to run at least 2-3 minutes.

After the measurement is completed, divide the total volume by the time in minutes (minutes+seconds/60). This will give the uncorrected volume flow in L/min.

Correction:

Once the volume flow rate is determined from the number of rotations and time, a series of corrections need to be made.

The corrections are necessary because the gas in the Wet Test Meter is not at standard temperature, standard pressure, and it contains water vapor from evaporation.

Pressure correction:

The pressure inside the Wet Test Meter is measured against ambient pressure via a manometer tube containing water. From this manometer, the height difference can be read in inches of water. If the temperature of that water is assumed to be the same as in the Wet Test Meter, the density of water can be calculated using a fit:

$$\rho_{water}\ [kg/m^3] = 1001.1 - 0.0867*T_{WTM}[C] - 0.0035*T_{WTM}[C]\text{^}2 \qquad \text{Eq. A1}$$

T_{WTM}: Temperature of Wet Test Meter. Read from the thermometer at the bottom (3L Model) or top (0.25cft Model). Note, that the Wet Test Meter will be colder than the ambient temperature due to the continuous water evaporation.

The pressure inside the Wet Test Meter then follows:

$$p_{WTM}\ [atm] = p_{amb}[atm] + \rho_{water}[kg/m^3] * 9.807[m/s^2] * \frac{\Delta p[in.H_2O] * 0.0254[m/in.]}{101300[Pa/atm]} \qquad \text{Eq. A2}$$

where:

p_{amb}[atm]: Ambient barometric pressure

Δp [in. H_2O]: Pressure difference between Wet Test Meter and ambient in inches of water (read from manometer on Wet Test Meter).

Since the gas leaving the Wet Test Meter is saturated with water, the vapor pressure is needed at the operating temperature. It is calculated from the Antoine equation:

$$p_{vap}[atm] = \frac{10^{\left(4.08245 - \frac{1346.382}{T_{WTM}[K] - 53.508}\right)}[bar]}{1.013[bar/atm]} \qquad \text{Eq. A3}$$

The corrected volume flow at standard conditions is then calculated from the uncorrected volume flow by removing the water content, multiplying by the pressure

and temperature correction. This assumes that the standard conditions for SLPM are 0°C (273.15 K) and 1 atm. Note, that the temperature of the water in the Wet Test:

$$V_{corr}[SLPM] = V_{uncorr}[\frac{L}{min}] * \frac{p_{WTM}[atm] - RH * p_{vap}[atm]}{p_{WTM}[atm]} * \frac{p_{WTM}[atm]}{1[atm]} * \frac{273.15[K]}{T_{WTM}[K]} \quad \text{Eq.A4}$$

RH : Relative Humidity as fraction. 1 refers to full saturation of the gas with water.
T_{WTM}[K]: Temperature of Wet Test Meter (read from the thermometer at the bottom).

Simplifying the equation leads to the following final equation:

$$\mathrm{V_{corr}[SLPM]} = \mathrm{V_{uncorr}}[\frac{\mathrm{L}}{\mathrm{min}}] * \frac{\mathrm{p_{WTM}[atm]} - \mathrm{RH} * \mathrm{p_{vap}[atm]}}{1[\mathrm{atm}]} * \frac{273.15[\mathrm{K}]}{\mathrm{T_{WTM}[K]}} \quad \text{Eq.A5}$$

Figure A1 describes the calibration curves estimated for each flow-meters for MN measurements tests.

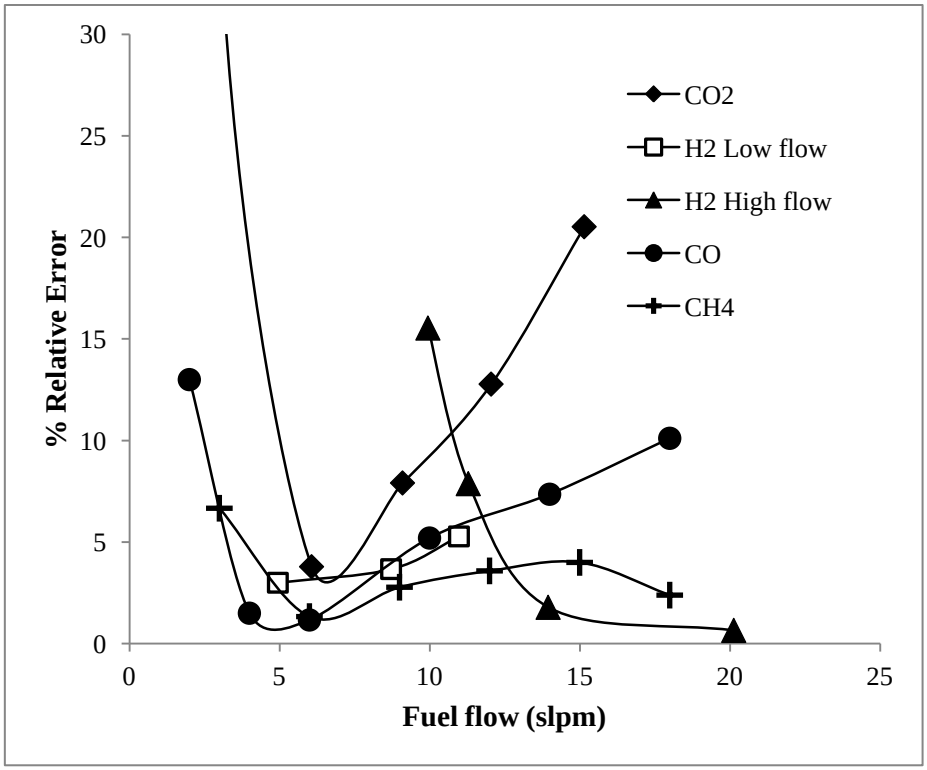

Figure A1. Calibrations curve for MN measurements.

Appendix B: Methane Number uncertainty determination

By definition, the MN of a fuel blend is equal to the volumetric fraction of methane in a binary mixture of hydrogen and methane. Therefore, the Methane Number is given by:

$$MN = \frac{100 * \dot{Q}_{CH_4}}{\dot{Q}_{CH_4} + \dot{Q}_{H_2}} \quad \text{Eq. B1}$$

Thus, the MN uncertainty due to reference gas compositions is defined as:

$$\delta MN = \left[\left(\frac{\partial MN}{\partial \dot{Q}_{CH_4}} \delta \dot{Q}_{CH_4} \right)^2 + \left(\frac{\partial MN}{\partial \dot{Q}_{H_2}} \delta \dot{Q}_{H_2} \right)^2 \right]^{1/2} \quad \text{Eq.B2}$$

where :

$$\frac{\partial MN}{\partial \dot{Q}_{CH_4}} = \frac{100}{\dot{Q}_{CH_4} + \dot{Q}_{H_2}} - \frac{100 * \dot{Q}_{CH_4}}{\left(\dot{Q}_{CH_4} + \dot{Q}_{H_2}\right)^2} \quad \text{Eq.B3}$$

$$\frac{\partial MN}{\partial \dot{Q}_{H_2}} = \frac{-100 * \dot{Q}_{CH_4}}{\left(\dot{Q}_{CH_4} + \dot{Q}_{H_2}\right)^2} \quad \text{Eq.B4}$$

When MN is greater than 100, the MN is defined as:

$$MN = 100 + \frac{100 * \dot{Q}_{CO_2}}{\dot{Q}_{CH_4} + \dot{Q}_{CO_2}} \quad \text{Eq.B5}$$

The MN uncertainty due to reference gas compositions is defined as:

$$\delta MN = \left[\left(\frac{\partial MN}{\partial \dot{Q}_{CH_4}}\delta\dot{Q}_{CH_4}\right)^2 + \left(\frac{\partial MN}{\partial \dot{Q}_{CO_2}}\delta\dot{Q}_{CO_2}\right)^2\right]^{1/2} \quad \text{Eq.B6}$$

where

$$\frac{\partial MN}{\partial \dot{Q}_{CO_2}} = \frac{100}{\dot{Q}_{CH_4} + \dot{Q}_{CO_2}} - \frac{100 * \dot{Q}_{CO_2}}{\left(\dot{Q}_{CH_4} + \dot{Q}_{CO_2}\right)^2} \quad \text{Eq.B7}$$

$$\frac{\partial MN}{\partial \dot{Q}_{CH_4}} = \frac{-100 * \dot{Q}_{CO_2}}{\left(\dot{Q}_{CH_4} + \dot{Q}_{CO_2}\right)^2} \quad \text{Eq.B8}$$

Mathematically, the flow-meters uncertainties are defined as:

$$\delta\dot{Q}_{CH_4} = \delta_{fm,CH_4} + \delta_{calibration,CH_4} \quad \text{Eq.B9}$$

$$\delta\dot{Q}_{H_2} = \delta_{fm,H_2} + \delta_{calibration,H_2} \quad \text{Eq.B10}$$

$$\delta\dot{Q}_{CO_2} = \delta_{fm,CO_2} + \delta_{calibration,CO_2} \quad \text{Eq.B11}$$

where δ_{fm} represents the uncertainty of the flowmeter and $\delta_{calibration}$ is the error estimated by using the flowmeter calibration curve.

Appendix C: DEVELOPMENT OF A COMPUTATIONAL TOOL FOR COMBUSTION ANALYSIS

German Amador, Carlos Bravo, Adalberto Salazar, Orlando Olaciregui, Lesme Corredor

gjamador@uninorte.edu.co cabravo@uninorte.edu.co nadalberto@uninorte.edu.co

omolaciregui@uninorte.edu.co lcorredo@uninorte.edu.co

CONTENT

FIGURE LIST

TABLE LIST

INTRODUCTION

The efficient analysis of the experimental data obtained in the experiments requires a large amount of time and computational resources. This document describes in detailed the computational tool developed to carry out these analysis. The computational tool is compound of three modules which has been programmed in VBA of Excel. The modules are: KOCA Analysis, Mass Fraction Burned (MFB) and the Heat Release Analysis. The raw data used consists in pressure traces of 1410 cycles as a function of crank angle ranging from 360° bTDC to 360° aTDC with a step of 0.1 crank angle. This means that there are available 7201 data points for processing manually, which is a tedious work. Table C-1 shows the average time required for processing manually the first 300 cycles of the 1410 cycles available.

Table C- 1 Average time required for processing manually 300 cycles

Process	Time(min)
Data Filtering and KOCA	168
Average MFB	140
Heat Release Analysis	105
Total	423

The objective of these programs is to optimize the analysis of a large amount of data. The programs can be used regarding of the engine power and size.

The System Requirements needed to guarantee a correct performance of the programs are described as follow:

a) The active version of the Excel program must be equal or greater than 2013 version.

b) The *developer option*, and *Macro permissions* must be activated in Excel. If these options are not active, the module will not work.

c) These modules must be handled as it is indicated in this document in order to obtain good results.

MODULE 1: KOCA ANALYSIS

The objective of this module is to determine experimentally the Knock Occurrence Crank Angle (KOCA) of a fuel as a function of a given engine operating condition. Figure C-1 shows schematically the algorithm employed to determine the average KOCA.

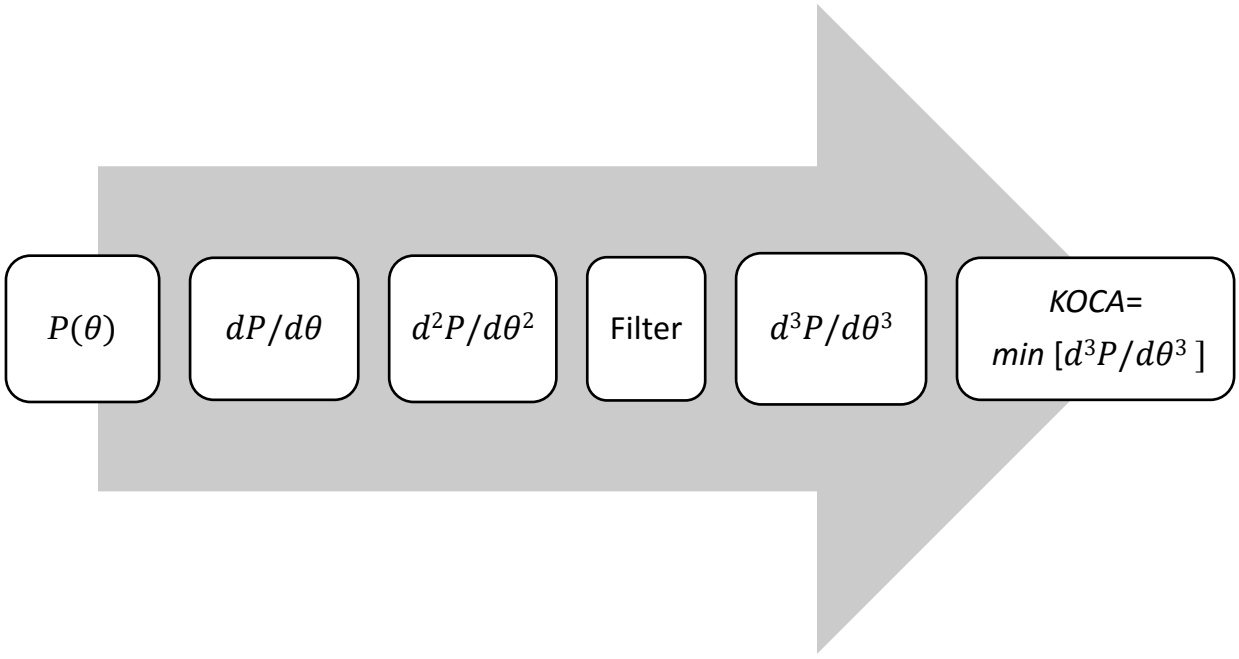

Figure C- 1 Scheme of the KOCA ANALYSIS algorithm

This algorithm is applied to each filtered cycles, which are selected through the individual knock intensity. Cycles with FFT amplitude higher than 1 were selected for the analysis. From the individual KOCA estimated, a confidence interval of KOCA is calculated by using the statistical distribution T-Student:

$$\overline{KOCA} - t_{(\frac{\propto}{2},n-1)} * \frac{S}{\sqrt{n}} < \mu < \overline{KOCA} + t_{(\frac{\propto}{2},n-1)} * \frac{S}{\sqrt{n}} \qquad \text{Eq.C1}$$

where S is the standard deviation of the sample,n is the number of data in the sample, $\overline{KOCA}$ is the arithmetic average of KOCA in the sample and α is the type l error of the analysis.

The analysis starts by defining the SOC and EOC crank angles. These values are determined previously by using the methodology proposed in Chapter 4. For instance, Figure C-2 shows a dialog box with the interval where the combustion takes place; the SOC is 50° bTDC and EOC is 40° aTDC. Depending on the fuel used, these values can change. The negative value of the SOC means that the crank angle is before of the top dead center (bTDC).

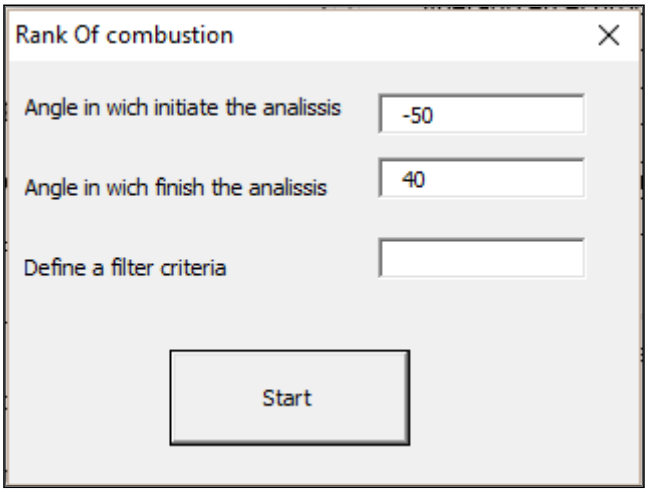

Figure C- 2 Dialog box for defining the SOC, EOC and the filter criteria as input data

The raw data must be organized according to Figure C-3. The sheet of Excel must contain the in-cylinder pressure as a function of the crank angle and the knock intensity defined as the maximum FFT. This data must be previously filtered in order to obtain representative cycles with high knocking tendency. The KOCA analysis modulus effectively filters the raw data coming from the data acquisition system. The knock intensity must be defined in order to filter the data. This thesis considers as reference an individual knock intensity of 1.

	Untitled	Untitled 1	Untitled 2	Untitled 3	Untitled 4	Untitled 5	Untitled 6	Untitled 7	Untitled 8	Untitled 9	Untitled 10	Untitle
Cylinder 1 FFT Knock Knock Hz	2,03648615	1,59080267	0,91635275	0,8628884	0,80706894	1,15344977	1,39079177	1,13958383	0,44820663	1,71257758	0,46325362	1,1956
Crank Angle [deg]												
-50	501,569336	519,924561	509,620117	506,72168	531,195068	523,144775	515,094238	525,720947	512,518311	506,721924	522,500488	517,02
-49,90000153	502,857422	520,568359	510,586182	511,22998	531,839111	525,076904	515,738281	528,297119	514,450439	508,653809	523,788818	517,6
-49,79999924	504,467529	522,822754	512,196289	508,97583	533,77124	527,331055	518,636475	529,906982	515,416504	511,230225	526,042725	520,24
-49,70000076	506,72168	524,11084	513,806152	511,22998	535,381348	528,940918	519,924561	531,839111	517,67041	512,196289	527,331055	521,85
-49,59999847	507,687744	526,36499	514,772217	512,840088	537,313477	530,229248	522,178711	533,449463	518,95874	513,484131	531,839111	523,46
-49,5	508,975586	528,297119	516,704346	515,41626	538,601318	531,839111	523,788818	534,415527	519,602539	515,094238	530,873047	524,1
-49,40000153	508,975586	529,584961	517,67041	516,060303	540,21167	534,415283	525,076904	536,347412	522,500977	517,026367	532,483154	526,04
-49,29999924	512,517822	532,161377	519,602783	517,67041	542,465576	535,703369	526,042969	537,313477	523,467041	519,602539	534,093262	528,61
-49,20000076	513,806152	533,127441	522,178711	519,602539	544,075684	536,347412	528,297119	537,635742	523,789063	519,924561	535,381348	535,38
-49,09999847	517,992188	534,415283	522,822754	520,890625	545,686035	537,95752	528,941162	541,177734	526,042969	522,178711	538,601563	531,51
-49	517,67041	536,669678	524,433105	523,788574	547,295898	540,21167	532,161133	543,109863	528,941162	523,144531	538,923584	532,80
-48,90000153	519,280273	537,313477	527,009033	525,076904	548,583984	541,177734	532,80542	544,397949	528,941162	526,042725	540,533691	534,73
-48,79999924	521,534424	539,567627	528,297119	526,36499	550,838135	544,075928	535,381592	546,330078	529,263184	526,687012	542,46582	535,70
-48,70000076	523,144775	541,177734	529,907471	528,296875	551,482178	545,364014	536,669434	548,262207	530,873535	528,618896	544,075928	538,27
-48,59999847	524,754639	543,753906	531,8396	530,551025	554,702393	546,007813	537,95752	548,262207	534,737549	530,551025	546,330078	539,88
-48,5	527,008789	545,364014	533,771484	532,161133	555,668213	547,618164	539,567627	552,448486	536,025635	531,195313	546,974121	542,14
-48,40000153	527,974854	546,6521	534,737549	534,415527	555,346436	549,550293	541,822021	553,092529	538,279785	539,889648	549,228271	542,78
-48,29999924	532,483154	547,618164	536,347656	535,703369	558,888672	551,1604	543,109863	555,024658	539,889893	535,381348	550,516113	544,39
-48,20000076	530,873047	549,872314	538,601807	538,279541	561,464844	553,414307	544,719971	556,956787	541,822021	538,601563	550,194336	546,00
-48,09999847	533,449219	552,126465	540,211914	538,601563	563,396973	555,024658	546,974121	560,177002	543,432129	539,24585	554,702637	548,26

Figure C- 3 Screenshot of the data after of the filter process

Once the data have been filtered, the module computes the characteristic KOCA, which depend on the engine operating conditions and the fuel. Later, a GUI is displayed with the desired information as shown in Figure C-4. The result obtained is the confidence interval which is based on the T student's distribution. In addition a plot of the third derivative as a function of crank angle is shown to verify the most negative derivative that defines KOCA. The computational time required to obtain this result is 5 minutes approximately. This is a substantial reduction of time taking into account the time required for processing the data manually.

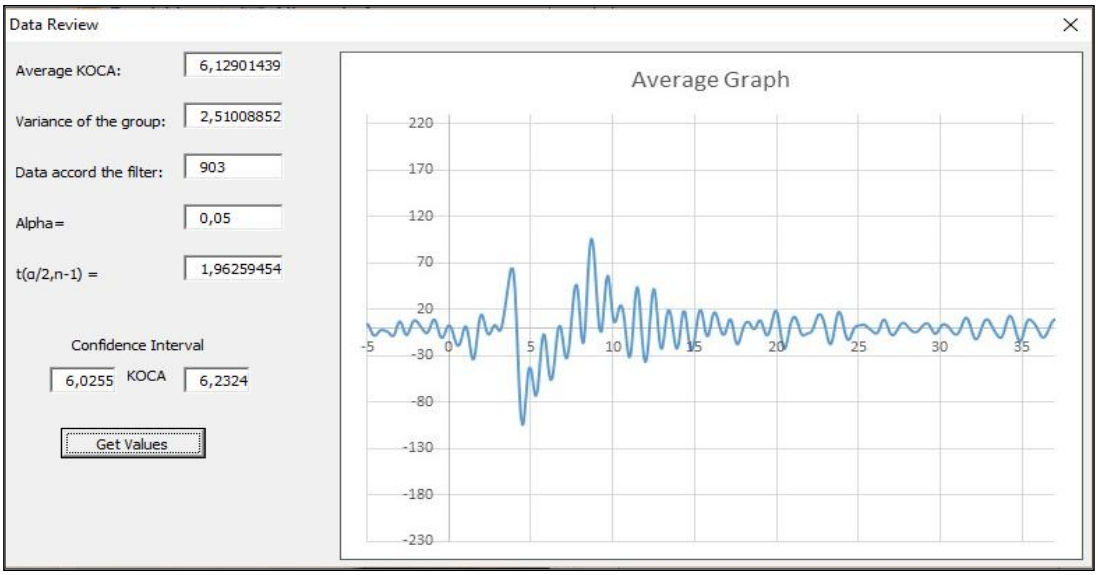

Figure C-4 Dialog box displaying the results of the analysis

MODULE 2: MASS FRACTION BURNED DETERMINATION

This module computes the Mass Fraction Burned (MFB) of each cycle recorded and then the average MFB, which is used for modeling ICE. This module was developed by using Excel (Visual Basic developer tool). The data obtained from this tool are: a plot with the average MFB trace, the crank angle at 10% of MFB (SOC), crank angle at 90% MFB (EOC) and the 50% MFB crank angle (Intermediate point). Moreover, the combustion duration is given from the point SOC and EOC determined previously. The input data required for the module are:

a) IT: Ignition Timing
b) r_c: Compression ratio
c) V_d: Volume displacement of the engine
d) R: connecting rod length /radius ratio

A scheme of the module operation is illustrated in Figure C-5. The input data required are: geometrical properties of the combustion chamber, in-cylinder pressure as a function of the crank angle and the Ignition timing.

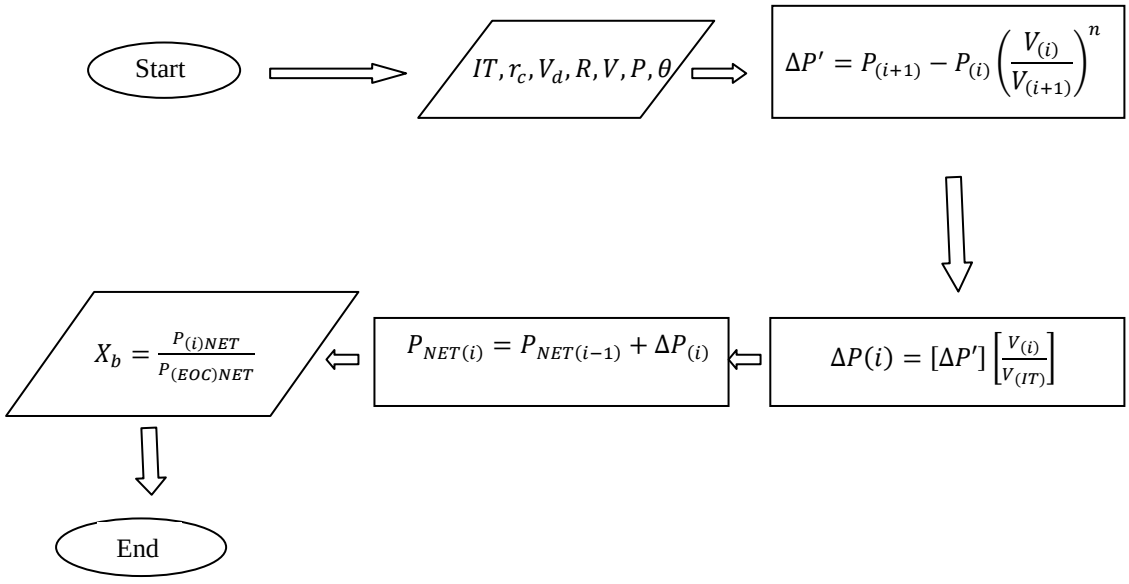

Figure C-5 Scheme of the module operation for MFB estimation for one cycle

This algorithm is applied to each filtered cycle; therefore, MFB of each cycle is possible to obtain according to the necessity of the user. The equations used for MFB estimation were describes in Chapter 4. However, in this section are described again:

$$\Delta P_K = \left[P_{K+1} - P_k \left(\frac{V_K}{V_{K+1}}\right)^n\right] \frac{V_K}{V_{IT}} \quad \text{Eq.C2}$$

$$P_{net(K)} = P_{net(K-1)} + \Delta P_K \quad \text{Eq.C3}$$

By definition:

$$\theta_{EOC} = \theta \quad \rightarrow (P * V)_{maximum} \quad \text{Eq.C4}$$

Then:

$$X_b = \frac{P_{netK}}{P_{net(EOC)}} \quad \text{Eq.C5}$$

For a correct use of the module, the user needs to organize the in-cylinder pressure data as appear in Figure C-6. It is important to highlight that the raw date must be carefully handled as if it is not copied properly, wrong results will be obtained.

	1	2	3	4	5	6	7
1	Crank Angle	Untitled	Untitled 1	Untitled 2	Untitled 3	Untitled 4	Untitled
2	-360	90,6730957	100,3339844	98,07910156	98,72338867	91,63916016	93,24951
3	-359,899994	91,31738281	99,68969727	97,75732422	97,43554688	91,63916016	92,60522
4	-359,799988	90,6730957	100,6557617	98,07910156	97,11352539	90,99536133	93,57128
5	-359,700012	90,99560547	100,0119629	97,75732422	96,79174805	92,92749023	91,9609
6	-359,600006	90,6730957	100,0119629	96,79125977	97,11352539	91,63916016	92,60522
7	-359,5	90,6730957	100,9780273	96,79125977	97,75732422	90,35107422	92,92700
8	-359,399994	90,6730957	99,04589844	97,11303711	97,11352539	91,31713867	94,85913
9	-359,299988	89,06323242	99,36791992	96,79125977	96,14746094	90,99536133	91,9609
10	-359,200012	90,35131836	99,04589844	95,82519531	97,75732422	91,63916016	92,28344

Figure C-6 Correct organization of the raw data

The steps required for activating the module are described as follow: click on the *developer tab* and then select the *Macros* command. A dialog box will appear wherein the MFB option must be selected. Then, click on the *Run* button to execute the macro as shown in Figure C-7.

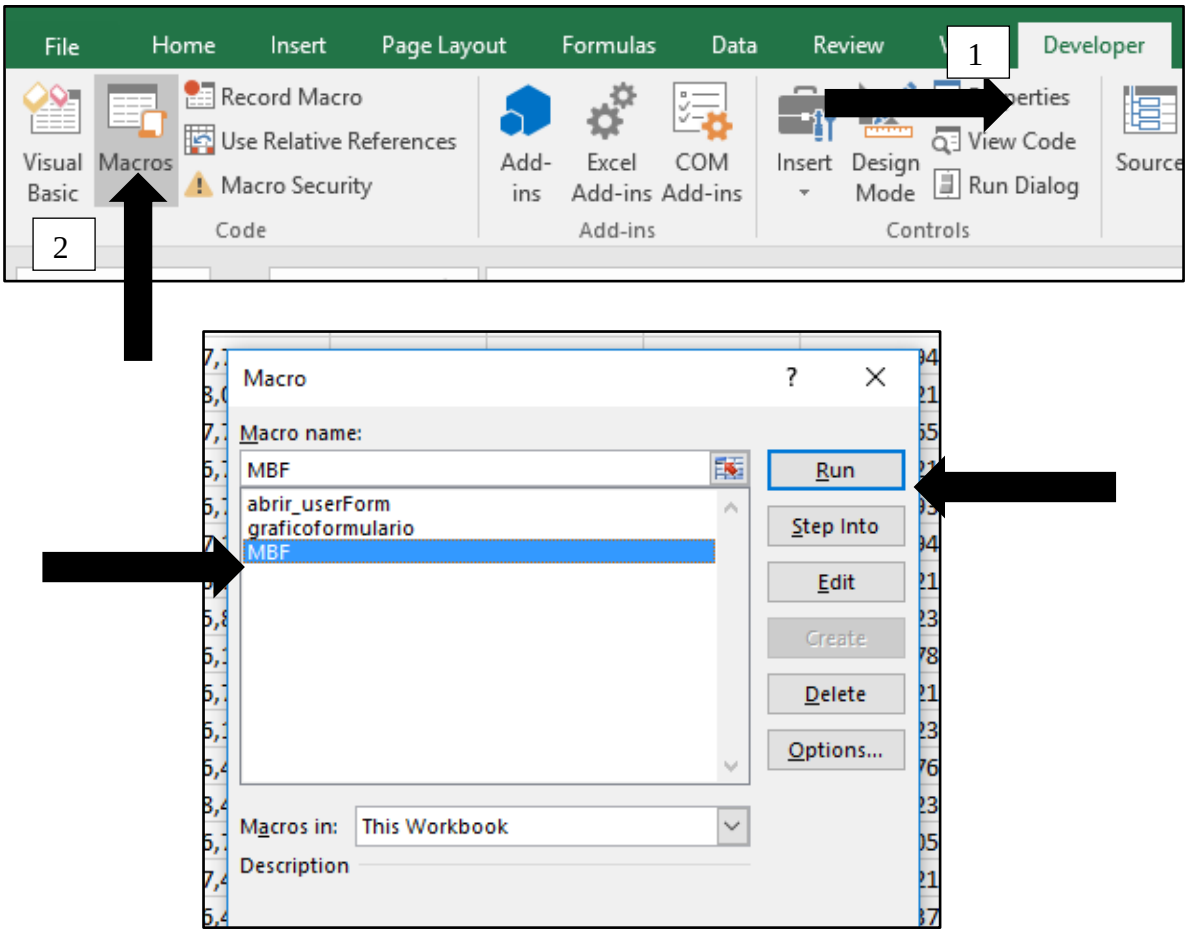

Figure C-7 Steps required for activating the macro

Once the raw data has been processed, a GUI will appear as illustrated in Figure C-8. The ignition timing and geometrical properties of the engine must be supplied by the user. This option permits to analyze combustion process of engines of different size and therefore different power. Then, press I*nput* button for saving the data. When process has finished successfully, a box dialog will appear with the message "successful process" as illustrated in Figure C-9. Then, the "*OK*" button must be clicked for displaying the results. Figure C-10 shows the results obtained which consist in the average MFB of the cycles analyzed and the SOC, EOC and CD characteristic of the air fuel mixture. To display the results, the *"Show Values"* button must be clicked.

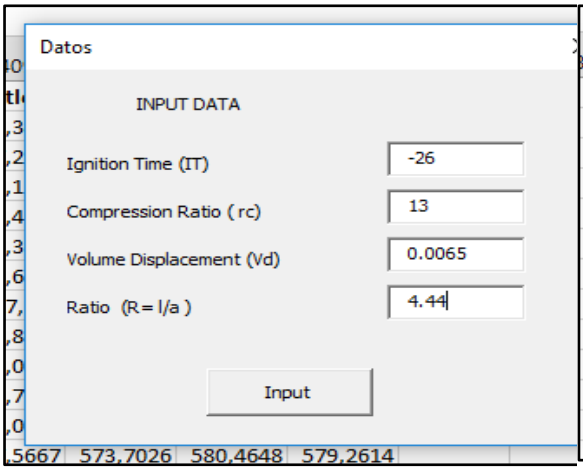

Figure C-8 Dialog box for supplying ignition timing and geometrical properties of the engine

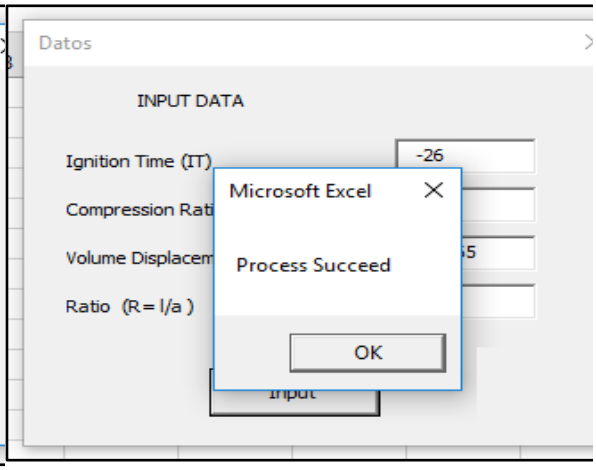

Figure C-9 Dialog box that indicates a successful process

The time required for processing the data is around 10 minutes. There is a substantial reduction of time, taking into consideration that the time required for process that data manually was 140 min. If the user desires, the module also gives the individual MFB which is recorded in a sheet of Excel.

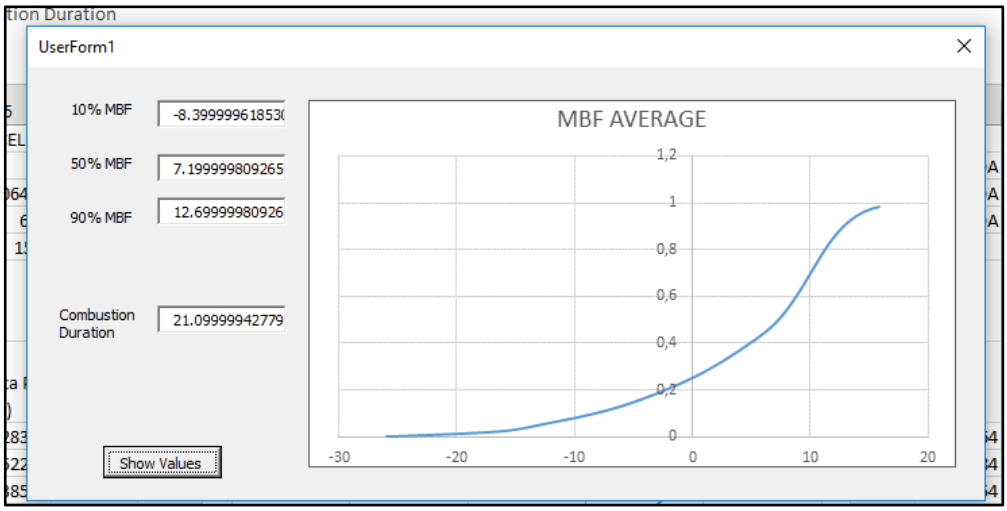

Figure C-10 Average MFB and combustion properties obtained

MODULE 3: HEAT RELEASE ANALYSIS

The objective of this module is to estimate the Net Heat Released by the fuel. It uses the ignition timing, the heat specific ratio, the in-cylinder pressure and the combustion chamber's volume as input data. Figure C-11 shows a schematic representation of the algorithm implemented.

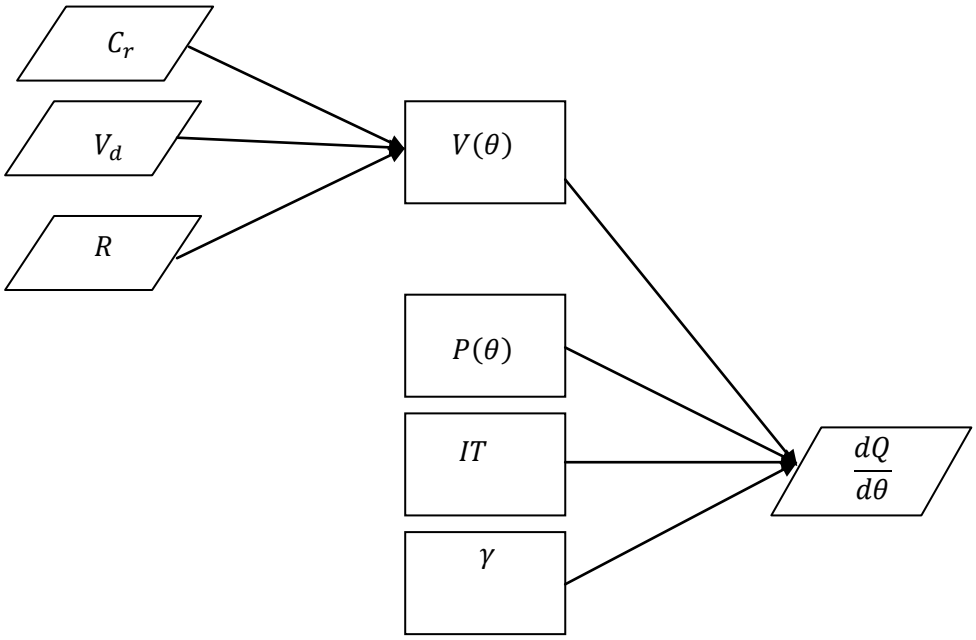

Figure C- 11 Schematic representation of Heat Release algorithm

The geometric properties of the engine are used to compute de combustion chamber's volume. The equations used for this estimation was described in Chapter 4; however, it is presented again as follow:

$$V(\theta) = \frac{Vd}{r_c - 1} * \left[1 + 0.5(r_c - 1)\left(R + 1 - cos\theta - \sqrt{R^2 - \sin^2\theta}\right)\right] \qquad \text{Eq. C-6}$$

Figure C-12 illustrates the dialog box where the geometric properties of the engine are supplied. To save the data, the "*Ingresar*" button must be clicked

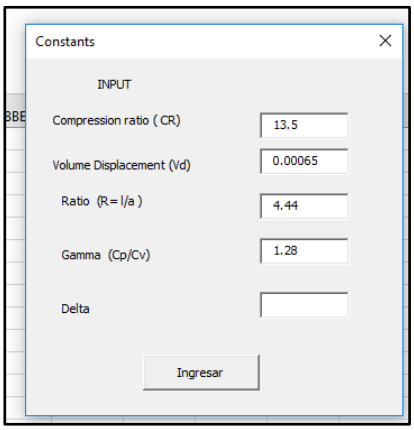

Figure C-12 Screenshot of the dialog box used for supplying the geometric properties of the engine

As mentioned above, this dialog box permits to analyze the heat released by a fuel regarding of the engine size and power.

The equation used for estimating the heat release is given by:

$$\frac{dQ}{d\theta} = \frac{\gamma}{\gamma - 1} P \frac{dV}{d\theta} + \frac{1}{\gamma - 1} V \frac{dP}{d\theta} \qquad \text{Eq. C-7}$$

The derivatives are calculated by means of Eq. 3-3. Figure C-13 shows the average Heat Release estimated by means of the module developed. It is important to highlight that the data that appear in the figure are arbitrary.

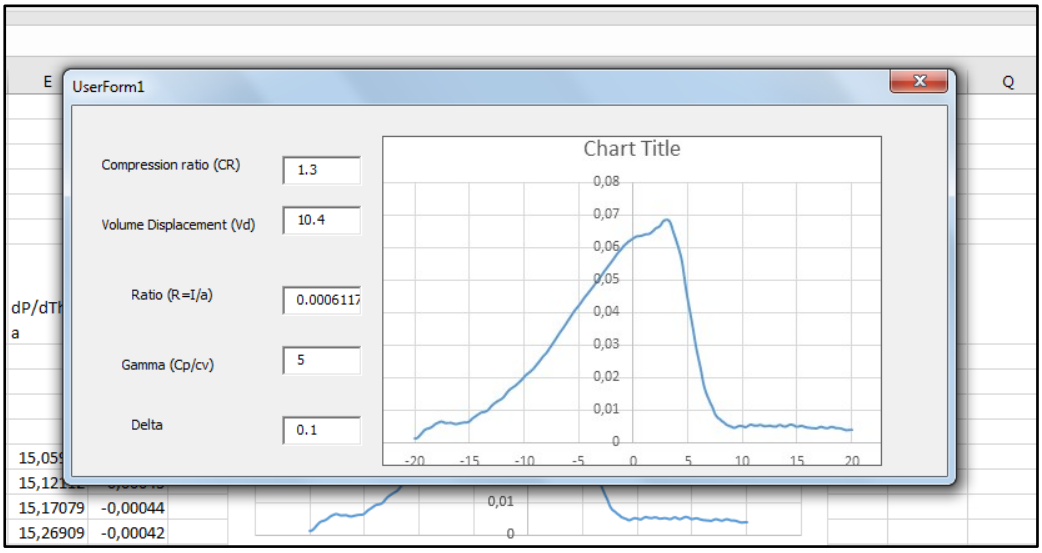

Figure C-13 Heat Release Analysis developed by means of the module

These modules are a useful tool for efficient analysis of a large amount of raw data. According to Table C-2, a reduction of 90 % of time was achieved in comparison with the analysis developed manually.

Table C- 2 Time required for combustion analysis by using the modules developed in the present thesis

Process	Time(min)
Data Filtering and KOCA	10
MFB Determination	11
Heat Release Analysis	25
Total	46

Appendix D : MATLAB CODES

```
function I=Integral(x)
global T_ivc n P Angle Koca
X1=x(1);
X2=x(2);
X3=x(3);
R=8.314;
I=zeros(length(Koca),1);
for i=1:length(Koca) %i representa el numero de ciclos
    i;
    P_ivc=P(1,i);
    Tu=T_ivc*(P(:,i)/P_ivc).^((n-1)/n);
    f=1./(X1*P(:,i).^-X2.*exp(7000.*X3./(R.*Tu)));
    Ang_koca=Koca(i,1);
    for j=1:length(P);
        if (Angle(j)<=Ang_koca)&&(Angle(j+1)>Ang_koca)
            Ind_koca=j;
        end
    end
    I(i,1)=(trapz(Angle(1:Ind_koca),f(1:Ind_koca))-1)^2;
end
I=sum(I);
End
```

MAIN CODE TO FIND X_1 , X_2 *and* X_3

```
clc
clear all
global T_ivc n P Angle Koca
load('DatosPresionCH4H2_27.mat')
T_ivc=365;
n=1.28;
P=DatosPresion(:,2:end);
Angle=DatosPresion(:,1);
X1=0.1;% Semillas
X2=0;% Semillas
X3=0;% Semillas
x0=[X1 X2 X3];
options
=optimset('Display','iter','MaxIter',10000,'MaxFunEvals',100000,'Algor
ithm','lm-line-search','TolFun',1e-15);
[X,fval] = fminunc(@Integral,x0,options);
```

MAIN CODE TO FIND CHARACTERISTIC PRESSURE AND TEMPERATURE

```
clc
clear all
load('DatosPresionCH4H2_32.mat')
X1=1.1347;
X2=-0.79;
X3=0.2548;
R=8.314;
n=1.28;
T_ivc=365;
```

```
for i=1:length(Koca)
    theta_koca=Koca(i,1);
    P=DatosPresion(:,i+1);
    P_ivc=P(1,1);
    Tu=T_ivc*(P/P_ivc).^((n-1)/n);
    I=((theta_koca+146)./(X1.*P.^(-X2).*exp(7000*X3./(R*Tu)))-1).^2;
    [~,IndP]=min(I);
    P_car(i,1)=P(IndP,1);
    T_car(i,1)=Tu(IndP,1);
%     plot(DatosPresion(:,1),I)
end
P_mean=mean(P_car);
T_mean=mean(T_car);
```

Appendix E: Estimation of the standard uncertainty of target data: ignition delay time

The standard uncertainty of experimental data reported in the literature was calculated by using Microsoft Excel®. For example, the model proposed to estimate the standard uncertainty of the data set reported by Peschke and Spadaccini (1985) is given by:

$$\ln(\tau, ms) = \alpha \ln[H_2] + \beta[CO] + \gamma[CO_2] + \frac{k}{T\,(K)} \qquad \text{Eq.E1}$$

The statistical analysis of the model proposed is shown in Figure E-1. The typical error corresponds to the standard uncertainty of ignition delay time data.

Estadísticas de la regresión	
Coeficiente de correlación múltiple	0,96715541
Coeficiente de determinación R^2	0,93538958
R^2 ajustado	0,92696213
Error típico	0,41479847
Observaciones	53

Estimated standard Uncertainty of ignition delay time data

ln (t)=0,414 t = +/- 1,51 ms

ANÁLISIS DE VARIANZA

	Grados de libertad	*Suma de cuadrados*	*Promedio de los cuadrados*	*F*	*Valor crítico de F*
Regresión	6	114,583502	19,0972504	110,993244	1,14437E-25
Residuos	46	7,91465756	0,172057773		
Total	52	122,49816			

	Coeficientes	*Error típico*	*Estadístico t*	*Probabilidad*	*Inferior 95%*	*Superior 95%*	*Inferior 95,0%*	*Superior 95,0%*
Intercepción	20,0351089	12,9661421	1,545186587	0,12915377	-6,064381107	46,1345989	-6,06438111	46,1345989
ln[h2]	-0,06180091	0,55066635	-0,112229322	0,9111299	-1,170234773	1,04663295	-1,17023477	1,04663295
ln[co]	-1,02394672	0,3277798	-3,123885999	0,00308606	-1,683733229	-0,36416022	-1,68373323	-0,36416022
ln[co2]	-0,86644657	0,34862326	-2,485337848	0,0166401	-1,568188782	-0,16470437	-1,56818878	-0,16470437
ln[o2]	-6,60365509	3,18151884	-2,075629732	0,04354599	-13,00772025	-0,19958993	-13,0077203	-0,19958993
ln[n2]	-1,1105225	0,7610232	-1,459249211	0,15129204	-2,642382717	0,42133772	-2,64238272	0,42133772
1/T	7227,46639	289,401201	24,97386452	2,1442E-28	6644,931996	7810,00079	6644,932	7810,00079

Figure E-1 Statistical analysis of the regression model proposed

Figure E-2 shows the experimental data with the standard uncertainty estimated with the regression model. Then, the standard uncertainty of the data reported by Peschke and Spadaccini (1985) is $\sigma_u = \mp 1.51\ ms$

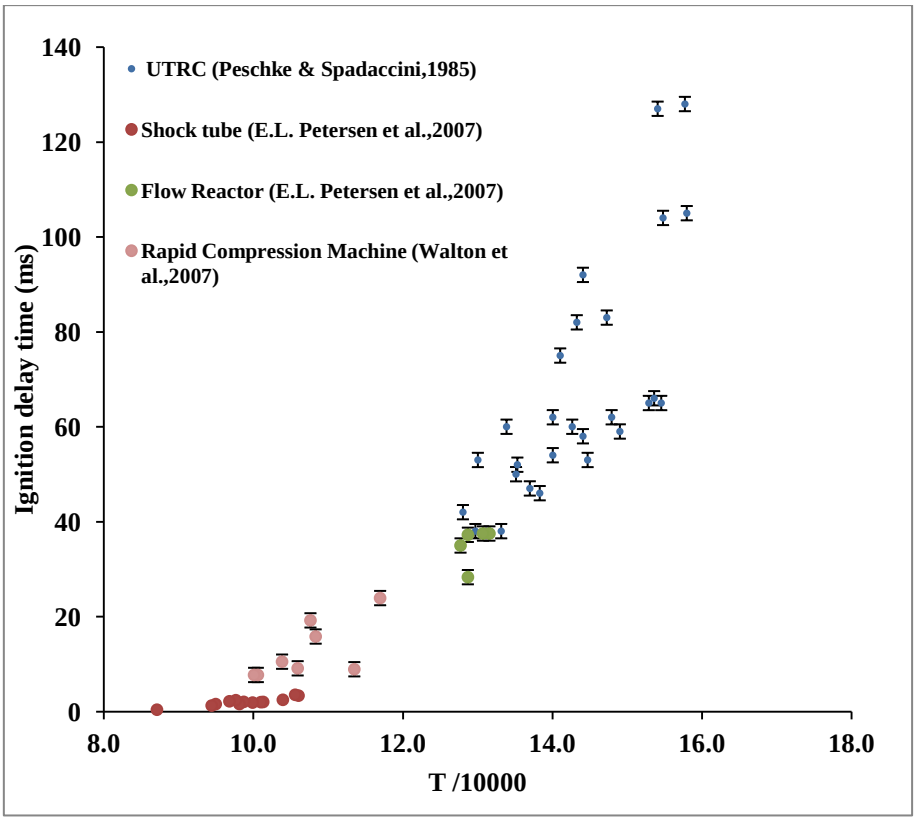

Figure E-2 Ignition delay time vs temperature